Extrusion: Second Edition
M. Bauser, G. Sauer, K. Siegert, editors, p 141-194
DOI:10.1361/exse2006p141

CHAPTER 4

Metallurgical Principles

Martin Bauser*

4.1 Introduction

THE EXTENSIVE USE of metals over thousands of years, but in particular during the industrial age, can be attributed to their specific properties. In addition to their good electrical conductivity—associated with good thermal conductivity—and visual properties, the most important are the mechanical properties and the good workability. The use and range of application of different metals depends on these and many other properties, including, for example, the corrosion resistance. However, the production costs also play a decisive role.

These extend from the accessibility and the extraction of the ore, the cost in the refining up to and including the casting and processing. Extrusion is suitable as a deformation process in different ways for the different materials. The well-used expression "extrudability" is a way of expressing this.

Knowledge of deformation technology alone is not sufficient to be able to understand and control the processes taking place during extrusion. The quality of the billet materials, the processes taking place within the extruded material during extrusion, and the properties of the extruded section can be understood only from a metallurgical viewpoint.

This chapter, therefore, explains the basic terminology of metallurgy—naturally in the context of the aims of this book—to provide the tools needed by those involved in extrusion. More detailed explanations can be found in the literature, e.g., [Hor 67, Guz 70, Ber 83, Sch 81, Dah 93, Hou 93, Blu 93, Alt 94].

This materials science chapter is concerned only with metals. The atoms are held together by the so-called "metallic bond," which differentiates them from the nonmetals (covalent bond, ionic bond). A characteristic of this metallic bond is the ease of movement of the outer electrons, which are no longer attached to individual atoms but form an electron gas. This mobility of the electrons is the reason for the good electrical conductivity of metals.

Nonmetallic crystalline materials can, as a rule, be extruded only with difficulty, if at all. There is insufficient ductility in the working range of temperatures and pressure. Glass with its amorphous structure is, however, an exception because it softens on heating.

Recently, metal and nonmetal composite materials have been extruded. Nonmetallic particles or fibers are uniformly embedded in a metallic matrix, usually artificially, to improve the mechanical properties and often to reduce wear. These materials are also discussed briefly in this chapter.

4.2 Structure

4.2.1 Lattice Structure Single Phase

All metals consist of crystallites (small crystals), the arrangement, size, and shape of which are referred to as the structure. Polishing of

*Casting and Cast Structure, Homogenizing of Aluminum Alloys, Wolfgang Schneider; Casting and Cast Structure of Copper Alloys, Adolf Frei; Deformation, Recovery, Recrystallization, Martin Bauser

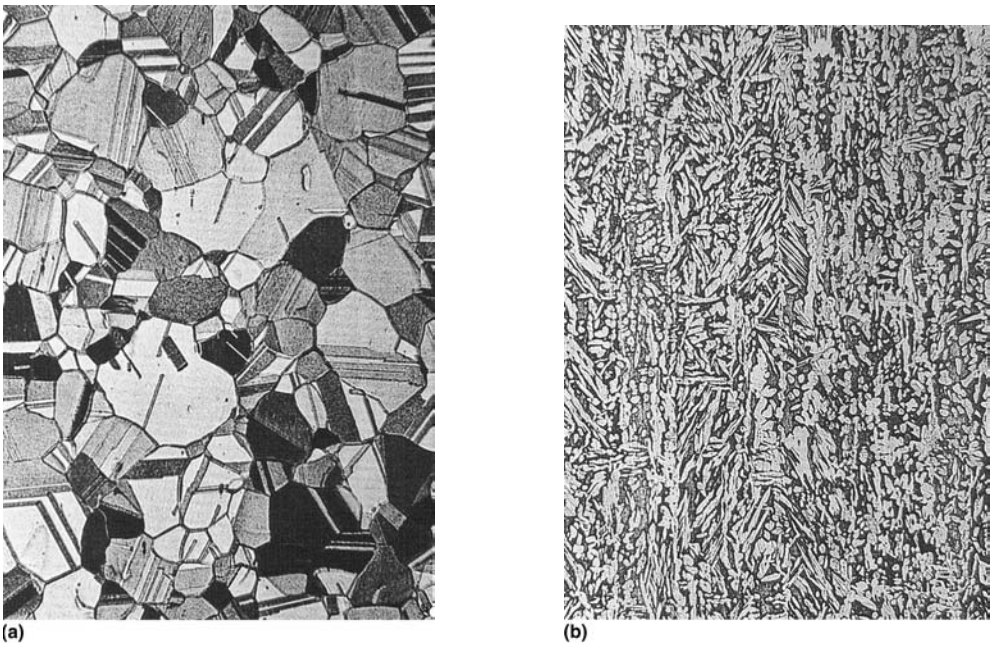

Fig. 4.1 The structure of brass [Wie 86]

metal specimens and suitable methods of etching are used to reveal the structure—usually under the microscope (Fig. 4.1).

The crystallites that form during solidification from the melt change during the cooling. They are stretched by the deformation and reform by recrystallization after annealing a deformed material. They are, however, always crystallites with an ordered lattice structure that constitute the metal.

If a metal consists of only one type of crystallite, it has a *single-phase structure*.

The regular arrangement of the atoms of each crystallite forms the lattice structure. The smallest component of this lattice is referred to as the *unit cell*. A real crystallite, also called a grain, consists of many unit cells arranged uniformly in adjacent rows like building blocks.

The unit cells are very small. The edge length, known as the lattice constant, is of the order of 10^{-7} mm so that a crystallite with a mean diameter of 0.1 mm contains 10^{18} elementary lattice building blocks.

The location of a lattice—a simple cubic lattice is shown in Fig. 4.2—is defined by the direction of the edges of the elementary cell. This is referred to as the orientation of the lattice.

In a real metal body consisting of numerous crystallites, the latter can be differentiated by their orientation, which is usually completely random.

This is shown schematically in Fig. 4.3. The different types of metal lattices have a significant effect on their behavior during deformation. The most important lattice structures are shown in Fig. 4.4. They are face-centered cubic (fcc), body-centered cubic (bcc), hexagonal, and body-centered tetragonal lattices. Figure 4.4 also shows the lattice structure of the important metals at room temperature.

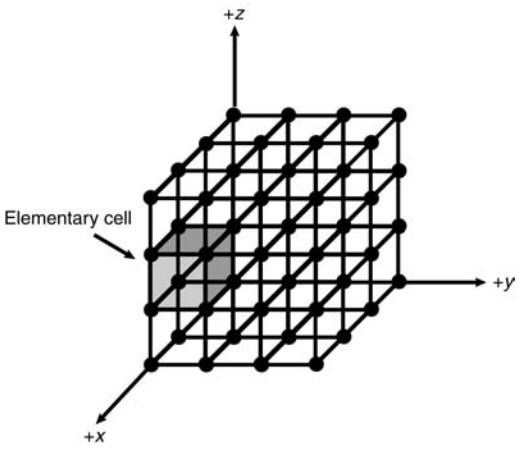

Fig. 4.2 Elementary cell in a simple cubic lattice [Sch 81]

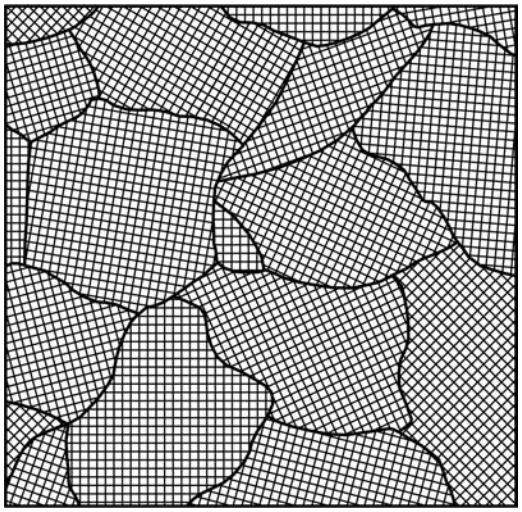

Fig. 4.3 Diagram of a polycrystalline structure

The description of a space lattice by surfaces and direction is usually given by Miller's indices (see the Appendix to this chapter).

In the solid state the metal atoms try to achieve the highest packing density. The fcc and specific hexagonal lattices posses the densest spherical packing. The atoms are assumed to be spheres that preferentially form these arrangements when shaken together. A bcc lattice has a spatial filling of 68%. Face-centered cubic lattices and the hexagonal close-packed structure have a spatial filling of 78% of the maximum possible. It is therefore clear that the density of a metal depends not only on the atomic weight but also on the crystal structure.

The size and shape of the crystallites can be influenced by control of the solidification from the melt and by recrystallisation during the annealing of a deformed metal. Extremely fine crystallites can have diameters well below 1 μm and large grains several mm. It is also possible to grow single crystals. These are particularly suited for studying the basics of the deformation processed within crystals. Cylindrical specimens several centimeters long are produced for this purpose.

Defect-free ideal crystals do not occur in practice. Indeed, specific defects are necessary for plastic deformation and diffusion processes to occur at all. The most important types of defects are shown schematically in Fig. 4.5 and 4.6 and include:

- *Vacancies:* Numerous lattice sites are unoccupied. The number of vacancies increases exponentially with temperature. In the equilibrium state, e.g., in an undeformed aluminum crystal at room temperature, approximately one in every billion lattice sites is unoccupied. In contrast, one in a thousand is unoccupied just below the melting point.
- *Interstitial atoms:* In pure metals embedded atoms of the same type between the regular lattice sites. In alloys specific foreign atoms that are significantly smaller than the atoms of the base lattice can be embedded into the interstitial places (e.g., C and N in Fe).
- *Foreign atoms that substitute the base metal atoms:* Foreign atoms, particularly those with a similar atomic radius and with a similar lattice structure can replace atoms of the base structure.
- *Dislocations:* Step dislocations are lines at which an atomic plane ends. On one side of the slip plane—so called because the dislocation line can move in this plane—there is one more lattice plane than on the other (Fig. 4.6a). In a screw dislocation, the lattice areas are displaced relative to each other so that

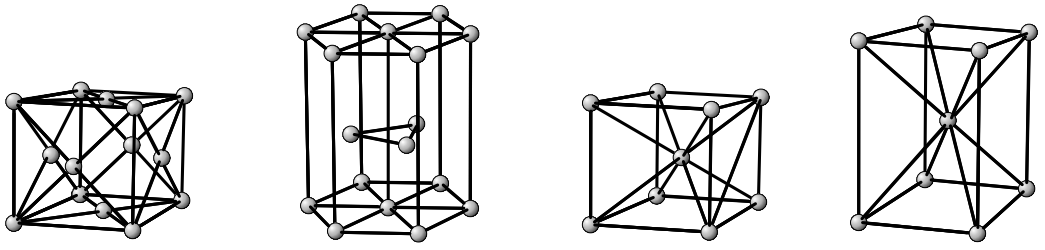

Face-centered cubic lattice
Copper, α-solid solution, nickel, aluminum, lead

Hexagonal close-packed lattice
Zinc

Body-centered cubic lattice
β brass lattice, α iron

Tetragonal body-centered lattice
Tin

Fig. 4.4 The most important types of metal lattice structures [Wie 86]

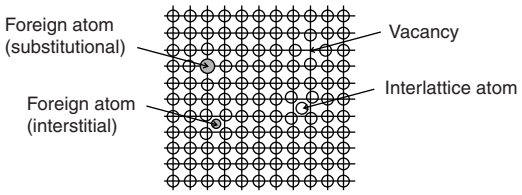

Fig. 4.5 Point type of lattice defect (vacancies, interlattice atoms, substitutional and interstitial foreign atoms)

the atoms are arranged around the dislocation line like a spiral (Fig. 4.6b). A real, usually randomly curved dislocation line in a slip plane can be considered to consist of edge and screw elements. The dislocation line consists of a closed ring or ends at a grain boundary or particle. In an undeformed structure, there can be up to 1 km of dislocation lines/mm^3 (dislocation density 10^6 to 10^8/cm^2.

If the orientation of two adjacent crystallites differs only slightly, the grain boundary between them can be considered to consist of dislocations located above each other (low angle grain boundary; subgrain-boundary) (Fig. 4.7a). Subgrains differ in their orientation from each other by only a few minutes of arc up to a few degrees [Dah 93, Ber 83]. A grain boundary between crystallites with very different orientations (large angle grain boundary) is, in contrast, a severely distorted region with defects of various types (Fig. 4.7b).

Twins represent a special form of crystallites in contact with each other. Their orientation is a mirror image at a plane boundary surface (Fig. 4.8).

A metallic structure that consists of only one type of atom contains dislocations, vacancies, and interstitial atoms. If a metal contains two or more different atoms, it is an alloy containing embedded or substituted foreign atoms. These can accumulate readily in the more or less severely distorted grain boundaries. Every type of defect naturally causes internal stresses within the lattice. Internal stresses are decreased when foreign atoms migrate to grain boundaries because they are able to fill the voids that are present.

4.2.2 Multiphase Structure—Equilibrium Diagrams

Alloys, materials that consist of two or more metals, can have one or more phases (types of crystal).

If only one type of crystal is present in a metallic material—pure metal or alloy—it has a single phase referred to as a *homogeneous structure.* Correspondingly, a *heterogeneous structure* consists of several types of crystals (phases). The well-known free-cutting brass CuZn39Pb, for example, contains both the fcc α brass as well as the bcc β brass, in addition to undissolved lead inclusions as a chip breaker. Figure 4.1 shows a micrograph of a single phase α brass and a binary phase α-β brass.

The structure, the quantity, and the distribution of the various phases of an alloy depend on the content of the individual metals, the previous history, and the temperature. An alloy can pass through several states as it cools from the melt. The amounts of the individual phases that form in the thermodynamic equilibrium state, i.e., the state with the lowest energy, are described by the equilibrium diagram. The spatial distribution of the crystallites of the phases that occur are studied using metallographic images and image analysis techniques.

4.2.2.1 Binary Systems

The simplest equilibrium diagrams are those with only two alloying partners involved. This is referred to as a binary alloy. The abscissa

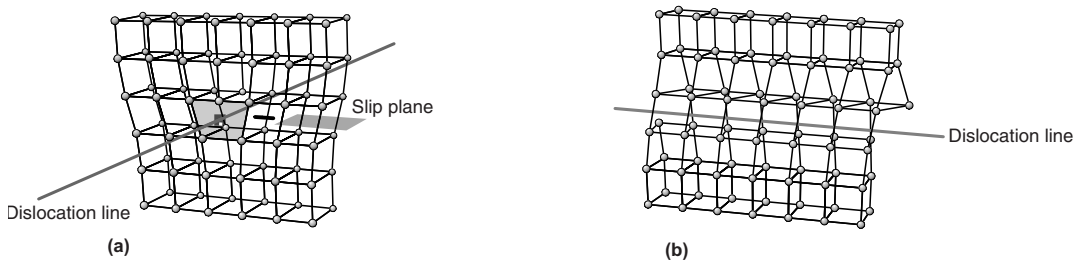

Fig. 4.6 Dislocation = linear lattice defect. (a) Edge dislocation. (b) Screw dislocation [Wie 86]

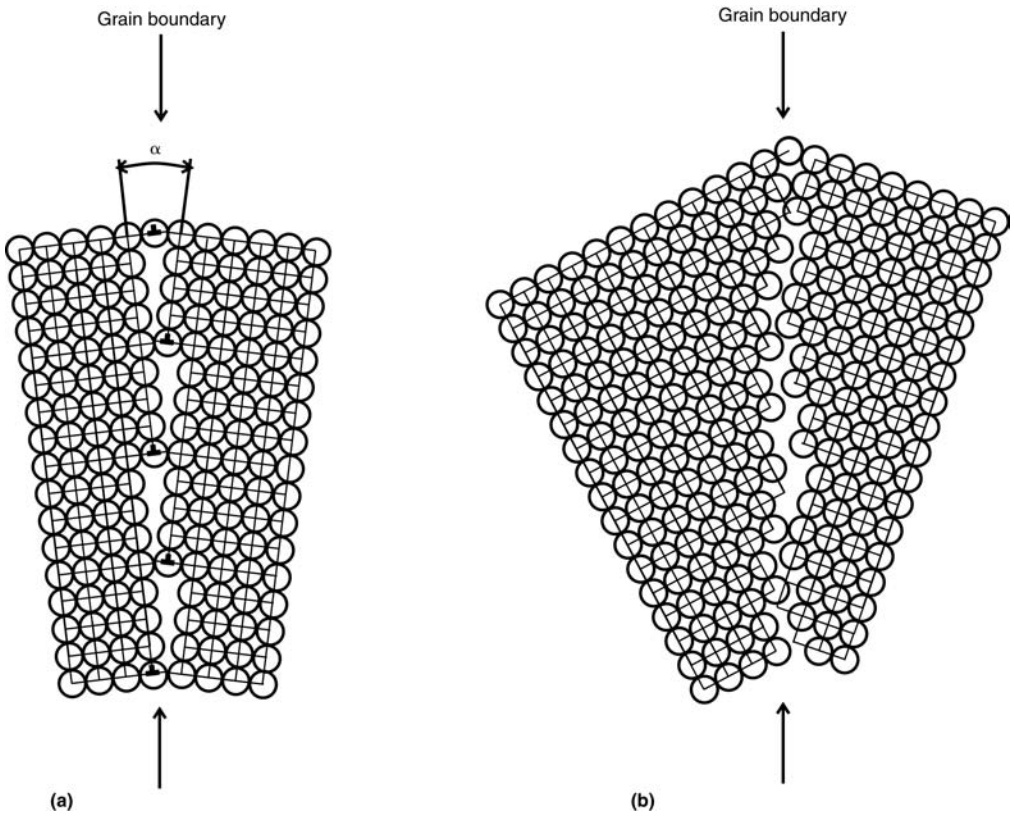

Fig. 4.7 Grain boundary structure. (a) Low angle boundary. (b) High angle boundary [Alt 94, Sch 81]

gives the amount of the two atoms (in weight percent) and the temperature is plotted along the ordinate.

Figure 4.9 shows schematically some of the frequently occurring basic types of binary phase systems. The equilibrium diagrams of most binary systems can be constructed from these examples.

The liquidus temperature (at which solidification commences during cooling from the melt) and the solidus temperature (at which solidification is complete) can be read as well as the occurrence of the phases and the melting interval (the temperature difference between the liquidus and the solidus temperature). In the melting interval, solidified particles float in the melt.

In pure metals, the liquidus and solidus coincide because there is only one solidification temperature. It is identical to the melting temperature as the solid metal transforms to the liquid state at the same temperature on heating.

The different basic types of the equilibrium diagram are shown in Fig. 4.9.

Continuous Solid Solution (Type 1). The lattice type of the parent metal A is retained over the full range of solution up to the pure metal B. The atoms B replace to an increasing extent the atoms A in their lattice positions. This is referred to as atoms B dissolving in lattice A, analogous to the processes in liquids. The solution of one atom type in another is favored where the atom radii differ only slightly from each other, e.g., copper and nickel, which therefore form a continuous solid solution.

In field **a** the metal occurs as a liquid, in field **b** both as solidified particles and as liquid, and in field **c** as 100% solidified solid-solution format.

Because both metals usually have different melting temperatures, the liquidus and the solidus temperature vary with the alloy addition.

Eutectic System (Type 2). In this case, the atoms of type B are completely insoluble in the atoms of type A—usually when there are very large differences between the atom radii. If B is alloyed to A, then B forms its own second phase. The fraction of phase B increases in the equilibrium diagram uniformly to the right and the fraction of phase A decreases accordingly. In the

eutectic system there is one concentration E where the liquidus and the solidus temperature coincide at the minimum melting point. A typical eutectic structure forms at this concentration during solidification, usually consisting of alternating layers of atom A and atom B. If, on the other hand, an alloy outside the eutectic concentration on the A-rich side cools, the A phase first solidifies from the melt when the liquidus line is crossed. The residual melt from which the metal A is removed increases in concentration in the metal B as cooling continues. At the eutectic temperature the residual melt has reached the eutectic composition and solidifies entirely eutectically. The structure shows the primary solidified grains of type A surrounded by the eutectoid from the residual melt.

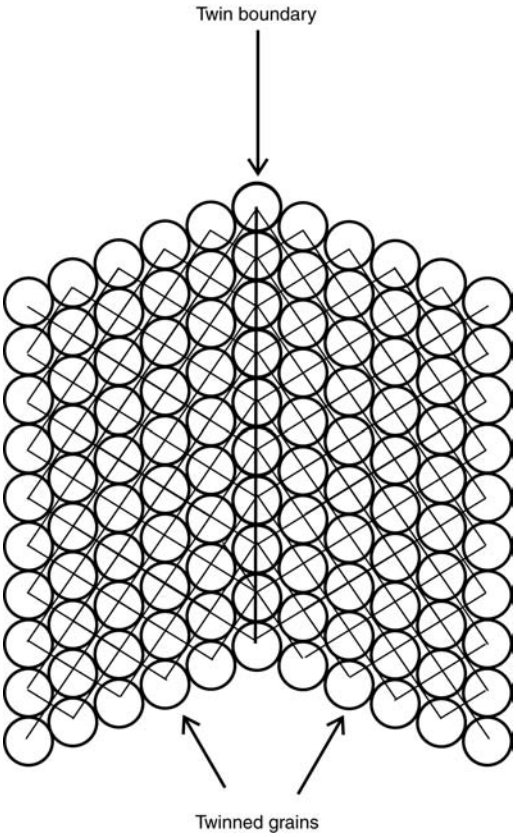

Fig. 4.8 Twinned grains and twin boundary

Eutectic System with Solid Solution (Type 3). This type of binary system occurs frequently when the atoms of type B dissolve in small concentrations by substitution of atoms A in the lattice (field **c**). As soon as a limiting concentration is reached, the internal stresses produced by the inclusion of the second atom type B become so high that the formation of a second phase becomes energetically more favorable (field **d**). As mentioned previously, the structure always tries to achieve the state of lowest energy.

The composition of the A-rich phase in field **d** corresponds to the concentration on the left boundary line to **c**, the composition of the B-rich phase to the concentration of the right boundary line $\mathbf{c_2}$ at the corresponding temperature. The more the displacement of the composition of the alloy from the left boundary line to the right, the greater is the number of grains of the B-rich phase and, correspondingly, the fewer the grains of the A-rich phase in this two-phase field.

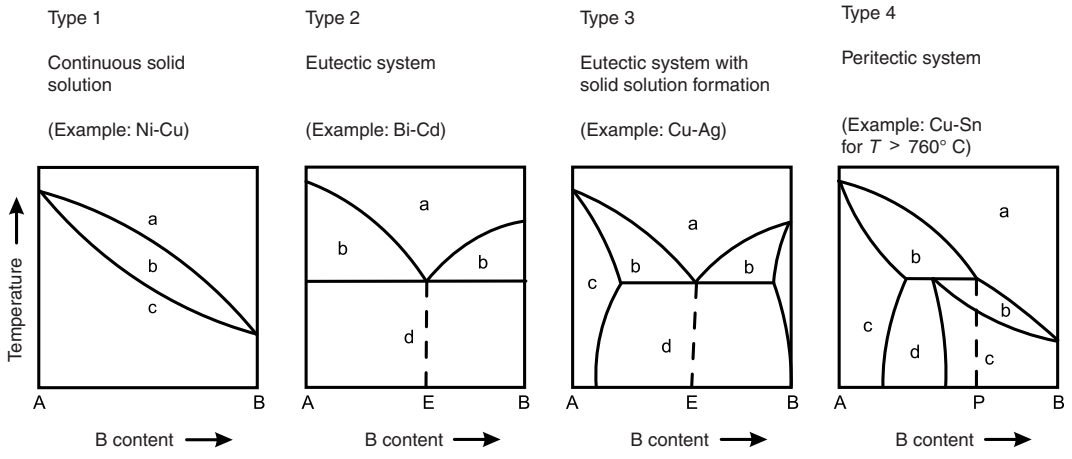

Fig. 4.9 Basic types of phase diagram. a, melt; b, melt + solid crystals; c, solid solution (homogeneous); d, two different crystals (heterogeneous); E, eutectic point; P, peritectic point [Wie 86]

In Fig. 4.10, the structures corresponding to different compositions are sketched under the equilibrium diagram of such a eutectic system with solid solution formation:

- *Concentration α:* Crystals of the phase $\mathbf{c_1}$ solidify here, surrounded by layers of the eutectoid E formed at the eutectic temperature **E**.
- *Concentration β (eutectic composition):* The structure consists only of the layers of the eutectoid of the phases $\mathbf{c_1}$ and $\mathbf{c_2}$.
- *Concentration γ:* Grains of phase $\mathbf{c_2}$ form initially and are surrounded by the eutectoid on further cooling.

As can be seen from the diagram, the solubility of the second atom type decreases in the solution regions (fields $\mathbf{c_1}$ and $\mathbf{c_2}$) with decreasing temperature, which must result in the precipitation of particles of the second phase even after solidification to maintain equilibrium (see also Fig. 4.13, section 4.2.3).

This type of eutectic system equilibrium diagram with solid-solution formation rarely represents the real state of an alloy because the mobility of atoms decreases so strongly with decreasing temperature that the elimination of the nonequilibrum state is possible only after a long holding period, if at all.

The structural state at high temperatures can, therefore, be "frozen" by quenching from this temperature so quickly that the atoms have no time to form the room temperature configuration.

Peritectic System (Type 4). A peritectic reaction occurs when the melt (field **a**) forms a

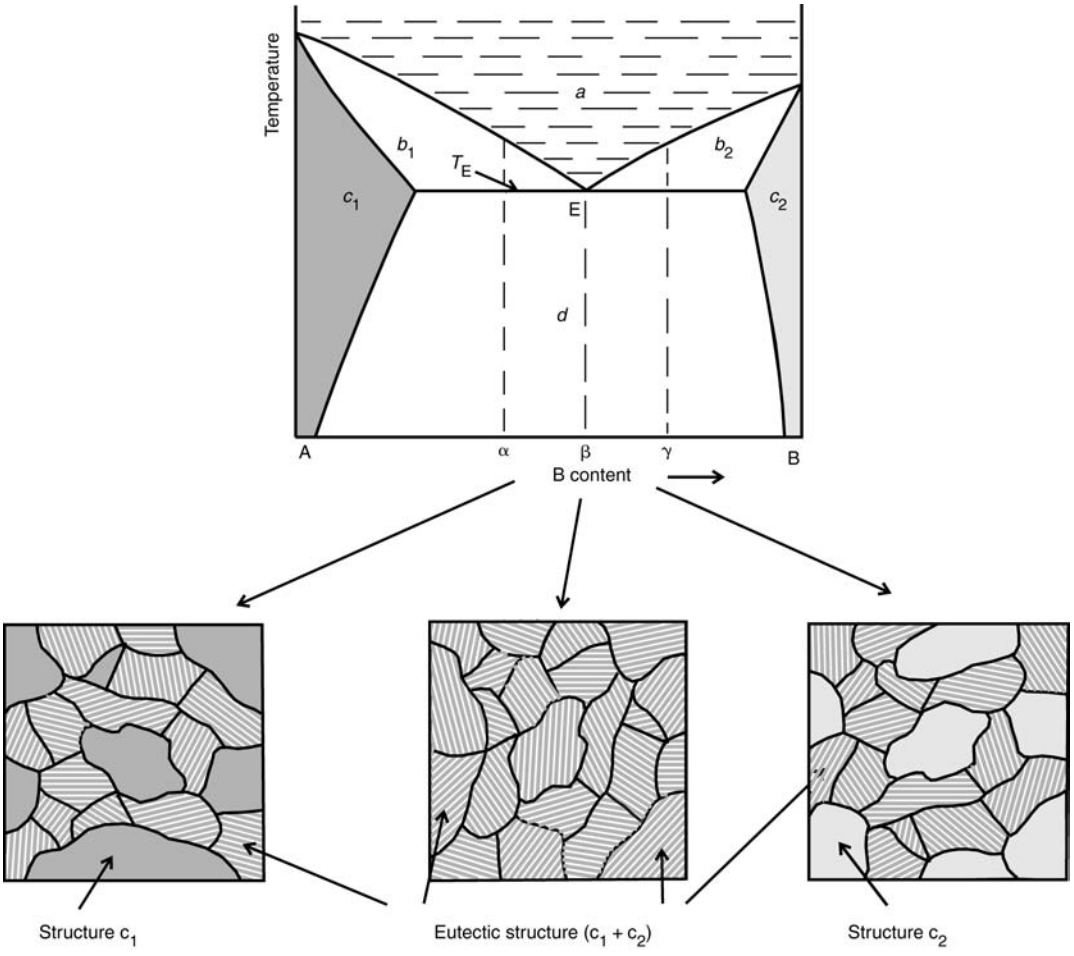

Fig. 4.10 Structure of a eutectic binary alloy [Ber 83]

new solid phase with a primary precipitated solid phase. The α grains are then surrounded by a shell of the β phase. In the peritectic concentration point a peritectoid structure forms that appears similar in micrographs to the eutectoid. The development of the equilibrium state on further cooling is very restricted and can be achieved only after long holding periods at the corresponding temperature.

4.2.2.2 Intermediate Phases

A solid solution consists, as previously mentioned, of the parent metal with interstitial or substitutional foreign atoms that are distributed randomly or only slightly ordered.

Intermediate phases occur when two or more types of atom are bonded together in an ordered, usually complex, structure. Intermediate phases have little or no deformability and are very brittle.

4.2.2.3 Multicomponent Systems

If an alloy consists of more than two types of atoms in a significant amount, it is not possible to depict it completely in a two-dimensional diagram. Two different depictions are used for three-part systems (ternary systems), as shown in Fig. 4.11:

- *Isothermal section:* The diagram consists of an equilateral triangle representing the three alloying partners. Each point within the triangle can be related to a specific concentration of the alloying elements A, B, C (in the example point P: 35%A, 40%B, 25%C). This type of diagram naturally shows the state at a specific temperature. In order to represent all phase states, therefore, it is necessary to have numerous similar isothermal sections that are often depicted within each other.
- *Quasi-binary section:* The proportion of two types of atoms are fixed (in the example shown A:B = 3:2) and the phase states studied for increasing amounts of atom type C. This diagram can be read in the same way as a binary system.

4.2.3 Diffusion, Precipitation, Nonequilibrium

The phase diagrams show that in many alloys both the composition of the individual phases of

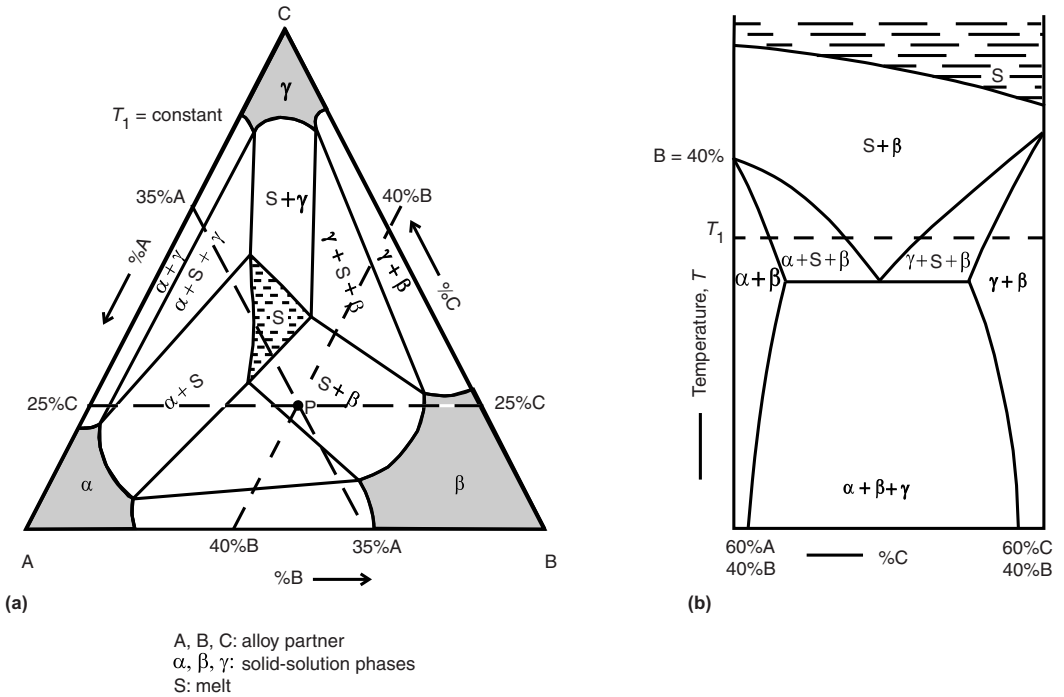

Fig. 4.11 Tertiary system representation. (a) Isothermal section (temperature T_1 = constant). (b) Quasi-binary section (alloy component B, e.g., 40%) [Ber 83]

a multiphase structure as well as the fraction of the phases in the structure change during heating or cooling. Atoms have to migrate from one phase to another to maintain the new equilibrium when the temperature changes. This *diffusion* occurs by transposition processes, which, in the case of *substitution solid solutions,* requires a large number of vacancies. The migrating foreign atom always moves to the nearest vacancy position (Fig. 4.12).

The atoms of a crystal lattice are stationary only at absolute zero. As the temperature increases they oscillate more strongly about their location and can then more easily leave their position. When changing places, the migrating atom has to pass through a state of higher energy, known as the activation energy Q, which is easier in the energy-rich state of a higher temperature: diffusion processes occur faster at higher temperatures than at lower.

In interstitial solid solutions the significantly smaller foreign atoms (e.g., carbon or nitrogen in iron) migrate from one interstitial lattice place to the next without the assistance of vacancies. The diffusion activation energy is lower than with substitution solid solutions.

From diffusion laws, which also apply to gases and liquids, the rate of diffusion is not only temperature dependent but is faster the greater the concentration difference between the two regions that will be equalized by the diffusion process.

A precipitation process occurs if a second phase is formed in the solid state of a homogeneous alloy during cooling when the solvus line is crossed. Nuclei first form and continue to grow until phase equilibrium is reached. Typical examples are the age-hardening aluminum alloys (Fig. 4.13).

If a single-phase region is rapidly cooled from the solid solution (e.g., the dashed line X2 in Fig. 4.13), the foreign atoms initially are retained in solution because they are practically immobile at low temperatures. Only when aging occurs at a temperature that enables significant diffusion to take place can nuclei of the second phase form and grow.

Because this process of solution treatment with quenching followed by aging is usually associated with an increase in strength, it is referred to as "age hardening."

Energy also has to be expended for the nucleation of precipitates, but this is usually lower at specific crystal defects or in a grain boundary than in the interior of the undistorted lattice. With a low precipitation pressure—e.g., slow

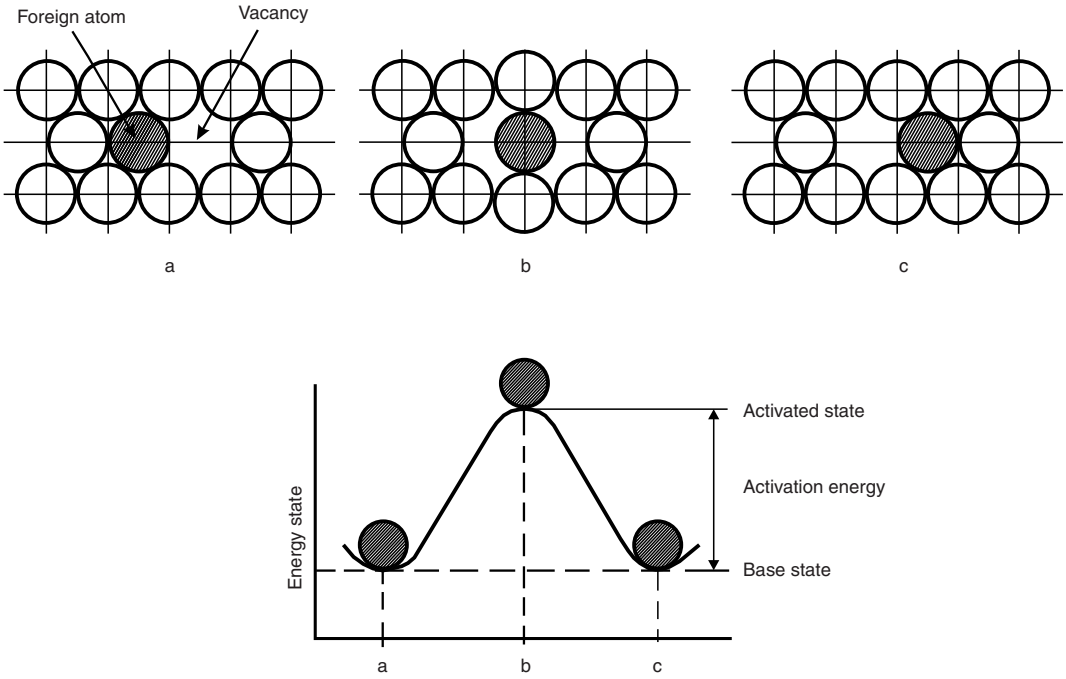

Fig. 4.12 Transposition through vacancies in diffusion [Ber 83]

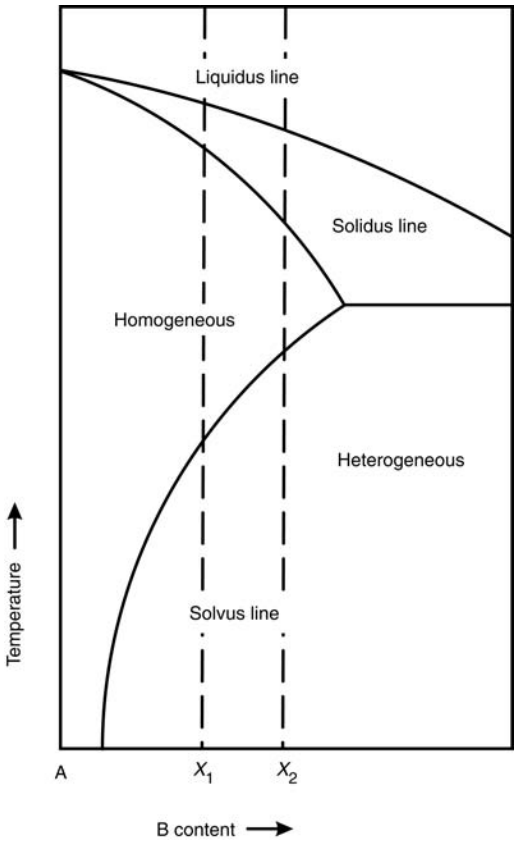

Fig. 4.13 Precipitation of a two-phase system [Wie 86]

cooling—the nuclei preferentially form at these defects and grain boundaries. The foreign atoms have sufficient mobility at higher temperatures to cover large distances to these nucleation points and grow there to precipitates.

However, after quenching and aging at lower temperatures, the precipitation pressure is high enough for large quantities of nuclei to form in the less-distorted zones of the crystal interiors, which can then be reached by atoms in the immediate neighborhood in spite of the lower mobility at these lower temperatures. The precipitates are then so fine that they cannot be detected under the microscope.

If a suitable material is hardened by solution treatment and aging, the rate of cooling from the solution region needed for freezing increases the further the equilibrium state at low temperatures is from the solvus line. Accordingly, with AlMgSi0.5 (line X1 in Fig. 4.13) cooling from the solution temperature at about 500 °C in stationary or slightly moving air is required, whereas, with AlMgSi1 (line X2), water quenching is needed to retain the solid-solution state.

This ideal picture can change if foreign precipitates or inclusions are present: manganese in AlMgSi0.5 acts as a nucleating agent so that rapid cooling has to be used in this case—similar to the higher-alloyed AlMgSi alloys—in order to retain the solution state [Sca 64].

The change with time (the kinetics) of transformation of the solid solution that is supersaturated by the quenching can be represented in the time-temperature transformation (TTT) diagram. The time is the abscissa and the temperature is the ordinate. The degree of transformation is quantified by curves showing suitable parameters (phase fraction in micrographs, hardness, age hardenability).

The *isothermal TTT diagram* shows the transformation progress of rapidly cooled samples at a constant temperature.

In many cases the *continuous TTT diagram* is more informative. This shows the precipitation behavior for different cooling rates from the solution temperature. The minimum cooling rate can be read from the diagram. Above this, no significant precipitation of the second phase occurs and the full hardening effect is obtained from the subsequent age hardening (Fig. 4.14). This is known as the *critical cooling rate.*

Figure 4.14(a) also shows the *freezing temperature* T_E, below which diffusion processes no longer occur. It occurs approximately at $0.3 \times T_S$ (T_S = the melting point) for diffusing substitution atoms. Figure 4.14(b) shows constant hardness curves in the continuous TTT diagrams.

If the cooling process from the solution temperature can be sufficiently accurately characterized by a specific parameter—e.g., the cooling time t_a to 200 °C—it is possible to use this parameter t_a as the abscissa and to plot against it a parameter that indicates the degree of transformation.

In steels and other materials that have different crystal lattices at different temperatures, the change in the transformation with time analogous to segregation can be depicted by isothermal or continuous TTT diagrams.

Grain growth follows the nucleation of the second phase as additional foreign atoms collect at the nucleus by diffusion. In the case of finely distributed precipitates, a coarsening process finally occurs after further thermal treatment. This is referred to as *coagulation* (Fig. 4.15).

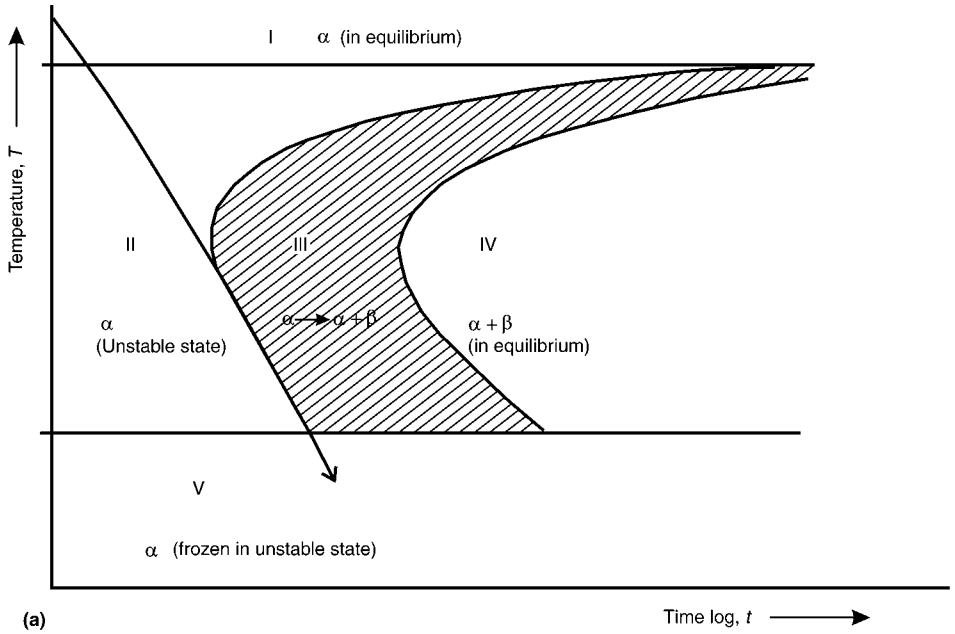

(a)

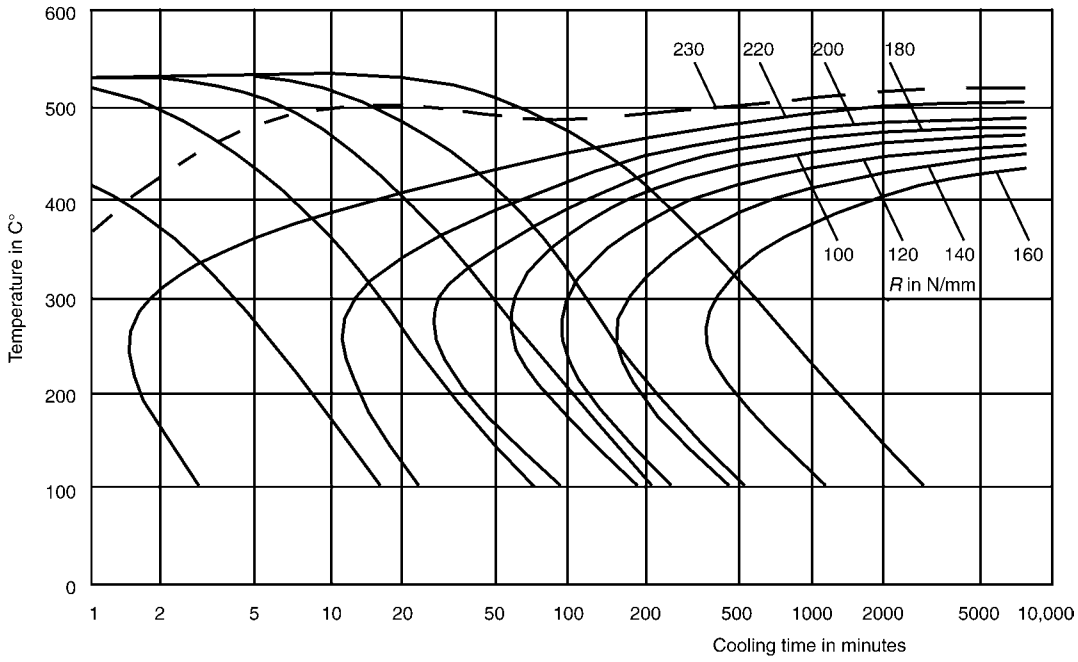

Curves of constant strength after age hardening for 10 h at 160° C

(b)

Fig. 4.14 Time-temperature transformation (TTE) diagram. (a) Principle [Ber 83]. (b) Continuous TTE diagram for AlMgSi0.5. I, solid-solution α (B dissolved in A) in equilibrium; II, solid-solution α (B still dissolved in A) in unstable state; III, second phase β precipitates to an increasing state from the solid-solution α; IV, equilibrium between phases α and β; V, frozen unstable state of the α phase

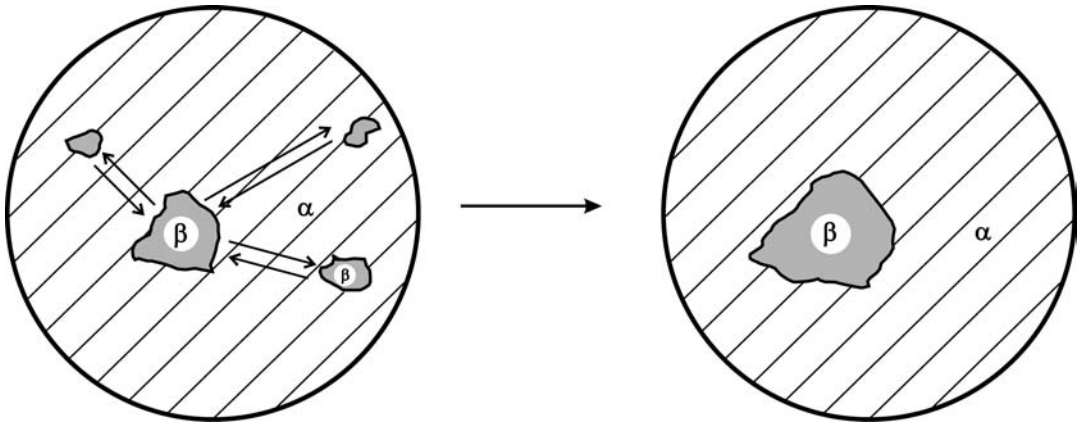

Fig. 4.15 Coagulation of precipitates [Ber 83]

During this coagulation process, atoms migrate by diffusion from smaller to larger precipitates. The small precipitates gradually disappear and only the large precipitates remain. Many small precipitates have a higher total of boundary surfaces between the phases than a few large ones. Because these boundary surfaces are energy rich coagulation reduces the energy levels.

The *martensitic transformation* is a special type of phase transformation in which the atoms adopt new positions without diffusion. This movement takes place extremely quickly after quenching and produces significant stresses between the old surrounding lattice and the new martensitic structure that is usually needle or plate shaped. The formation of martensite is mainly known in the behavior of steels, but it does occur in other materials, including α-β brasses.

4.2.4 Melting and Casting Processes

The structure in the billet is very important for the extrusion process. It has a strong influence on the extrusion load, the maximum possible extrusion temperature and speed, as well as the structure and properties of the extruded section.

The change from chill casting to continuous casting—now used for most metals—alone brought a significant quality improvement. This prevented the severe billet segregation associated with chill casting. The aim of numerous developments in continuous casting initially concentrated on the production of a fine structure with the minimum segregation that solidified from the bottom to the top rather than from the outside to the interior.

The formation of the solid phase by cooling of a melt takes place by nucleation and growth when the liquids line has been crossed in a similar way to the precipitation of a second phase in the solid state described previously. Nuclei first form where the melt is cooler, which is at the mold wall in the casting process. As the undercooling of the melt increases the nucleation work needed reduces so that the number of nuclei increases and a finer structure is produced.

Casting and Cast Structure, Homogenizing of Aluminum Alloys

Wolfgang Schneider*

4.3 Development of the Continuous Cast Structure

Figure 4.16 shows the development of the continuous cast structure in a simplified manner. The heat extraction through the water-cooled mold wall, also referred to as indirect

*Casting and Cast Structure, Homogenizing of Aluminum Alloys, Wolfgang Schneider

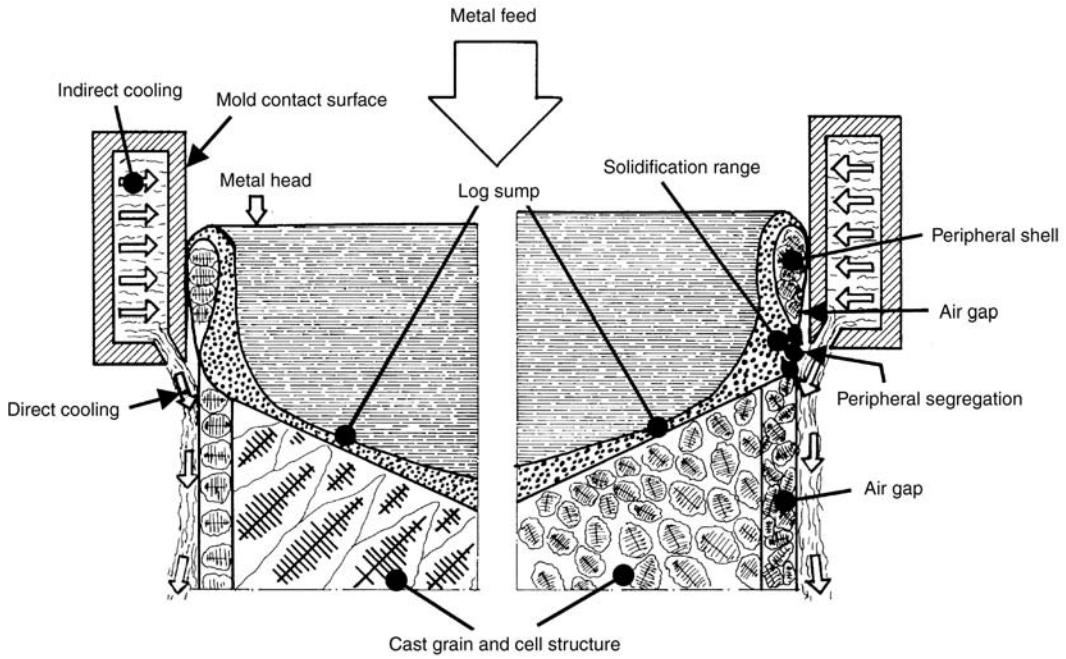

Fig. 4.16 Schematic of the formation of the continuous cast structure

cooling, causes the solidification of the peripheral region, i.e., to the formation of the so-called *peripheral shell*. This shrinks away from the mold wall and forms an air gap between the cast surface and the mold wall. This air gap hinders further heat extraction, resulting in reheating of the peripheral shell up to temperatures in the solidification range; i.e., partial or even complete melting of the peripheral shell is possible. *Peripheral segregation* can form during the dwell time in the air gap region as a result of the partial melting. The surface of the cast log is characterized by this and by the solidification of the peripheral shell itself, particularly in the meniscus region. The cast log finally emerges with the peripheral shell from the bottom of the mold and is hit by the cooling water flowing from the mold to complete solidification, referred to as direct cooling. This results in the formation of the cast grain and cell structure and, finally, the eutectic cast phases on the grain and cell boundaries as well as a characteristic profile of the solidification front across the cast log cross section, which is also known as the cast sump (Fig. 4.16).

The formation of the structure of the cast log is significantly influenced by the mold technology. The parameters of mold technology, which can be assumed to have a controlling influence, are the height of the effective mold wall and the metal head in the mold, the shape of the metal feed into the mold, and the direct cooling of the cast log. The direct cooling of the cast log is carried out by either spray water or mist cooling so that the mold has to have corresponding nozzles that will produce these methods of cooling. In aluminum continuous casting mist cooling predominates because aluminum has a high coefficient of thermal conductivity. In this case the application of a closed water mist below the mold is sufficient for rapid cooling of the cast log, and the use of additional specific cooling zones is not necessary.

The cooling of the cast log by direct cooling results in the development of stresses as a result of the temperature gradient from the interior of the cast log to the periphery; these can lead to the formation of hot or cold cracking, depending on the alloy system. The hot cracks usually form in the center of extrusion billets. Cold cracks, on the other hand, can occur over the full cross section. Alloys of the type AlMgSi are sensitive to hot cracking, whereas cold cracks are more likely to develop in AlCuMg and AlZnMgCu alloys.

The formation of the continuous cast structure is influenced by the casting parameters as well as the mould technology. The most important are

the casting speed, the volume of cooling water and the casting temperature or the temperature of the melt as it enters the mould. The casting speed, in particular, is extremely important. Accurate selection of the casting speed and the mould wall height for the alloy composition is very important, for example, to avoid hot and cold cracking.

4.3.1 Peripheral Shell and Peripheral Segregation

The peripheral region of the cast log in the form of a peripheral shell is of particular importance in the continuous casting process. Numerous casting defects can occur within this peripheral shell, and these should not finish up in the semifinished product during subsequent processing of the cast log. Consequently, the extent and the cast structure of the peripheral shell are important and have to be controlled by the casting technology to minimize the peripheral shell thickness and defects.

The extent of the peripheral zone is largely determined by the mold wall height and the alloy composition [Scn 85]. The larger the solidification interval of the alloy being cast and the higher the mold wall, the thicker is the peripheral shell. In comparison, the casting parameters exert only a small influence on the thickness of the peripheral shell.

The cast structure of the peripheral shell usually consists of a fine and a coarse cellular region. The fine cellular zone solidifies in direct contact with the mold wall, whereas the formation of the coarse cellular region can be attributed to the insulation effect of the formation of the air gap already described.

The mechanical properties of the solidifying peripheral zone tend toward low values. They are influenced by the cast structure formation and the temperature of the peripheral zone, in particular by the actual temperature in the solidification interval and subsequently by the fraction of solid phase during the dwell of the peripheral shell in the air gap region [Ohm 88, Ohm 89].

The casting defects that are usually found in the peripheral zone include peripheral segregation. Zones of peripheral segregation are characterized by an above-average high concentration of alloying elements and a sharp concentration jump to the adjacent structure [Mor 69]. There are also often alloying element impoverished zones below the peripheral segregation zones. This can be clearly seen in the example in Fig. 4.17.

The occurrence of peripheral segregations has to be considered in relationship to the solidification of the peripheral shell. Peripheral segregation forms during the dwell of the peripheral shell in the air gap region. Transport of residual melt regions enriched in the alloying elements towards the surface of the cast log takes place. The main transport mechanism is the metallostatic pressure of the melt before the peripheral shell. This is referred to as air gap segregation. A further mechanism for the formation of peripheral segregation is the residual melt enriched with alloying elements overflowing the meniscus curvature of the peripheral shell. This is referred to as meniscus segregation. Both these segregation methods described are shown schematically in Fig. 4.18 [Bux 77].

Various segregation formation shapes can be differentiated in peripheral segregation. Two examples are shown in Fig. 4.19. The nature of the segregation depends on the alloy type but also to some extent on the mold technology.

4.3.2 Cast Log Surface

The surface structure of the cast log is largely determined by the peripheral segregation.

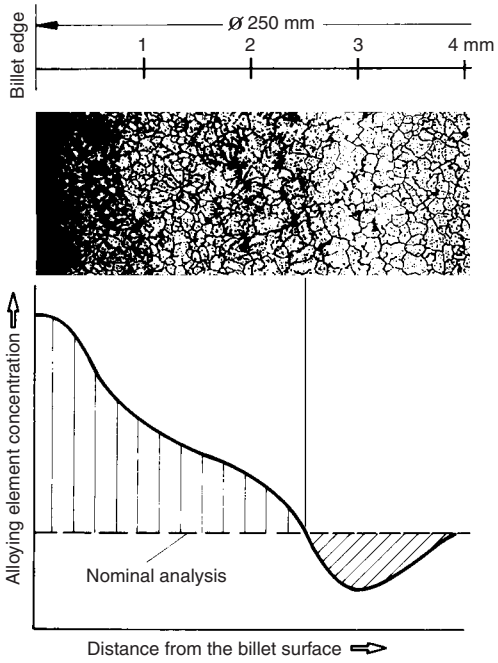

Fig. 4.17 Typical profile of the alloying element concentration in the peripheral segregation region

The different forms of peripheral segregation shown in Fig. 4.19 also result in correspondingly different cast log surfaces. Figure 4.20 shows examples of surfaces caused by different types of segregation.

Cold shuts are one surface feature that is not related to the peripheral segregation. An example is shown in Fig. 4.20. The formation of cold shuts can be attributed to the freezing of the melt meniscus in contact with the mold wall followed

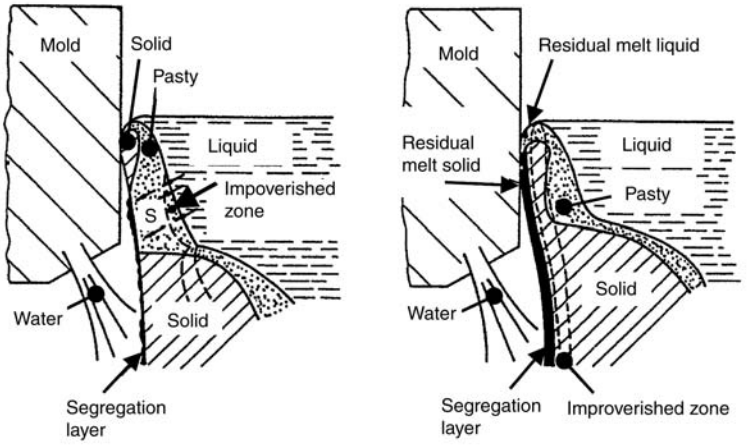

Fig. 4.18 Schematic of the peripheral segregation mechanism [Bux 77]

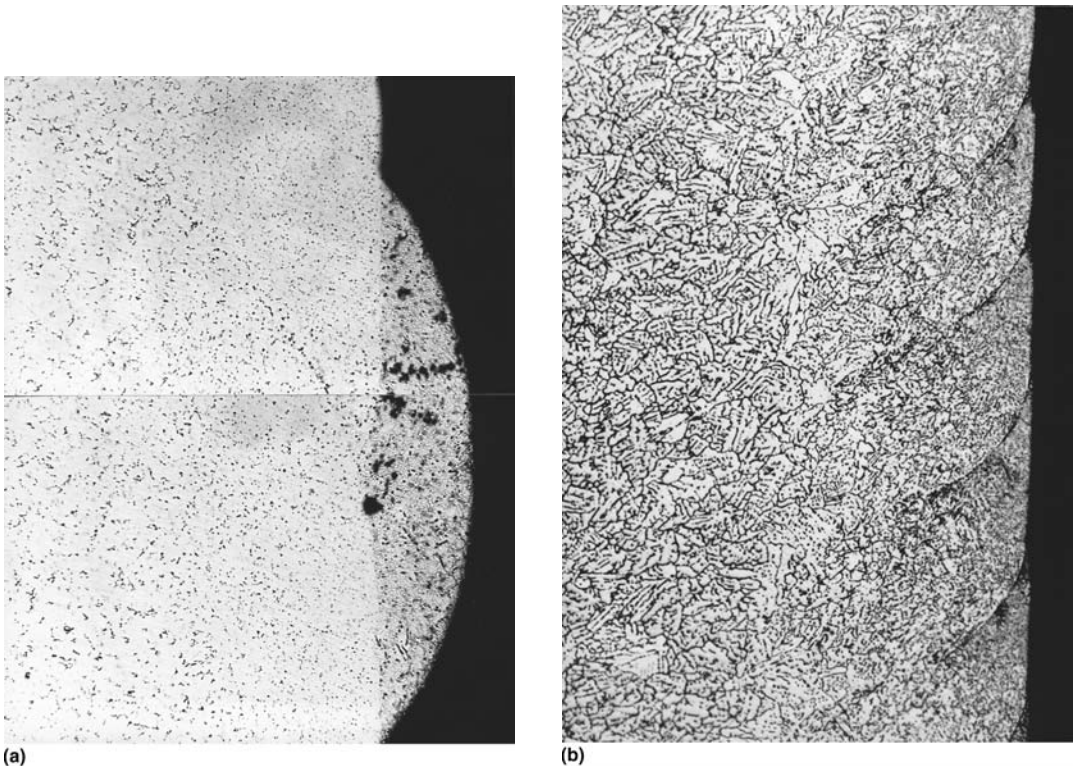

Fig. 4.19 Examples of types of peripheral segregation. (a) Sweating beads. (b) Lap segregations. Casting direction downward. The width is approximately 0.75 mm

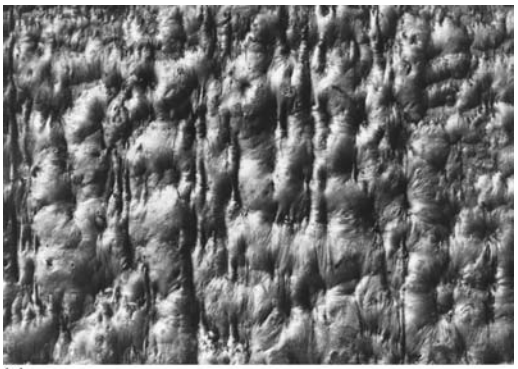
(a)

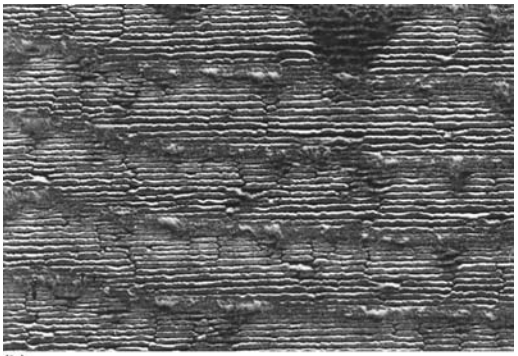
(b)


(c)

Fig. 4.20 Examples of types of cast log surfaces. (a) Surface with sweat beads. (b) Surface with segregation beads. (c) Surface with cold laps. Casting direction downward

by the melt flowing over the frozen peripheral shell. This surface defect is observed when the casting speed or the casting temperature is too low [Alt 65].

One type of surface that appears on the cast log and is best described as a surface defect is the surface tear that occurs in the form of cracks transverse to the casting direction. These tears are attributed to the frictional forces between the peripheral shell and the mold wall.

The types of surface appearance just described are always found on cast logs. The formation of the peripheral shell is indeed important for the formation of the surface. However, a reduction of the peripheral shell thickness should not always be associated with an improvement in the surface quality. In general, the aim is to produce a smooth surface, but in many cases this is merely a purely optical effect. In other words, a smooth surface is not definitely associated with a good peripheral structure quality. This means that more value should be placed on producing a good peripheral structure quality for the subsequent processing of the cast logs.

4.3.3 Cast Grain and Cell Structure, Intermetallic Phases

An important requirement of the structure of the cast log is a fine and uniform globulitic formation of the cast grain structure. The production of a fine cast grain reduces the hot and cold crack sensitivity, depending on the alloy system. In addition, the hot-working behavior of the cast logs and the surface appearance of the extruded product after surface treatment also are affected. The globulitic cast grain structure is achieved using a grain-refining treatment (Fig. 4.21).

Grain-refining alloy additions of the type AlTiB are used [Los 77]. These are added during the casting as a 9 mm thick wire into the melt in the casting launder. The grain-refining action of the AlTiB alloy is attributable to complex nu-

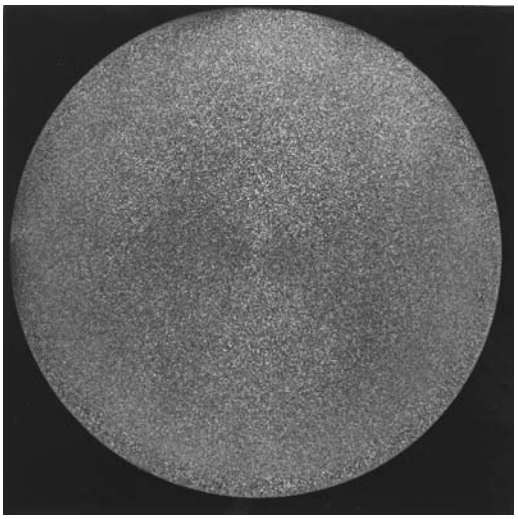

Fig. 4.21 Cast structure of a round billet (200 mm Ø) after grain-refining treatment

cleation processes in the melt [Rei 80]. The most important constituent of the alloys is insoluble TiB_2, which exists as fine particles and plays a direct role in the nucleation processes. Alloy additions of 0.2 to 1.5 kg/t aluminum are needed to obtain adequate grain refining depending on the alloy composition.

The majority of commercial wrought materials cast by the continuous casting process exhibit a cellular to dendritic type of solidification [Fle 74]. This, in turn, determines the cast grain structure. Figure 4.22 shows an example of a cellular/dendritic solidified cast structure.

The grain and cell boundaries of the cast grains are lined with intermetallic phases that occur as eutectics during the solidification. The grain and cell structure is also characterized by grain segregations, i.e., by nonuniform distribution of alloying elements in the structure. These grain segregations, which can be attributed to nonequilibrium solidification with an enrichment of the alloying elements from the grain center to the grain boundary, can result in the formation of eutectic phases on the grain and cell boundaries even in those alloy systems where they cannot occur according to the equilibrium diagram.

The cell structure of a cast log should be fine and uniform [Los 83]. This results in a corresponding fine and uniform distribution of the cast phases in the semifinished product after deformation of the structure. This requirement is particularly important for semifinished products that are given a surface treatment for decorative applications. Variations in the cell size can produce a banded surface.

The cast cell structure of aluminum cast logs exhibit a characteristic profile over the cross section as shown in Fig. 4.23 for different billet diameters [Bux 77a].

There is a coarse cellular structure in the peripheral region of the cast log. This is the region of the peripheral shell. Next to this is a region with a very fine cell structure. Toward the center of the cast log, the cell size increases, reaching the maximum in the center. It should also be recognized that the quantitative profile of the cell size strongly depends on the diameter of the cast log. This relationship can be explained using the diagram in Fig. 4.24 [Bux 77a].

The faster the corresponding volume element of metal is transformed from the liquid to the solid state, then the finer the cell structure. If it remains too long in the partially solidified state between the liquidus and the solidus state, coarse cells form because these have a high "local solidification time" [Kat 67].

Figure 4.24 shows that the distance between the liquidus and solidus line varies across the cross section of the cast log. The distance is the greatest in the center of the log where the highest local solidification time occurs and, accordingly, the maximum cell size forms. The cell

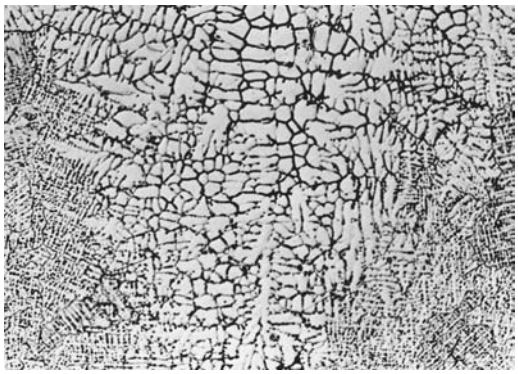

Fig. 4.22 Example of a cellular/dendritic solidified structure. The width is approximately 1.0 mm

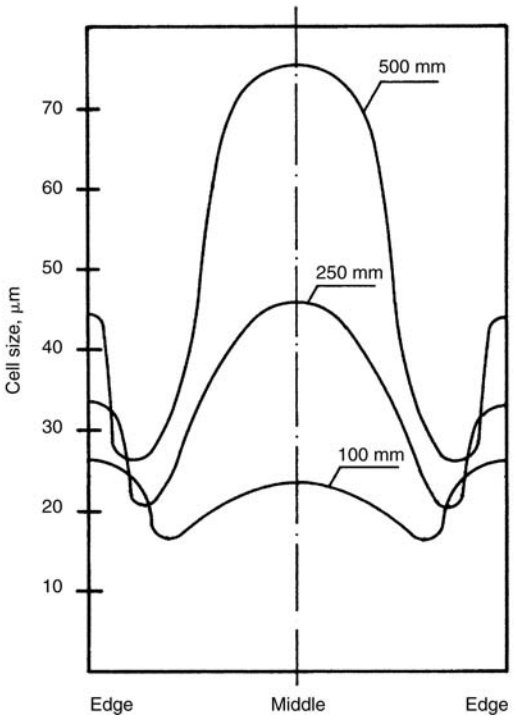

Fig. 4.23 Characteristic variation of the cast cell size over the billet cross section for different billet diameters [Bux 77a]

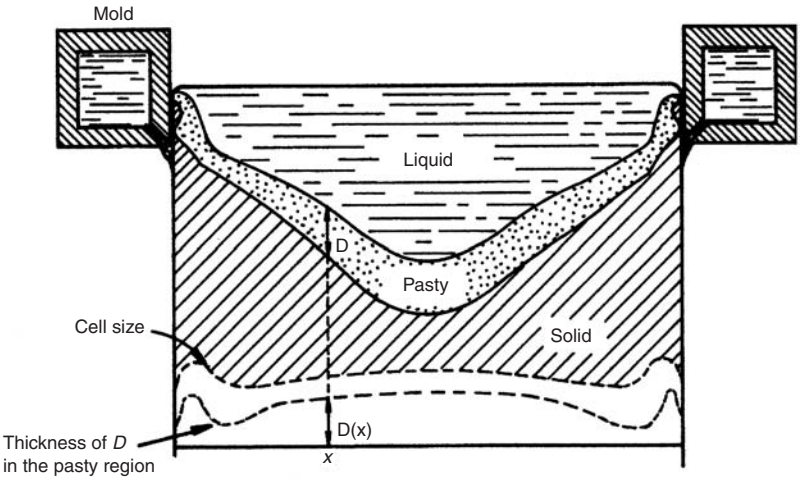

Fig. 4.24 Relationship between the distance between the liquidus and the solidus line and the cell size across the billet cross section [Bux 77a]

size minimum coincides with the contact point of the cast log direct cooling, because this is where low local solidification times exist because of the high solidification rates. Correspondingly, the distance between the liquidus and the solidus lines is smaller than in the log center where the cooling conditions in continuous casting result in the lowest solidification rates.

4.3.4 Homogenizing

The cast structure produced in continuous casting is neither the optimum for the subsequent processing nor for any surface treatment of the semifinished product. As mentioned previously, there is marked grain segregation in the continuous cast structure as well as a supersaturation of alloying elements. The volume fraction of eutectic precipitates is also increased. Therefore, a homogenization treatment consisting of high temperature annealing at temperatures between 450 and 600 °C is carried out to remove grain segregation and supersaturation.

The heating time at the homogenization temperature depends on the cell size and the rate of diffusion of the specific alloying constituents [Ake 90]. A fine cell structure is therefore advantageous because the concentration equalization within a cell can occur more quickly because the diffusion path is shorter.

The cooling of the logs from the homogenization temperature is also important in the homogenization process. Depending on the cooling rate, secondary precipitates form in various quantities and sizes from the α-solid solution as a result of decreasing solubility. The actual precipitation state influences the extrudability of the billets, as is well known from the AlMgSi alloys [Res 92]. If the cooling rate is too slow, coarse Mg_2Si phases can preferentially form on grain and cell boundaries in the temperature range above 400 °C. These coarse phases do not dissolve quickly enough in solution during heating to the extrusion temperature and can melt during extrusion if their melting point is exceeded during the extrusion process. The consequence is a reduction in the extrudability of the billet because surface defects can form on the section even at lower extrusion speeds. Mg_2Si phases that precipitate at temperatures below 400 °C are so fine they can redissolve even during short times at the extrusion temperature.

If the cooling rate from the homogenizing temperature is too high, fewer and finer secondary precipitates form. This is the same as increasing the content of dissolved silicon and magnesium in the α-solid solution. This raises the initial extrusion pressure and reduces the extrusion speed at a constant extrusion load. Figure 4.25 shows the structure of cast logs of AlMgSi0.5 alloy before and after homogenization. Figure 4.25(a) shows the cast state with needles of AlFeSi phases on the cell boundaries. Figure 4.25(b) shows the structure after a defined annealing and cooling. The precipitated secondary phases (Mg_2Si) can be seen in the α-solid solution.

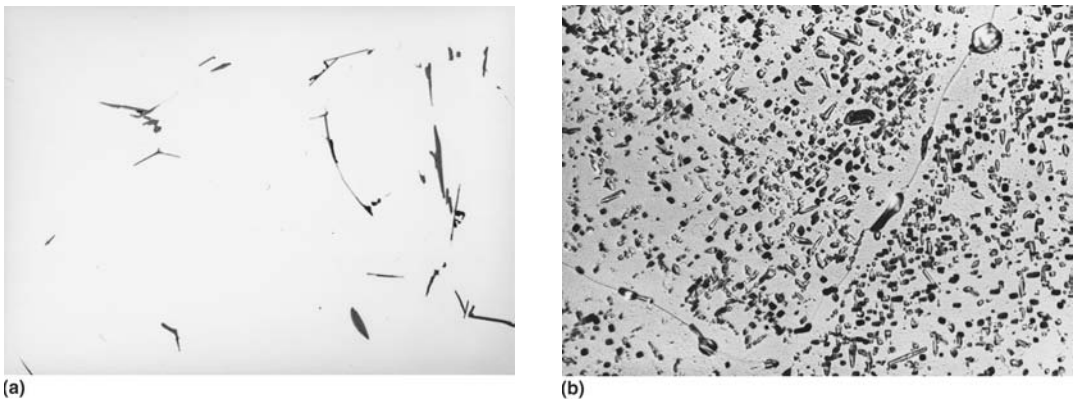

Fig. 4.25 Cast structure of AlMgSi0.5 round billet as-cast and after homogenization. (a) As-cast. (b) Homogenized

According to the previous discussion, therefore, the homogenization including cooling should be designed to give fast cooling to 400 °C to avoid the precipitation of coarse phases. This should be followed by slow cooling to reduce the content of dissolved alloying constituents [Ake 88].

Casting and Cast Structure of Copper Alloys

Adolf Frei*

Similar to aluminum alloys, the crystal growth is largely influenced by the temperature profile in the mold. The cast structure usually consists of a narrow very fine grain peripheral zone connected to a coarse globulitic or lamina structure extending to the core. Frequently, some form of single crystal is found in the center of copper billets.

Figure 4.26(a) shows the typical structure of a copper billet with a large columnar grain fraction, and Fig. 4.26(b) shows a brass billet with a globulitic core.

Direct cooling by water impingement is usually situated below a relatively short mold for the continuous casting generally used today for the casting of copper alloys (see Chapter 6). The indirect cooling through the mold wall is thus reduced and that from the water impingement directly below the casting mold increased (Fig. 4.27).

4.4 Segregation and Gas Porosity

The solidification in the mold is described using a copper-tin alloy with 8% tin as an example (Fig. 4.28). As soon as the liquidus line (at point 1 in Fig. 4.28 at temperature T_1) is crossed, nuclei of the solid phase with composition "a" grow. The residual melt is impoverished in copper atoms and enriched in tin atoms. In the equilibrium state the last residue of the residual melt at temperature T_2 has the composition "b." A fully solidified structure has zones with large variations in composition, i.e., *segregation,* particularly with slow cooling.

Specific crystallographic directions are characterized by high rates of growth leading to preferentially orientated columnar grains that suppress others and enable a cast structure to develop. Preferred growth direction is the reason for the formation of fir tree dendrites seen, for example, in cast iron alloys.

The numerous nuclei that form with rapid cooling and simultaneously grow produce a fine distribution of residual melt constituents in the solid state, which ensures that the segregation is less severe and more finely distributed.

In the solid state, there is both grain segregation, which is a variation in concentration in and around the individual grains of the solidified structure, and billet segregation, which pro-

*Casting and Cast Structure of Copper Alloys, Adolf Frei

Fig. 4.26 Cast structure of copper alloys. (a) Copper billet. (b) Brass billet

duces differences between the billet periphery and the core by the growth of a solidification front from the cold mold wall toward the interior of the billet. The core is richer in the second (in the example the tin containing) phase corresponding to the phase diagram.

If gases are dissolved in a melt (e.g., N_2 or H_2), their solubility in the solid state is usually significantly lower than in the melt; i.e., the gas precipitates in the form of pores during solidification. In chill mold casting where the melt slowly grows from the periphery toward the center, these gas pores collect like pearl strings in the center of the cast billet. In continuous casting they are found in the segregations of the residual melt, i.e., in the boundaries of the grains of the cast structure.

Segregations are, as mentioned previously, supersaturated zones outside the equilibrium state of the solidified structure. The segregations solidified from the residual melt possess a composition that produces crystallites of brittle phases, which hinder working. In addition, because these segregation zones, which solidified at lower temperatures, also melt at lower temperatures than the parent metal during heating, there is a risk of grain-boundary melting during hot working.

4.5 Cooling and Casting Defects

In spite of the indisputable advantages of continuous casting compared with the older processes, there still exists the possibility of defects. Billets with the optimum extrudability can be achieved only by careful control of the casting parameters.

The best billet quality would be obtained with a flat solidification front perpendicular to the casting direction. This would require the entire heat extraction to take place in the direction of the log axis. This can be achieved only with uneconomic casting speeds.

Practice is a long way removed from the ideal case because both indirect and direct cooling remove the heat from the cast log mainly perpendicular to the axis. The casting sump (region of liquid metal in the cast log) has a U- or V-shaped section.

As a rule of thumb, approximately one-third of the heat to be extracted is taken through the mold and the rest by direct cooling of the cast log.

If the direct cooling of the log is not exactly symmetrical, this results in distortion of the emerging log. This bending can quickly become so large that it makes direct extrusion very difficult and indirect extrusion with its longer billet lengths of up to 1.5 m impossible.

4.5.1 Cast Log Surface

The appearance of the surface of the cast log is largely determined by the processes in the mold. The melt transferred into the mold initially solidifies in direct contact with the mold

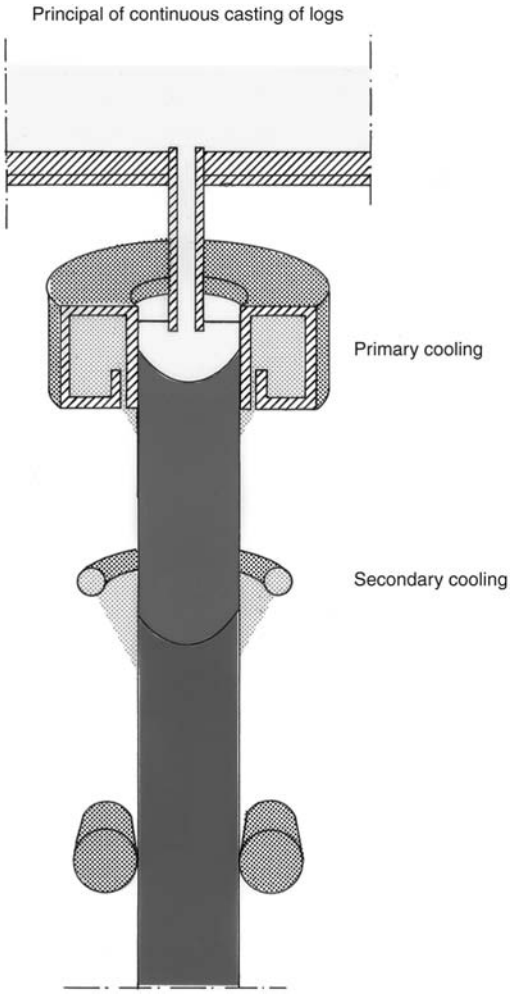

Fig. 4.27 Direct and indirect cooling in the continuous casting mold for copper alloys

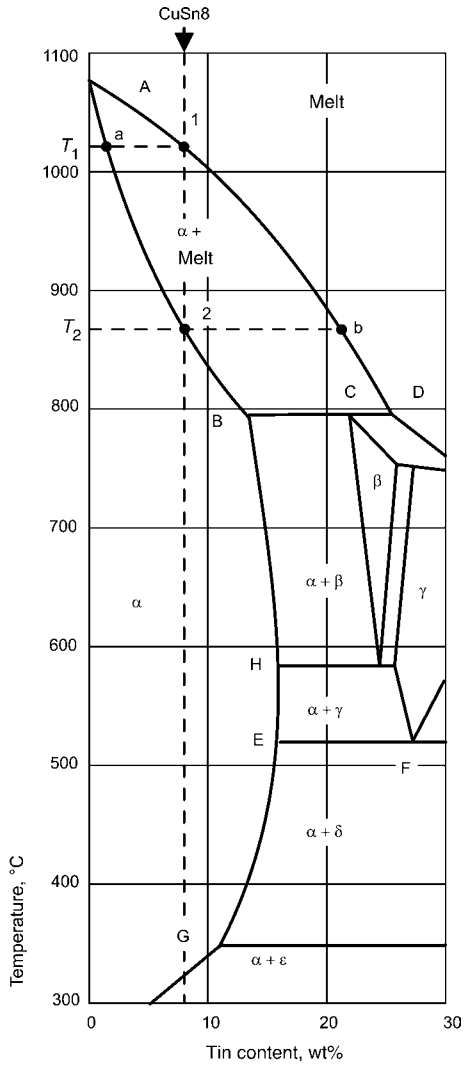

Fig. 4.28 Section of the copper-tin phase diagram [Ray 49]

wall to a thin shell, which pulls away from the mold wall after a few centimeters because of the solidification shrinkage. This produces a shrinkage gap that restricts further heat flow from the cast log. The interaction between the temperature of the melt, the method of metal feed, and the cooling conditions can lead to surface defects as the cast log passes further through the mold:

- Longitudinal cracks when the shell is pushed out by the metallostatic pressure of the melt in the sump and tears because of its low strength
- If the shell is pushed outward as an annular bead into the shrinkage gap, this can cause so much friction at the mold wall that transverse cracks occur ("cold shuts").
- In the extreme case, the log shell can locally melt from the still liquid core. The metal that emerges into the shrinkage gap solidifies as thin strings on the log surface.
- When casting high zinc containing brasses zinc can evaporate from the hot log shell and condense on the cold mold wall. From time to time it is stripped away by the cast log and forms "zinc flakes" on the surface of the log.

In the continuous casting of alloys with wide solidification intervals, for example, tin bronzes, "inverse segregation" can occur. The solidification shrinkage results in the tin-rich re-

sidual melt, which solidifies last, being enriched under the log surface and being partially pushed outward into the shrinkage gap. Good extrusion results can be obtained with these billets only by turning off the tin-rich peripheral layer and homogenization. CuSn8 is homogenized at approximately 700 °C for several hours to dissolve segregations of the brittle, tin-rich low-melting-point δ-phases.

The shrinkage gap is reduced in molds that are tapered toward the bottom, and the effects described can at least be suppressed to some degree. These molds are preferred for the casting of copper. The taper has to be carefully matched to the casting speed and the cooling conditions. The optimization is helped by computer programs.

If the metal head in the mold is not constant during the casting, inclusions of the covering agent and slag can occur under the surface of the cast log.

Excessive direct cooling can cause longitudinal cracks in the surface of the cast log, particularly with stress-sensitive alloys.

When casting is carried out with a salt cover, a thin salt film is initially formed on the surface of the cast log, and this has to be rinsed off in the region of direct cooling. If the composition of the covering salt is unsuitable or the direct cooling inadequate, the film can bond firmly to the cast log. It can then act as a lubricant between the billet and the container during extrusion and result in parts of the cast skin flowing into the extruded section, resulting in scrap due to laminations.

4.5.2 Interior of the Cast Log

Perfect results in extrusion can be achieved only from billets with smooth, clean surfaces and a dense structure over the complete cross section. Unsuitable casting conditions not only produce defects on the surface of the extruded section, but also within the section.

With a deep V-shaped casting sump there is the risk that gas bubbles can no longer escape but are retained in the region of the solidification point: porosity in the cast. In the region of the sump tip small zones of liquid metal can also be cut from the casting sump. When they solidify, the shrinkage results in small hollow spaces—solidification blowholes.

Solidification with a V-shaped sump results automatically in stresses in the cast log and, in the worst case, can result in longitudinal cracks in the core of the cast log. With very sensitive materials such as aluminum containing special brasses, these cracks can extend to the surface of the cast logs.

Unfortunately, it has to be assumed that such defects in the center of the billet along with the surface defects do not weld together in the extrusion press but produce material separation in the extruded section and thus scrap.

Exception: in the casting of copper billets with high casting speeds, shrinkage cracks can occur in the core along the grain boundaries with limited longitudinal extension. These "spiders" disappear during extrusion and do not have any detrimental effect on the section.

In the sections "Aluminum Alloys" and "Copper Alloys" in Chapter 6, detailed information on casting plants are given for the different materials.

Deformation, Recovery, Recrystallization

Martin Bauser*

As well as the references given at the start of section 4.2, the following works are recommended for a more detailed discussion of section 4.3: [See 85, Haa 84].

4.6 Deformation of Pure Metals at Room Temperature

4.6.1 Dislocations

In section 4.2.1, dislocations are described as linear defects in the crystal lattice as shown in Fig. 4.6. In real lattices, they form networks and are unevenly distributed (Fig. 4.29).

If an external force is applied, a crystal lattice initially deforms elastically following Hook's law. The elastic deformation is reversible—i.e.,

*Deformation, Recovery, Recrystallization, Martin Bauser

Fig. 4.29 Dislocation network in undeformed single crystal (transmission electron micrograph of aluminum $M = 10{,}000{:}1$) [Alt 94]

the lattice returns to the initial state when the load is removed.

As shown schematically in Fig. 4.30, a plastic nonreversible deformation results in atoms in specific planes and direction, the slip system, being displaced by one or more atomic spacings.

If all the atoms on a slip plane are simultaneously moved by one atomic spacing, a theoretical yield stress a hundred to a thousand times the real yield stress is required.

Dislocations make it possible for rows of atoms individually and successfully to spring to the next lattice place with only a low applied load. Figure 4.31 shows schematically the movement of an edge dislocation. As soon as a dislocation has passed through a slip plane, the entire crystal part on one side of the slip plane has been displaced by one atomic spacing relative to the other part.

The slip system in which the dislocation movements occur usually consists of planes with a dense atomic packing but with larger distances between each other. Their slip directions are particularly densely packed atomic rows.

Figure 4.32 shows the possible slip systems in cubic and hexagonal lattices. The planes and directions are identified by the Miller's indices used in crystallography (see the additional information in the appendix of this Chapter).

There are 12 favorable slip systems in the face-centered cubic (fcc) lattice and eight in the body-centered cubic (bcc) lattice. The close-packed hexagonal spherical packing on the other hand has only three. This gives an indication of the different degrees of workability of such different structures.

If two opposite dislocations meet during their migration on the same slip plane, they mutually cancel each other out. If they are located on two adjacent slip planes, they form a vacancy chain when they meet (Fig. 4.33).

Whereas edge dislocations are tied to their slip planes and can only slip on these, screw dislocations can also move in other slip planes. When they meet barriers they can move to a parallel slip plane by "cross slip" and overcome the barrier (Fig. 4.34).

This cross slip, however, is hindered by stacking faults. The slip of a dislocation by one atomic spacing takes place in two steps when this is energetically favorable. The dislocation is then split into two half dislocations (Fig. 4.35).

The larger the energy needed for the splitting, the "stacking fault energy" of a metal, the smaller is the separation. Therefore, the stacking fault hinders the cross slip because the separation has to be removed by contraction (Fig. 4.34b). The stacking fault energy is therefore a specific parameter for a metallic material—applicable not only to cross slip. It plays an important role in deformation and annealing processes at higher temperatures.

4.6.2 Single Crystals

Single crystals are particularly suitable for experimental investigations and for explaining the deformation processes in metals. If a single crystal is loaded in tension a dislocation moving shear stress is at a maximum at 45° to the specimen axis. Usually, therefore, only the slip system closest to this 45° direction is activated (simple slip in the principal slip system).

During the slip, further dislocations form at *sources* (Fig. 4.36). The dislocations therefore multiply but also hinder one another in real networks. During cold deformation the length of the dislocation lines can increase from originally 1 km/mm^3 in the undeformed state by a factor of 1,000 to 10,000 (dislocation density in the cast structure: 10^6 to 10^8, after a deformation; up to 10^{12}/cm^2) [Hou 93].

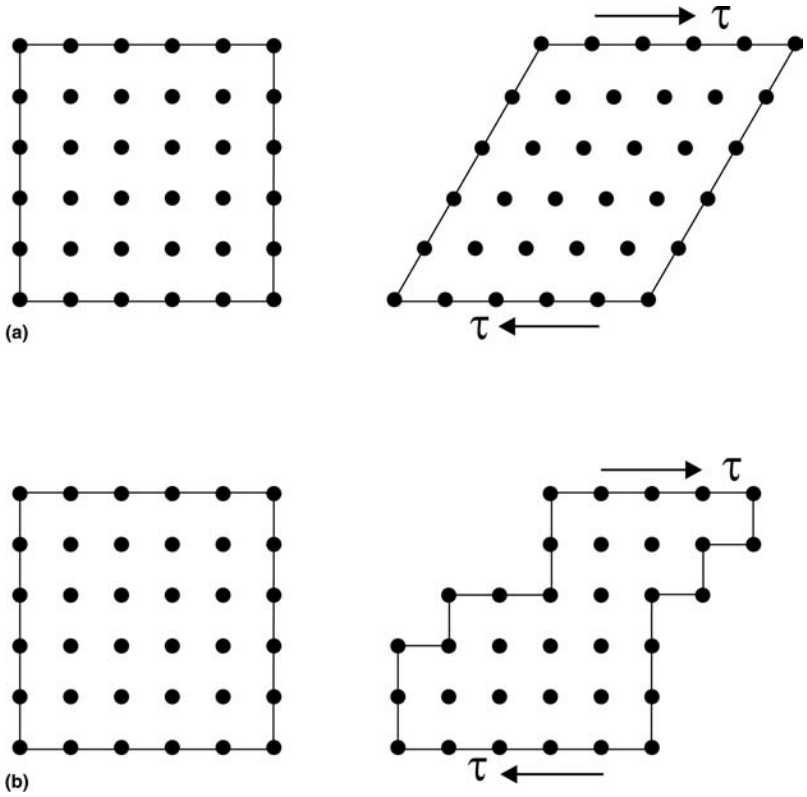

Fig. 4.30 Lattice structure during deformation. (a) Elastic deformation. (b) Plastic deformation

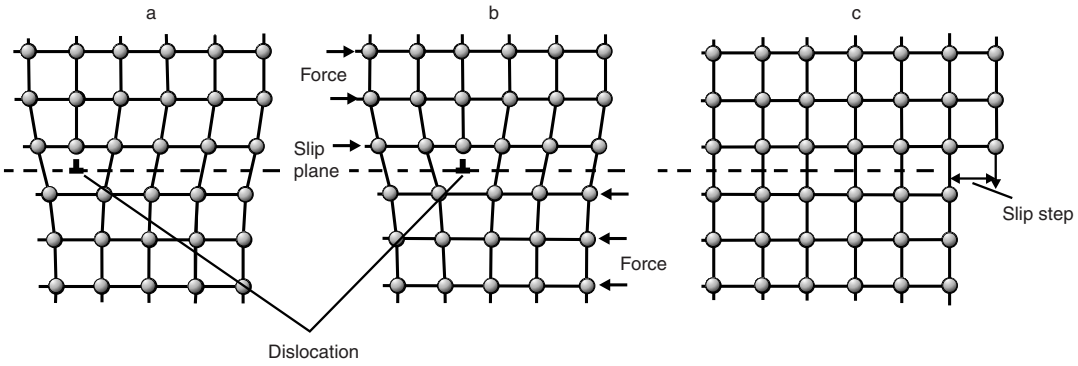

Fig. 4.31 Movement of an edge dislocation [Hou 93]

As slip continues the crystal rotates (Fig. 4.37). More and more slip systems then move into the 45° region and are activated (multiple slip).

In these additional slip systems, the dislocations that move have to cross the original ones and are trapped by them. These locations form defects at which following dislocations pile up. *Strengthening* means that dislocation movement is made more difficult by these and other barriers during the deformation.

4.6.3 Polycrystals

A polycrystal can be considered to consist of several single crystals of different orientations.

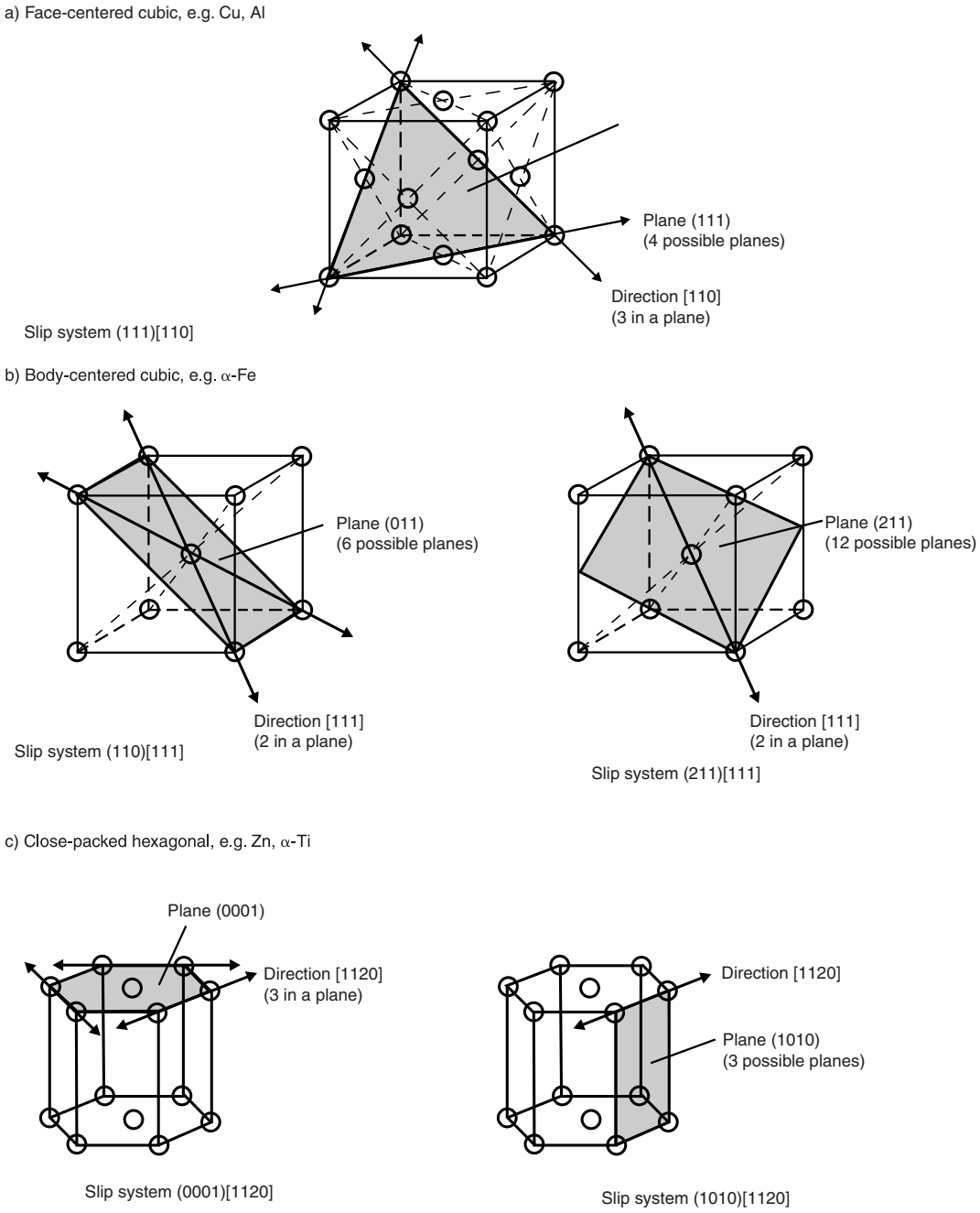

Fig. 4.32 Slip systems

Each single crystal will deform as discussed above in its principle slip system. The boundaries with the neighboring crystal, however, hinder this free movement.

In order to retain the cohesion between the individual deforming crystallites, at least five slip systems have to be active in each grain, which contributes to the strengthening.

Whereas in single crystals dislocation lines can disappear at the surface, they pile up at grain boundaries in polycrystals. If no grain boundary slip occurs, then the higher the number of grain

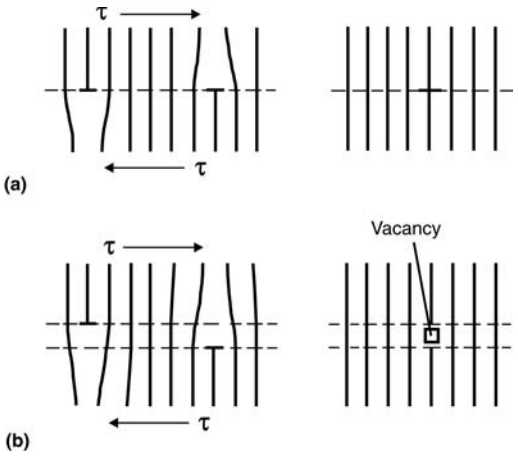

Fig. 4.33 Interaction of parallel dislocations of different signs. (a) Cancellation. (b) Formation of a vacancy

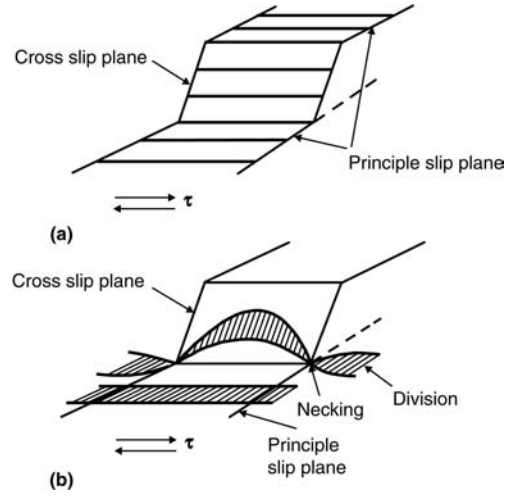

Fig. 4.34 Cross slip of a screw dislocation [Hou 93]. (a) Nondivided dislocation. (b) Split dislocation

boundaries, i.e., the finer the structure, the greater is the strengthening (Hall-Petch relationship).

Twins can form in individual grains during working to relieve the severe internal stresses formed during the deformation of polycrystals (Fig. 4.8).

With severe deformation of a polycrystal, the individual grains extend and align themselves by rotation so that crystal orientations accumulate in the deformed state in specific directions. This is referred to as a *deformation texture* described by Miller indices and pole figures (see Appendix, "Additional Information 2").

The deformation textures of different materials can vary. Also, different methods of deformation produce different textures. A rolling texture is not the same as a drawn texture.

Special *extrusion textures* occur when recrystallization during the extrusion process is completely or partially suppressed [Bag 81].

Textures also signify differences in the deformation behavior in different directions. In extruded bars that have not completely recrystallized, e.g., high-strength aluminum alloys, the strength in the extrusion direction is higher than in the transverse. This is referred to as the *extrusion effect*.

The stress-strain diagrams of polycrystalline materials frequently do not exhibit a marked yield point because individual favorably orientated grains start to flow earlier than others: the transition from the purely elastic to the plastic deformation state is thus smooth. The *0.2% deformation* $R_{p0.2}$ is therefore defined as the "yield stress" at which a permanent deformation of 0.2% occurs. The pronounced yield point, which is seen not only in steels, is described in the following section.

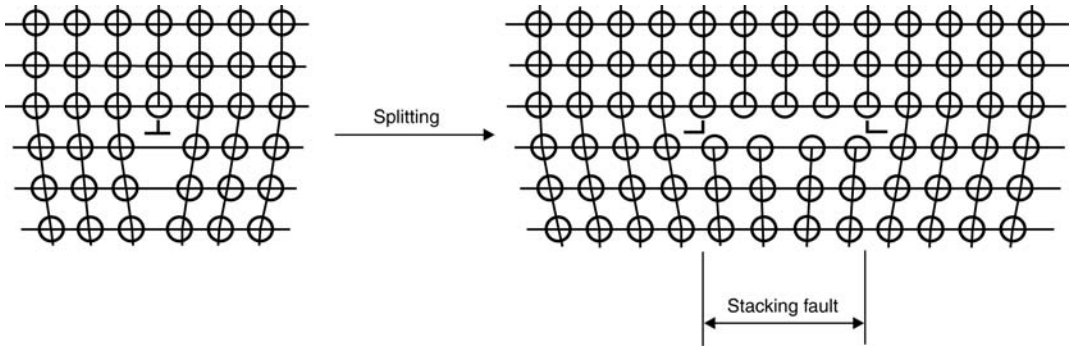

Fig. 4.35 Dislocation split by stacking defects

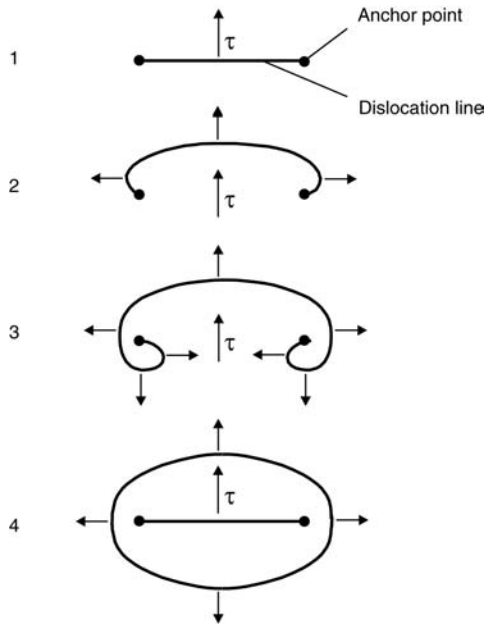

Fig. 4.36 Production of dislocations [Fra 50]

4.7 Deformation of Alloys at Room Temperature

The deformation, i.e., the movement of dislocations, can be hampered in many ways. Foreign atoms embedded in the solid solution or as secondary phases in the form of inclusions or precipitates and the self-producing obstructions from secondary slip systems described previously and neighboring grain boundaries.

In solid solution hardening, a substituted foreign atom in the base lattice causes a local distortion field the size of which increases the greater the difference between the atom radii. However, even with the base and foreign atoms having approximately the same size, interactions still take place because the foreign atoms influence the bonding forces between the atoms.

The movement of dislocations is therefore hindered by the foreign atoms. Because they have to cross their stress fields—analogous to slip friction between two solid bodies—this is referred to as *solid-solution friction,* which increases the deformation resistance.

The higher mechanical properties of the so-called naturally hard aluminum alloys (AlMg, AlSi) are attributable to solid-solution friction.

The action of foreign atoms in solid solutions is relatively weak compared with the particle hardening described subsequently. The yield stress and the increase in strength, however, do increase significantly with the fraction of dissolved atoms (Fig. 4.38).

Even at slightly increased temperatures, foreign atoms can accumulate at dislocations by diffusion particularly where they reduce the stress field of the dislocation. A dislocation is anchored by these foreign metal clouds (Cottrell clouds) and can only be released and set in movement by higher forces, which produces a *marked yield stress*.

Interstitial foreign atoms, e.g., carbon in iron, move more easily than substitutional atoms. Carbon clouds around dislocations are the cause of the well-known marked yield point of carbon steels.

Particle Hardening. The second phases in an alloy can take on many different shapes, sizes, and distribution, which determine the effect of the particles on the dislocation movement.

Dislocations can pass through so-called *soft particles*; they are "cut" (Fig. 4.39a).

One part of such a particle is displaced by one atomic spacing in the same way as the entire

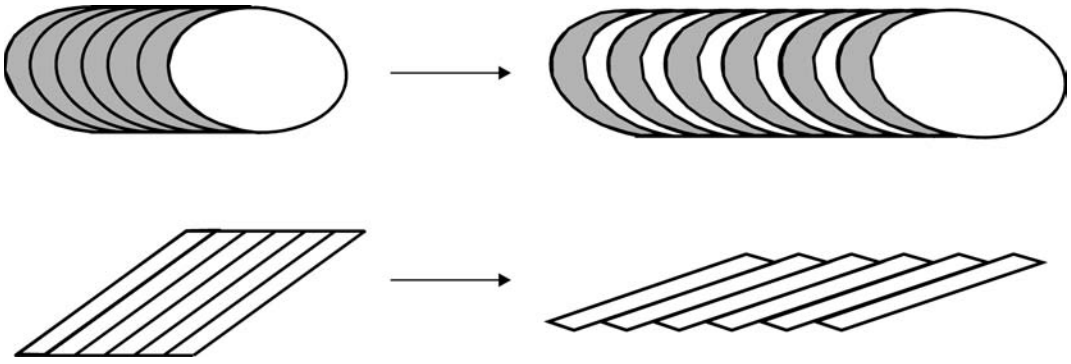

Fig. 4.37 Rotation of single crystal during deformation

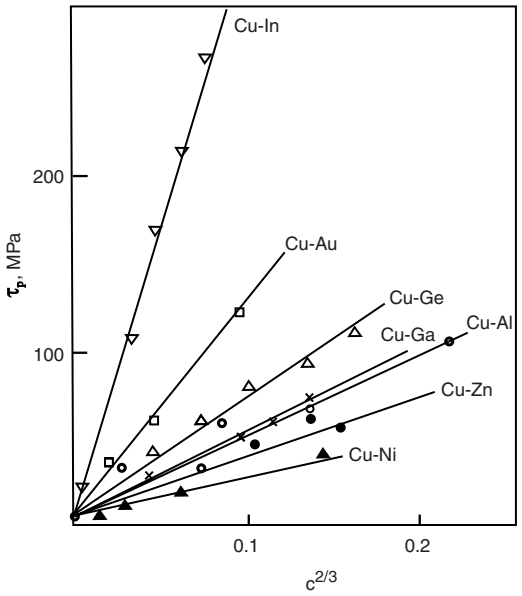

Fig. 4.38 Yield stress of single-phase copper alloys as a function of the content of foreign atoms

lattice along a slip plane. This requires the application of a higher force compared with dislocation movement through a single-phase lattice. The dislocation in the cutting process is therefore stretched like a rubber band and then relaxed after cutting. The greater the number of particles, the stronger is the effect. Only small coherent or approximately coherent precipitates in which the matrix and particle lattices have similar structures and orientations are cut.

An incoherent particle—which includes most precipitates—forms a barrier that cannot be overcome by cutting. The dislocation manages to go around these "hard particles" (Orowan process, Fig. 4.39b); as soon as a dislocation line has been stretched to such an extent that the positive and negative parts move close together, they meet and mutually cancel each other out. A dislocation ring remains around the particle, and this repels the following dislocation. This is because dislocations of the same sign mutually repel each other and those of the opposite sign attract. Therefore, with increasing deformation

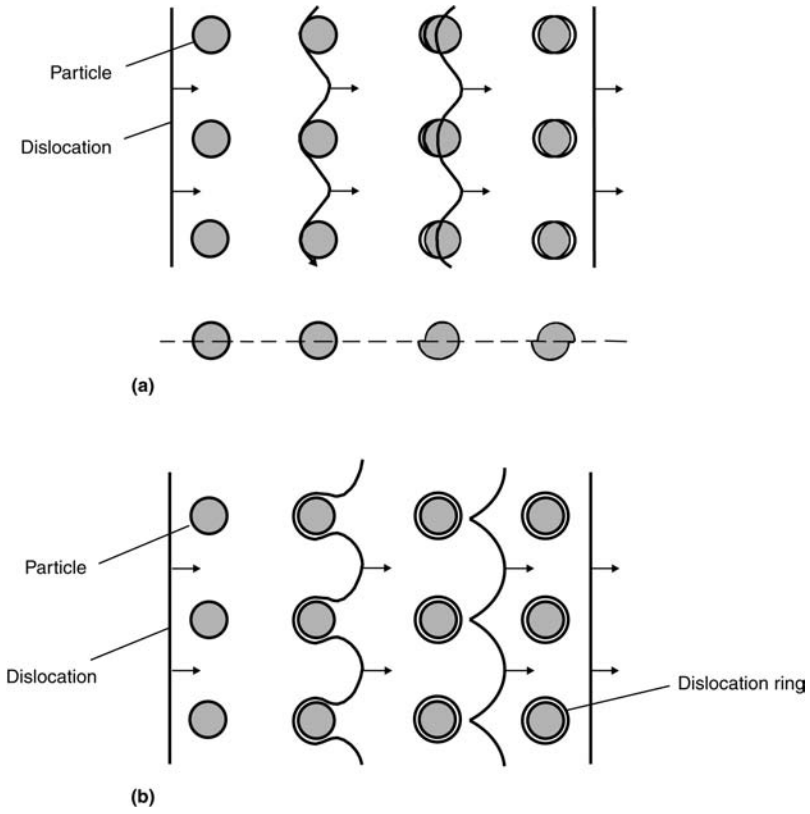

Fig. 4.39 Interaction of dislocations and particles [Ber 83]. (a) Intersection of "soft" particles. (b) Bypassing of "hard particles"

and thus an increasing number of dislocation rings around the particles, an additional type of hardening takes place. This is referred to as *precipitation hardening* or *dispersion hardening*.

The size of the particle does not influence this type of hardening, but their number and distribution do. The higher the number of particles that cannot be cut, the greater is the resistance to dislocation and thus the strengthening.

In hot age hardening, e.g., of a heat treatable AlMgSi alloy, as shown in Fig. 4.40, small and coherent particles of the second phase first form so that they can be cut. As the aging time increases, the particles become incoherent and increase in size and can no longer be cut, which increases the strength. If coagulation occurs after longer heat treatment, as described in Fig. 4.15, large particles grow at the expense of smaller ones and the number of particles decrease. The strength and hardening then reduce. This is known as *overaging.*

AlCu alloys, for example, exhibit an increase in strength even with cold age hardening (aging after solution heat treatment at room temperature) by the formation of coherent groups of copper atoms in so-called Guinier-Preston (GP) zones. They redissolve, however, during subsequent hot age hardening before the hot-age-hardening phases form.

Targeted alloy development and heat treatment enabled extremely high-strength materials with specific deformation properties to be developed. In addition to solid-solution hardening and precipitation hardening, they involve the inclusion of foreign particles as dispersions, e.g., by powder metallurgical processes.

4.8 Higher Temperatures with Pure Metals

As the temperature increases, the thermal movement of the atoms in the crystal increases, which increases the ease of transposition processes by, for example, diffusion.

The *climb of edge dislocations* also takes place (Fig. 4.41). In this process, complete atomic rows are removed or added; the dislocations are thus moved into another parallel slip plane. The climbing, therefore, naturally is only activated when it results in a reduction in the internal stresses and thus to a lowering of the internal energy of the crystal. This can take place by positive and negative dislocations mutually canceling each other and thus reducing the dislocation accumulation.

4.8.1 Annealing of Pure Metals

The first step in stress reduction by annealing of a deformation hardened structure is *recovery*. The crystallites retain their shape and orientation.

Dislocation freed from their forced location by climb and cross slip mutually cancel each

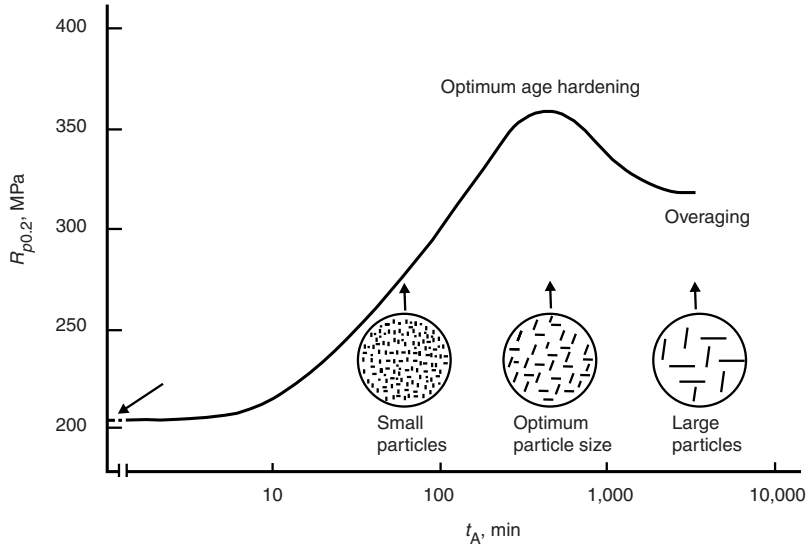

Fig. 4.40 Yield stress of age-hardening aluminum alloy as a function of the aging time [Blu 93]

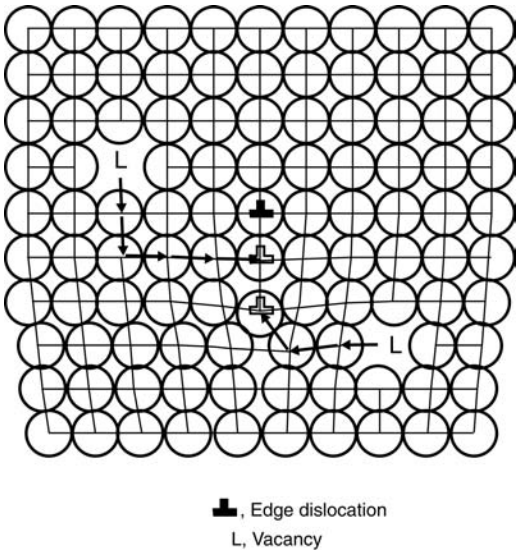

Fig. 4.41 Climb of an edge dislocation [Sch 81]

other out, as described previously (positive and negative dislocations), or move and accumulate in low stress subgrain boundaries, which are composed of a chain of dislocations of the same sign.

After recovery heat treatment an entire network of these subgrain boundaries is found—this is referred to as *polygonization* of the crystallite (Fig. 4.42). The orientation of the resulting subgrains differ only slightly from each other. The interior of the subgrains is practically dislocation free.

During recovery the internal stresses are not completely eliminated because there is still a high volume of dislocations in the subgrain boundaries.

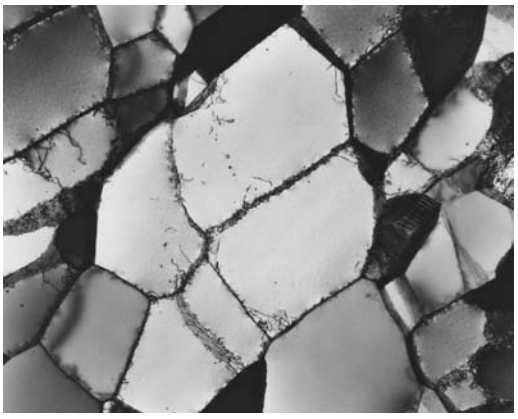

Fig. 4.42 Subgrain formation in Al99.99 (hot strip). The width is approminately 8.4 µm [Grz 93]

Stacking faults hinder not only cross slip but also the climb of dislocations and thus the recovery of metals. Low stacking fault energy metals, i.e., large stacking faults such as copper, nickel, and austenitic steels, therefore exhibit a low tendency to recovery. On the other hand, aluminum and alpha iron with high stacking fault energies and thus small stacking faults easily form subgrains during suitable heat treatment and therefore recover.

If a deformed structure is heat treated at a high temperature, recrystallization takes place. New grains that are largely free of dislocations and thus subgrains are formed during this process. The structure is free of internal stresses and therefore annealed. The deformation behavior largely corresponds with the undeformed cast structure.

Figure 4.43 shows schematically how a healed recrystallized grain grows into a dislocation rich work-hardened lattice.

Recrystallization usually occurs during a suitable heat treatment of a deformed metal without preceding recovery by nucleation after an incubation time.

The nucleation is followed by the growth of a grain that is sustained as primary recrystallization until all the deformed crystals have disappeared. In the subsequent secondary recrystallization (large grain formation), large grains grow at the expense of small recrystallized grains. The internal energy is reduced further by the shortening of the total grain-boundary surface. This is usually undesirable because of the associated irregular grain size [Alt 94].

Figure 4.44 shows the typical recrystallization process with time. As can be seen, after the incubation time there is initially a flat profile during the nucleation and a steep increase during the primary recrystallization. The gradient of the curve decreases with the subsequent secondary recrystallization.

The recrystallization nuclei form mainly at regions of high dislocation density. These can occur at grain boundaries between relatively undeformed original grains. Precipitates can also act as recrystallization nuclei [Wei 94, McQ 75].

During primary recrystallization, these nuclei grow by thermally activated migration of the grain boundaries into the work-hardened structure and consume it. The number of newly formed largely defect-free grains correspond to the number of nuclei capable of development.

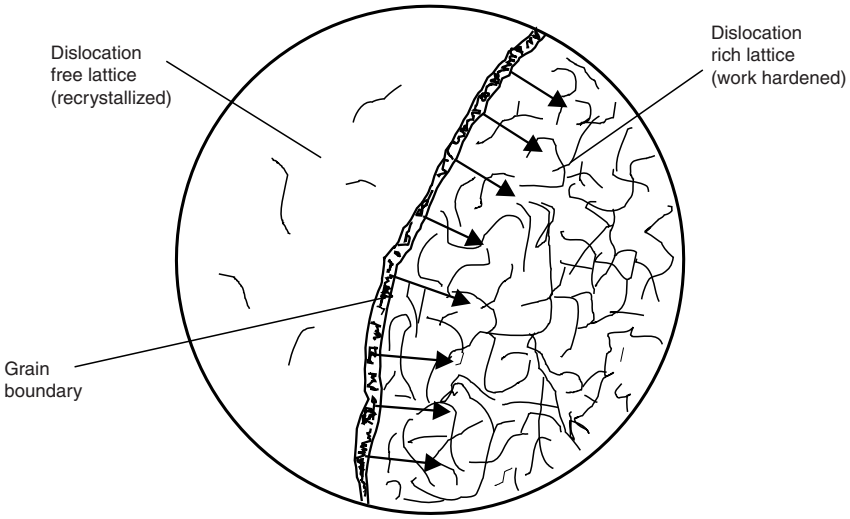

Fig. 4.43 Growth of recrystallized grain

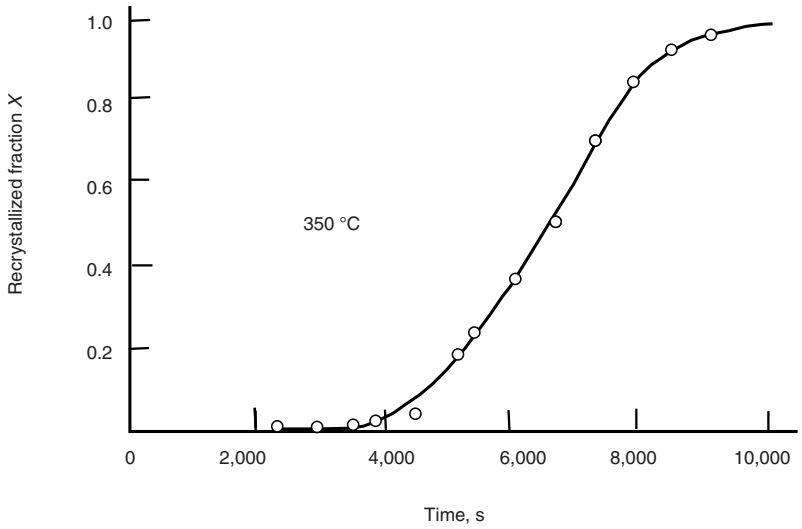

Fig. 4.44 Variation with time of recrystallization (Al99.5 after 5.1% tensile deformation) [And 48]

The rate of migration of the new grain boundaries and thus the rate of recrystallization is the greater the larger the preceding deformation and thus the larger the energy stored in the deformed structure. Naturally, a higher temperature promotes the grain-boundary migration and increases the rate of recrystallization.

Recovery preceding recrystallization, e.g., at low heat treatment temperatures, that has reduced the deformation energy stored in lattice by sub grain formation hinders recrystallization. In metals with high stacking fault energies like aluminum, it can even be completely suppressed by recovery—at low heat treatment temperatures and small deformation.

The recrystallization temperature above which recrystallization can be expected is usually related to the melting point of a metal:

$$T_{recr} \cong 0.6 \cdot T_s[°K]$$

This recrystallization temperature should not be considered unequivocal.

With deformed brass CuZn37, for example, the softening from recrystallization after high deformation starts at 400 °C but only at 500 °C after low deformation. With pure aluminum after 98% deformation recrystallization commences at 300 °C and at 400 °C after 20% deformation [Alt 94].It is, therefore, more correct to refer to a *recrystallization interval* instead of a recrystallization temperature.

If a structure textured by deformation is given a recrystallization heat treatment, the new structure can also exhibit preferred orientation, a so-called *recrystallization texture*. One cause can be that grains of a specific orientation in the deformed structure are less deformed than others. Nuclei of preferred orientation then grow from them into the severely deformed grains.

Deformation and recrystallization textures are closely related to each other but usually differ. Recrystallization textures are also characteristic for the deformation process and for the relevant lattice structure (e.g., AlCuMg [Moc 75]).

4.8.2 Deformation of Pure Metals at High Temperatures

If a pure metal is deformed at a higher temperature, both the yield stress and the work hardening are reduced (Fig. 4.45).

As the temperature increases, the dislocations can start to migrate through their slip systems at lower shear stresses due to thermal activation, which reduces the yield stress. The work hardening—that is, the gradient of the strength curve—is reduced because the vacancy diffusion at higher temperatures is also eased and hence piled up dislocations can move to energetically more favorable positions during the deformation by cross slip and climb. This means that recovery processes can proceed with the formation of a substructure during the work-hardening—and not only after heat treatment following cold working [Mug 84]. This is called *dynamic recovery*.

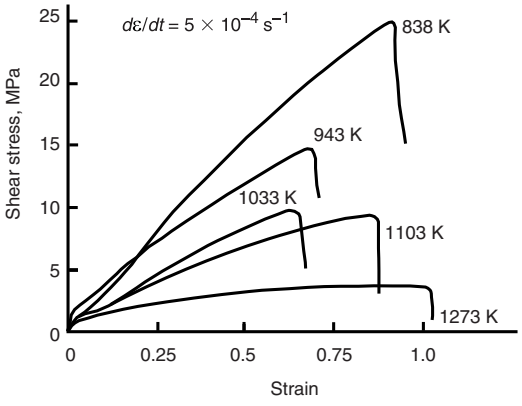

Fig. 4.45 Work-hardening curves of copper single crystals as a function of temperature [Got 84]

If deformation is carried out quickly enough at a high temperature, the work hardening can be so high despite the start of recovery that recrystallization can take place even during the deformation—this process is frequently observed in the extrusion of specific materials. It is referred to as *dynamic recrystallization* [Got 84].

The stacking fault energy plays an important role in the boundary between recovery and recrystallization during hot working.

High stacking fault energies and thus fewer divided dislocations occur in bcc alloys (e.g., α-iron, β-brass) as well as in certain fcc alloys (e.g., aluminum). In these cases, the cross slip and climb needed for subgrain formation and recovery is easier—recovery is more likely to take place in these cases in preference to recrystallization during hot working. Low stacking fault energies associated with large divided dislocations are found with a few other fcc lattices (e.g., copper and copper alloys). In these cases, recovery is more difficult, and dynamic recrystallization processes simplified during hot working.

The strength reducing recovery and recrystallization processes during hot working can take place so quickly after reaching a specific work hardening that there is equilibrium between softening and work hardening and the hardening curve remains horizontal (static case). Naturally, the dynamic recovery processes also result in a delay in the fracture-initiating mechanisms (see section 4.11), and the elongation to failure in tensile tests increases with increasing temperature.

If the events occurring within the structure in hot working are studied, it is clear that these processes depend not only on the temperature but also on the rate of deformation.

The slower the deformation rate, the greater is the time for the recovery and recrystallization processes to counteract the work hardening from the multiplication and piling up of dislocations. The work-hardening curve is, therefore, flatter and its horizontal leg lower the slower the deformation rate. At a fast rate of deformation, a relatively high flow stress has to be expected. This explains the high dependence of the deformation resistance on the rate of deformation in

hot working compared with cold working (Fig. 4.46).

The dependence of the flow stress on the temperature and the deformation rate in hot working is discussed in section 3 in the Appendix, "Additional Information 3," in this chapter.

The stress-strain curves obtained from torsion tests cover a much larger strain to failure than tensile tests because of the largely tensile-stress-free deformation.

They are therefore more suitable for assessing the behavior of metals in practical hot working, in particular extrusion, which also does not involve any tensile stress (Fig. 4.47) [Fie 57, Ake 66].

The hot stress-strain curves obtained from torsion tests exhibit after the initial increase, in which the number of dislocations and the internal stresses increase significantly, a large stationary region with hardly any additional work hardening. The work-hardening and recovery processes are in balance. The stress-strain curve starts to fall only when structural defects result in fracture.

Usually, no recrystallization occurs during the hot deformation of aluminum and many of its alloys. Subgrains are more likely to develop by recovery and their shape and size hardly change during the stationary region. If the load is removed and the temperature maintained or slow cooling permitted, recrystallization can occur—delayed significantly by the low internal energy. One example is the recrystallization during extrusion of low-alloyed aluminum alloys after leaving the die [McQ 90].

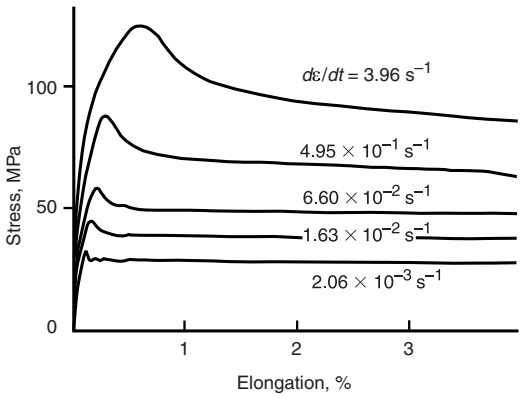

Fig. 4.46 Strain-rate dependence in hot working (stress-strain curves of nickel) [San 75]

4.9 Alloys at Higher Temperatures

4.9.1 Annealing of Alloys

In the annealing of deformed alloys—from the point of view of the deformation energy—in which there is thermal equilibrium at the annealing temperature, recovery and recrystallization processes play the main role as with pure metals. However, with single-phase alloys, the thermal activation of the climb and cross slip processes initiating thermal activation is more difficult because of the presence of foreign atoms. This also applies to the migration of grain boundaries during recrystallization because grain boundaries are frequently enriched with dissolved atoms and have to be torn away from them.

If the second phase exists in the form of fine precipitates (in the range of 0.04–0.4 μm diam), these also tend to retard recrystallization because they can exert a significant resistance to the necessary migration of grain boundaries, particularly where they accumulate. This can occur to such an extent that at a moderate annealing temperature recrystallization can be completely suppressed and only recovery takes place. The strength then does not fall completely during annealing and the deformation texture remains.

With two-phase alloys with large crystallites of the second phase, it is possible that only one phase with a low recrystallization temperature recrystallizes during the annealing process, whereas the second phase remains unrecrystallized.

Still more complicated is the case when a deformed alloy is in thermal unequilibrium during annealing. Softening processes then occur by recovery and recrystallization simultaneously with precipitation processes (or, in rare cases, dissolution processes) of second phases [McQ 90, McQ 90a]. The dependence of the mechanical properties on the annealing conditions is therefore complicated and difficult to explain.

There are more vacancies in deformed metals than in undeformed metals, which simplifies the diffusion of foreign atoms to precipitates. Therefore, the precipitation processes during annealing take place more quickly in the deformed structure than in the undeformed state.

It is possible today to construct high-strength materials in which specific alloy composition, heat treatment and deformation precipitation hardening and work hardening are combined without any significant softening processes tak-

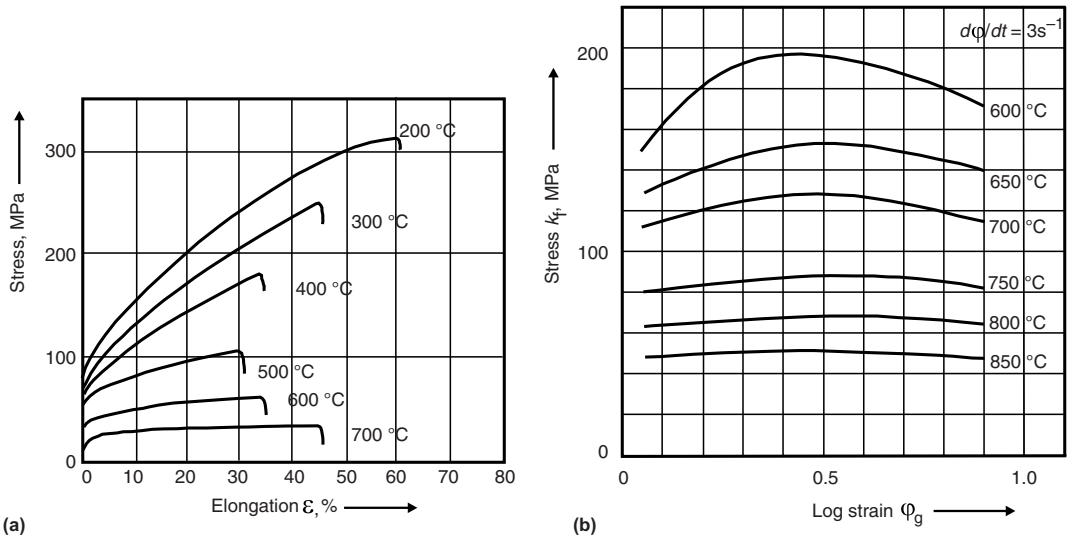

Fig. 4.47 Hot low curves for CuZn8 obtained from different methods. (a) Hot-tensile tests. (b) Torsion tests [Bau 63, DGM 78]

ing place during the permitted time at the intended working temperature [Ber 83].

4.9.2 Deformation of Alloys at Higher Temperatures

In single-phase alloys, the embedded foreign atoms hinder the migration of dislocations as in cold working but also impair dynamic recovery and recrystallization. The hot yield stress, work hardening, and hot strength increase with increasing foreign atom content (Fig. 4.48).

Precipitates, which retard static recrystallization, also naturally hinder dynamic recrystallization processes. Hot-strength curves are therefore steeper with alloys with precipitates and attain the stationary (horizontal) state later or at a higher temperature.

The high hot strength of high-alloy materials naturally makes hot working more difficult and thus materials "more difficult to extrude."

Because, as described above, a high vacancy concentration accelerates the process of precipitation processes, the rate of precipitation increases during the hot working of an alloy not in equilibrium.

The factors that determine whether and at what rate recovery and recrystallization takes place during hot working are the same as those governing annealing after previous cold working.

4.10 Processes in Extrusion

Billet heating before extrusion cannot be considered to be independent of the previous hot processes—casting, hot forging, or homogenization. In addition, the temperature and time of heating are determined by various, often conflicting, requirements:

- Low extrusion pressure
- High extrusion speed
- Limitation of the exit temperature to a maximum (surface quality) and to a minimum (recrystallization, with aluminum alloys solution heat treatment during extrusion).

When determining the preheat temperature, the deformation heat during extrusion (increasing the extrusion temperature) and the heat flow into the tooling (reducing the extrusion temperature) have to be taken into account.

If nonhomogenized billets of age-hardening alloys are used, the homogenizing effect during billet heating increases the longer it lasts. In this case, slower gas furnace heating is more effective than fast induction heating. Not only can segregations harmful to extrusion be reduced, but also precipitates dissolved and supersaturations reduced.

In contrast, previously homogenized billets of suitable aluminum alloys cooled to a specified

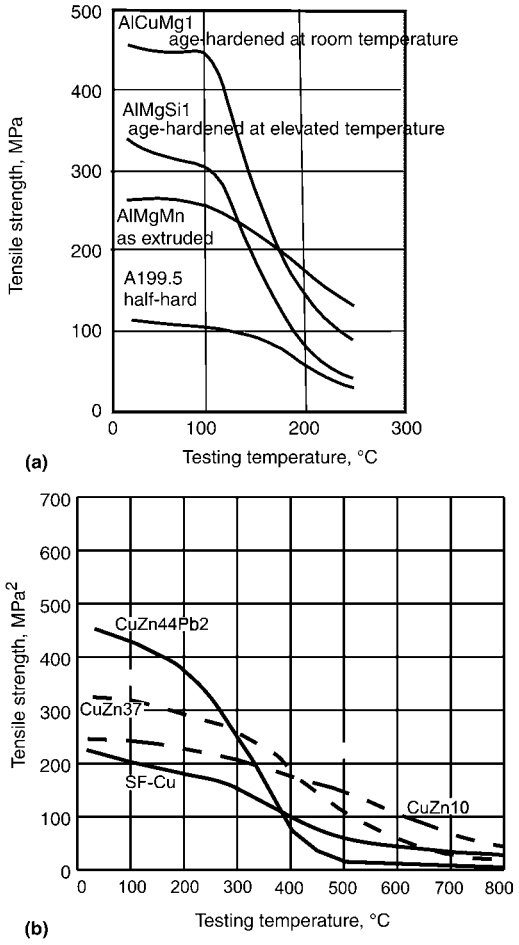

Fig. 4.48 Hot tensile strength of different alloys. (a) Aluminum alloy. (b) Brasses [Alt 94, Wie 86]

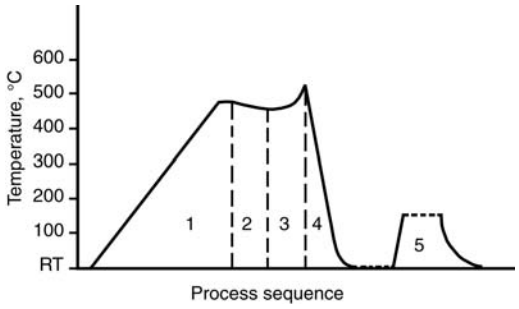

Fig. 4.49 Temperature variation in the processing of age-hardening aluminum alloys by extrusion. 1, Heating the billet; 2, transfer to the press; 3, extrusion = heating from the deformation = solution heat treatment; 4, section cooling; 5, elevated temperature age hardening. RT, room temperature [Alt 94]

degree of solubility have to be heated as quickly as possible and not too high in order not to destroy the desired structure. Induction heating is then recommended.

It is possible with AlMgSi alloys and CuCr and CuCrZr alloys to carry out extrusion at the solution annealing temperature and thus avoid a separate solution heat treatment prior to age hardening (Fig. 4.49).

With brass CuZn39Pb, which has an α-β structure at room temperature, the billet heating can develop a structure corresponding to the phase diagram (see the section "Extrusion of Semifinished Products in Copper Alloys," Fig. 5.51 in Chapter 5), in which the α brass that has poor hot-working properties is dissolved and only the readily hot-worked β brass is present.

The surface of the extruded billet quickly develops the temperature of the container liner wall, which at approximately 500 °C is cooler than materials extruded at moderate and high temperatures. There are materials—such as the free machining brass CuZn39Pb in which the surface cooling of the billet increases the content of the difficult-to-deform α brass—where the flow behavior close to the container wall drastically changes. The β-rich core then flows forward and the α-rich periphery is held back, resulting in the extrusion piping defect (see "Extrusion of Semifinished Products in Copper Alloys," Fig. 5.56, in Chapter 5).

Dynamic and recrystallization processes take place in front of and in the deformation zone of the die during extrusion. The stacking fault energy of the extruded metal plays an important role here. With a low stacking fault energy (copper, α-brass, austenite), dynamic recrystallization occurs in the extrusion deformation zone of the extrusion press at moderate and high extrusion speeds. On the other hand, aluminum and its alloys with a high stacking fault energy can repeatedly only recover—the extrusion leaves the press soft but with a fibrous unrecrystallized structure. However, in some cases, recrystallization processes can occur in the hot extrusion after it leaves the die.

The sketch in Fig. 4.50 schematically shows the influence of the high and low stacking fault energy.

In the shear zones (at the liner wall, at the funnel of the dead metal zones in flat dies and within hollow dies) the deformation in aluminum is up to 60 times larger than in the core [Ake 92].

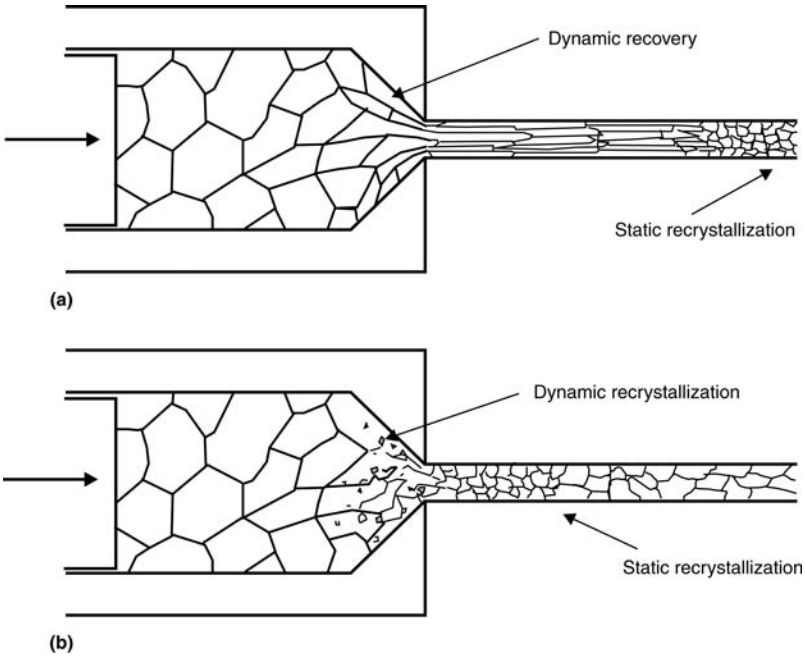

Fig. 4.50 Dynamic recovery and recrystallization processes in extrusion. (a) High stacking fault energy. (b) Low stacking fault energy [McQ 75]

If the fibers with higher deformation (e.g., close to the surface of the extruded section) are very elongated and thin (width approximately two subgrains), adjacent grains can grow together and the fibers appear shorter [McQ 90].

The grain structure, however, is so severely distorted in the shear zones that no grain boundaries are visible under the microscope and the precipitates present are randomly distributed. AlMgSi0.5 sections recrystallize with fine grains but only *after* leaving the die (static and not dynamic).

In alloys with recrystallization retarding additions (e.g., AlMgSi or AlCuMg with additions of Mn, Cr, or Zr), the recrystallization temperature is raised to such a level that no recrystallization occurs even after leaving the deformation zone (particularly following rapid cooling).

However, subsequent solution heat treatment reveals that the peripheral zone from the shear zone is more heavily deformed than the core and, therefore, statically recrystallizes, often with very coarse grains, whereas the more weakly deformed core remains unrecrystallized.

The unrecrystallized structures usually have a strong texture because of the high deformation in the extrusion press, whereby the strength in the longitudinal direction is much higher than in the transverse direction. This is referred to as the *extrusion effect*.

Recrystallization retarding additions in suitable aluminum alloys can, however, precipitate coarsely during annealing at high temperatures (defective homogenization, billet heating in a gas furnace). A second phase that has no effect on the recrystallization then forms (e.g., manganese in AlMgSi). Then the aluminum material can, as described earlier for AlMgSi0.5, fully recrystallize after leaving the die—while the section is still hot.

In the production of aluminum sections with a decorative surface, structural variations and textures can produce flecks and stripes. Because only the zone immediately below the surface of the section plays a role, attention has to be paid not only to the billet production (see section 4.2.4) but also to the die design. The procedures that have to be taken into account in the manufacture of aluminum sections are described in detail in the section "Extrusion of Semifinished Products in Aluminum Alloys" in Chapter 5.

Independent of the material, in extrusion without lubrication the zones close to the surface of the extruded zone are hotter than the core because of the concentration of the deformation in the shear zone and the friction between the die

land and the material. However, at the surface this friction also produces tensile stresses as the core of the extrusion accelerates. It is therefore no surprise that the billets with residual melt segregations with low melting points produce crack-sensitive extrusions. If these segregations are not previously eliminated by homogenization, the only option is to extrude at low temperatures and slow speeds. This prevents the temperature of the section surface from reaching the dangerous region of melting, which results in transverse cracks (see the section "Extrusion of Semifinished Products in Copper Alloys," Fig. 5.45, in Chapter 5).

In the extrusion of copper alloys and steels, spontaneous recrystallization usually takes place during the deformation as the extrusion temperature is well above the recrystallization temperature (which is 0.8–0.9 times the melting point T_S). It can happen that the start of extrusion, where the deformation is low and the temperature high, has a coarse secondary recrystallized structure, but the end of extrusion—where the deformation is high and the exit temperature lower due to cooling during extrusion—is fine grained.

In pure (and low-alloyed) copper so few recrystallization retarding precipitates are present that the grain boundaries migrate relatively easily. After the primary recrystallization in the deformation zone, a secondary coarse recrystallization has to be expected in the emerging extrusion (at 800–900 °C). Rapid cooling is used directly behind the die to prevent this.

4.11 Toughness, Fracture

The toughness of a material is—for the same temperature and the same deformation rate—dependent on the deformation conditions. For example, in a tensile test the toughness defining elongation to fracture is relatively low, but in the torsion test in which the deforming elements are subjected to other forces, it can be higher. In particular, in extrusion with its high hydrostatic contribution to the deforming loads much higher deformations can be achieved than in the simple tensile test. The phenomena occurring in the tensile test up to fracture should be understood (Fig. 4.51). A more detailed explanation is found in [Rie 87].

4.11.1 Ductile Fracture

In metal working the most common type of failure is ductile fracture following deformation. As a rule, the deformed metal is not defect free. During the deformation in the tensile test, initially small voids form at internal boundary surfaces with low adhesion, e.g., at inclusions, coarse precipitates or at existing gas pores, where the stress concentration becomes high enough during the working. Only very pure metals deform in tensile tests without this void formation.

The cross section of the tensile specimen in the region of the voids is reduced. The tensile force therefore exerts a higher stress, which leads to higher elongation in this zone, resulting in a localized necking. Once the necking has started this area continues to reduce in cross section as the stress increases, whereas the sections of the specimen that have not necked elongate only slightly. Soon the pores in the necked zone increase in size and grow together until fracture occurs between them. The fracture surfaces are rough and consist of craterlike depressions, each corresponding to an original void. The ductile fracture usually passes through the grains and is therefore transcrystalline.

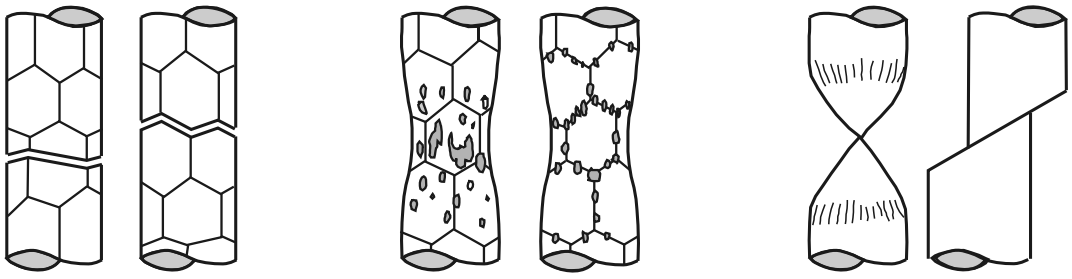

Fig. 4.51 Different failure methods (in tensile testing) [Ash 79]

At higher temperatures, as discussed previously, the yield stress and the work hardening are reduced by the onset of the recovery processes. This means that the stress needed to nucleate the voids, e.g., at inclusions, is first reached after a higher deformation. The elongation to fracture can then increase.

However, at higher temperatures the flow stress and the work hardening react more sensitively to the deformation rate, and accordingly the fracture behavior varies at higher speeds. As a rule, the elongation to fracture decreases as the rate of deformation increases.

Grain-boundary decoration by foreign atoms or inclusions and thin films of segregations can weaken the grain boundaries at high temperatures to such an extent that the crack propagates in an intercrystalline manner.

4.11.2 Brittle Fracture and Mixed Types

Pure deformation-free brittle fracture is rare; more common is low-deformation brittle fracture. Neither of these fracture types occurs during extrusion. Their explanation does, however, increase the understanding of the possible fracture processes.

At sufficiently low temperatures most metals fail without or with only slight deformation by brittle fracture. The starting point is a crack that is already present or forms after slight plastic deformation. The tip of this crack acts as a notch; i.e., a high stress concentrates here under a tensile load, which, when the so-called crack propagation stress is exceeded, results in a deformation free or low deformation cleavage fracture. The fracture surfaces are smooth.

With increasing temperature, the stress peak that forms at the initial crack under load is reduced by local deformation so that the crack propagation stress is reached only after higher work hardening, in other words, higher plastic deformation. The tendency to brittle fracture reduces with increasing temperature or disappears completely.

The cleavage fracture propagates along surfaces with low cohesion. If these are specific crystallographic planes, then the fracture is transcrystalline. With weakened grain boundaries attributed to higher temperatures or accumulated foreign atoms, segregations, or precipitations the fracture propagates between the grains and is thus intercrystalline. Frequently, a fracture shows both transcrystalline and intercrystalline components.

If the deformation is carried out at such a high temperature that existing segregations start to melt, an almost completely brittle fracture occurs.

4.11.3 Fracture during Hot-Working

The processes leading to fracture are now explained using hot torsion tests. Torsion tests correspond more closely to the processes in extrusion, but only a few suitable measured results are available.

Elongation and necking traverse in hot-torsion tests one or two minima. The examples of E-copper and of phosphorous containing tin bronze illustrate this (Fig. 4.52). With E-copper (Fig. 4.52a), the elongation to fracture and the necking initially reduce with increasing temperature (up to a minimum of approximately 500 °C) and then increase. As the temperature increases, severe grain-boundary cracks form perpendicular to the tensile direction. They form and grow by the migration of vacancies to the grain boundaries associated ultimately with weakening due to grain-boundary accumulation. Above the minimum temperature, where the elongation to fracture increases again, the processes of recovery and, in particular, recrystallization occur. Existing voids are dissolved and the susceptibility to fracture reduced.

A second minimum similar to that seen with 8% tin bronze (Fig. 4.52b) can be related to the effect of segregations that have a high mobility and readily melt [Bau 63]. In the example of the tin bronze it is a low melting point phosphorus containing phase on the grain boundaries.

4.11.4 Defects in Extrusion

Tensile stresses are usually required for crack formation and propagation. High shear stresses can also result in cracks—referred to as shear cracks.

In extrusion, the material in the die deformation zone is under three-dimensional compression. Only when it has passed through the die will the tensile stress developed close to the surface by the friction on the die bearing have an effect. The magnitude of this tensile stress depends on the friction and the die design. In lubricated extrusion (glass lubrication with steel and nickel alloys, hydrostatic extrusion) it is lower than in unlubricated (aluminum) or if only a flat die is lubricated (copper). The tensile stresses at the surface of the extruded section

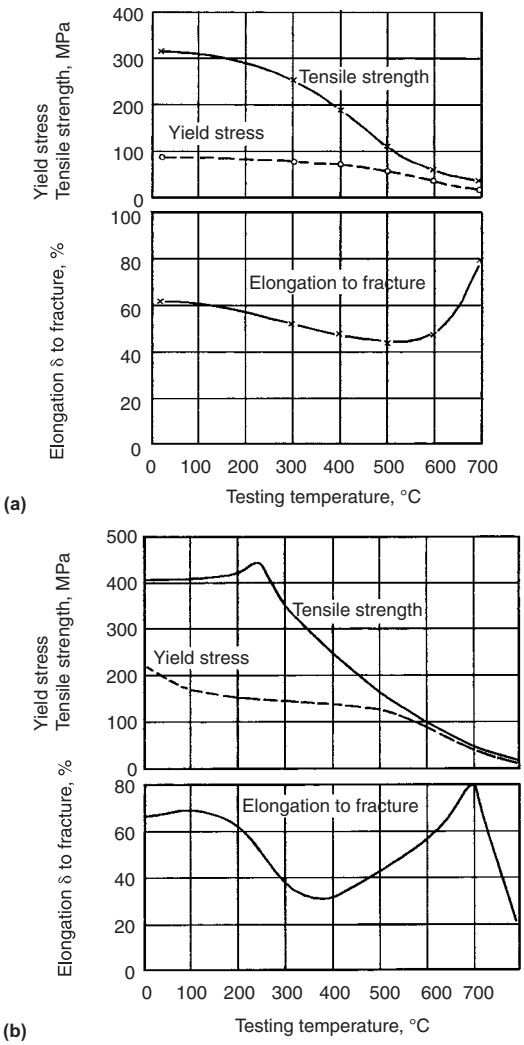

Fig. 4.52 Elongation to fracture as a function of temperature in tensile tests. (a) E-copper. (b) Tin-bronze CuSn8

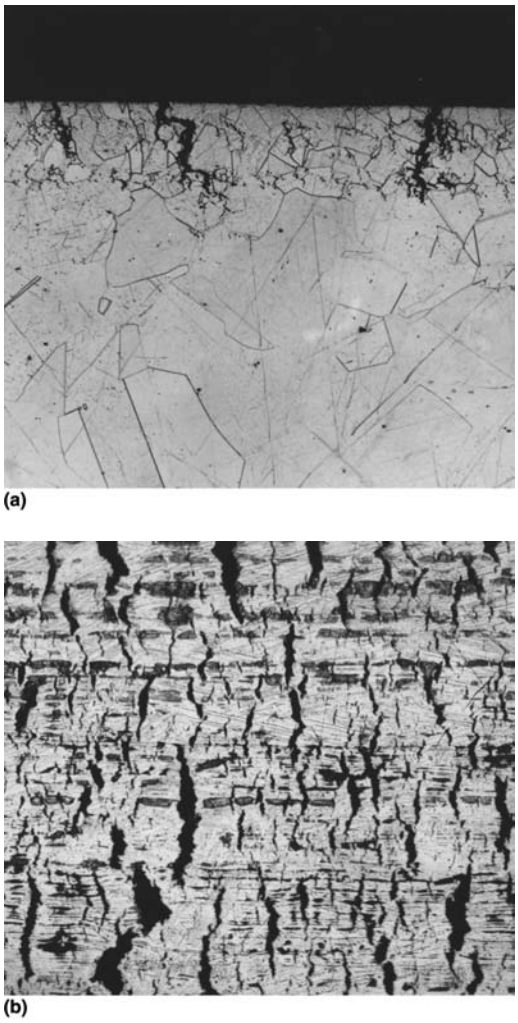

Fig. 4.53 Cracked surface of a CuZn28Sn (longitudinal section/surface image). (a) The width is approximately 0.66 mm. (b) The width is approximately 1.4 mm [Die 77]

combined with the temperature increase in the peripheral zone result in transverse cracks (fir tree defect) if an existing grain-boundary accumulation is severely weakened or even melted. Under the microscope these grain-boundary accumulations can be detected along with the predominantly intercrystalline nature of the cracks (Fig. 4.53).

Internal cracks in tubes have the same origin: if the friction between the material and the mandrel is high enough at the extrusion temperature to destroy the cohesion between grain boundaries transverse to the direction of extrusion, transverse cracks will form on the internal surface of the tube.

At a small extrusion ratio the core accelerates so quickly during extrusion relative to the surface zone that the shear stresses are sufficient to separate a surface shell from the core. This also requires correspondingly weakened zones.

With very small extrusion ratios, conical-shaped transverse cracks can develop because tensile stresses can occur along the billet axis before the die plane. These can result in voids and cracks at the affected areas.

Both types of defects—the peeling of a surface shell from the core and the core cracking—cannot be detected on the surface. Materials at risk must be tested using nondestructive methods when necessary.

4.12 Solid-State Bonding

Materials can bond together under pressure and at an elevated temperature without macroscopic shape changes (diffusion bonding). However, at least one of the bonding partners has to undergo a significant compressive deformation (compression, rolling, extrusion).

The bonding processes that occur during deformation is the reason for the use of the extrusion process in many cases.

The weld seams in hollow profiles, the production of composite profiles and the processing of composite materials as well as the extrusion of metal powders are discussed in this section.

4.12.1 Bonding Processes

The most common methods of joining two components are welding and soldering. In both cases the liquid phase takes the dominant role. In welding, the boundary layer between the components melts. The resolidified melt forms the "weld seam." In soldering, both the parts remain in the solid state, only the solder between them melts and solidifies. The joint is formed by adhesion and diffusion at the boundary surface.

When bonding in the solid state—referred to as *pressure welding*—the formation of a liquid phase usually is not required. The most common methods are roll cladding, friction welding, and ultrasonic welding (more information on pressure welding is found in [Tyl 68].

If two metallic surfaces meet, they can bond together if the surface atoms of both components are approximately a lattice spacing apart. The faces then act as a grain boundary and the metallic bonding forces of the electron gases act across the boundary surfaces. Experience shows that this adhesion process rarely occurs without the contribution of pressure and temperature. Absolutely flat and clean boundary surfaces are required and it is made easier or possible at all if the two components pressed together have identical, or similar, lattice structures.

A higher surface pressure always flattens very small irregularities and improves by plastic deformation of the roughness peaks the contact between the components pressed together over the maximum contact area. With pure aluminum the pressure welding commences after only 10% deformation of the two surface areas; however, it is only after 70% that the tear resistance of the joint matches the value of the parent metal.

At a higher temperature, this flattening and smearing together of the two surfaces is simplified, atoms changing places with each other can fit with the opposing lattice so well that the bond between the atoms at the boundary surface is optimized. There are hypotheses that the dislocations stacked together by pressure welding can traverse the boundary surface into the other partner.

Any existing coatings, e.g., fine oxide skins or films of lubricant, hinder any adhesive bond. If the areas of the components being bonded are increased during the bonding process, e.g., in roll cladding or extrusion, brittle coatings such as oxides cannot follow this expansion. Instead, they break up into individual pieces. Fresh metal forms between the pieces on the surface and this can now bond with the opposite side. Pressure welding requires both high pressure and a large deformation and thus an increase in the surface area. Since, in roll cladding and extrusion through a hollow section die there is also relevant movement between the two partners and frequently polyganization or even recrystallization occurs by recovery processes the grains orientate themselves into matching positions. If the bond is very good, it is impossible to detect the joint under the microscope (see Fig. 4.55).

If the surface coating can follow the increase in the contacting areas, i.e., smear, then bonding is not possible during the contacting process. One example is the damaging effect of lubricant in the extrusion of hollow aluminum alloy sections. This can prevent the formation of a sound pressure weld.

4.12.2 The Formation of Pressure Welds in Hollow Sections and during Billet-on-Billet Extrusion

If hollow sections are produced using bridge or porthole dies as described in Chapter 5, in the section on the extrusion of aluminum alloys, the divided strands bond together in the welding chamber immediately in front of the die into two or more longitudinal seams. These are not welds, as sometimes stated, but metallic bonds from solid-state adhesion. In these die zones, which are more correctly referred to as *bonding chambers,* the high transverse forces—almost equal to the hydrostatic pressure in the undeformed billet—act on the surfaces of the divided strands producing an increase in the surface area by the reduction of the cross section in the chamber. The adiabatic heating from the deformation also plays a role. The strands that are separated just prior to the bonding—and with the exclusion of

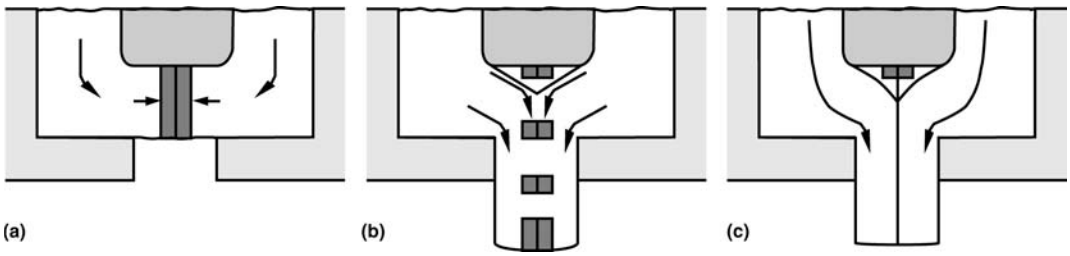

Fig. 4.54 Breakup of the surface layer in longitudinal welds in the production of aluminum hollow sections. (a) Meeting under the leg. (b) Breaking apart. (c) Clean longitudinal weld [Ake 92]

air—are free of any oxide or lubricant surface coating, assuming a clean die is used, that would hinder the bonding.

Oxide is brought into the welding chambers of the die only during the first filling when the free oxide coated end faces come together (Fig. 4.54a) [Ake 92]. The fractured remains of the oxide surface are mostly carried away with the first part of the section (Fig. 4.54b). The subsequent bonding takes place between material regions that have initially been compressed in front of the legs of the mandrel and have then flowed with extreme shearing along the flanks of the leg and combined at the dead metal zones beneath the legs. The strands that come together are free of any oxide film. The process of welding then consists merely of the initially small contact surfaces being extended over the entire length of the section and thus being increased by several orders of magnitude. Subgrains then form continuously even over the original contact surfaces. This repolygonization is linked to the movement of dislocations but does not require any atom diffusion.

In addition, the material recrystallizes usually in the deformation zone (e.g., copper) or immediately on leaving the die (e.g., AlMgSi0.5) so that the newly formed grains grow away from the contact faces freshly bonded by adhesion and heal them.

The contact faces that equate to a severely distorted grain boundary disappear during this recrystallization and cannot be identified under the microscope (Fig. 4.55).

The suitability for producing hollow sections varies from material to material. There are even differences between aluminum alloys, which appear to be predestined for hollow section production. Numerous precipitates or phase segregations with foreign lattice structures can impair the bonding. The hot strength of the high-strength materials can be so high that the large degree of deformation required to produce sufficient pressure in the bonding chamber is not reached and the use of hollow section dies made difficult or even impossible. Finally, with materials that do not recrystallize at the extrusion temperature, there is no possibility of healing the voids in the bonds by recrystallization [Ake 92a].

There are, however, cases where defects in the bonds occur even with materials well suited for hollow section extrusion. These problems are discussed in more detail in Chapter 5.

With copper and brass, which are extruded in the temperature range 600 to 900°C, the danger of separating oxides flowing in is greater than with aluminum alloys. This is one of the reasons why extrusion of these materials through hollow section dies is usually avoided (see Chapter 7, the section on tooling for copper alloys).

The ability of aluminum alloys to bond by pressure welding is not only utilized in the production of hollow sections but also in billet-on-

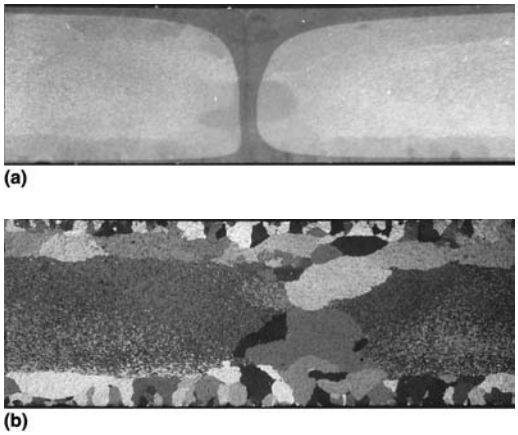

Fig. 4.55 Extrusion weld in aluminum. (a) Different etchant attack. (b) Full recrystallization across the weld [Ake 92]

billet extrusion where transverse welds form (Fig. 4.56).

There is—however rarely used—the case where the billet is extruded onto the discard of the previous billet (Fig. 4.56a). This is successful only after careful cleaning of the surfaces of the end faces and the removal of air to avoid blisters and material separation in the extrusion. This process is used in aluminum cable sheathing (see section 3.6 in Chapter 3).

With aluminum alloys, the discard is usually sheared off (solid section dies and porthole dies, Fig. 4.56c) or pulled off (bridge dies, Fig. 4.56d) before the next billet is extruded. If a solid section is extruded through a flat die, then a "feeder chamber" is normally used (Fig. 4.56b). The residue of the first billet remaining in this feeder chamber behaves in the same way as the residue in a hollow section die after removal of the discard. It can bond by adhesion with the subsequent billet. This usually occurs because the different flow conditions between the regions close to the surface and the core of the section result in the material of the next billet flowing as a tongue into the material from the preceding billet so that the contact surfaces are extensively increased.

4.12.3 Composite Extrusion

Composite extrusion is used to produce sections from two or more different materials, usually with a constant cross-sectional distribution over the entire length. The process and practical applications are given in Chapter 5 in the section "Extrusion of Semifinished products from Metallic Composite Materials." This section covers the mechanism of the bonding of two materials during extrusion.

Numerous metals react so severely at the high extrusion temperatures required by adhesion with the extrusion tooling that the latter is immediately destroyed unless protective measures are taken (See section 4.12.5).

This attack of the extrusion tooling and oxidation of the hot billet can be avoided by cladding the billet of the reactive material (Be, Ti, Zr, Hf, V, Nb, Ta) with copper or iron. Even alloy steel can be clad for specific purposes with mild steel, an aluminum alloy with pure aluminum, or even aluminum with copper to give just a few examples.

To ensure that a solid bond forms between the sheath and the billet by pressure welding, both carefully degreased components must undergo such severe deformation in the deformation zone (at least 50%) that any brittle surface coating present (oxide) breaks up and pure metals contact each other.

The diffusion of atoms across the boundary surface can simplify the bonding by transposition processes. On the other hand, these diffusion processes can also result in the formation of undesired alloy layers at the contacting surfaces. In the worst cases, a low-melting-point secondary phase can form from the atoms of the two components. Table 4.1 lists these low-melting-point phases in the corresponding binary system base material-cladding. The extrusion temperature must not exceed these limits [Ric 69].

If intermetallic brittle phases form by diffusion during the pressure welding between the sheath and the base material (e.g., between zirconium and iron), this is not always detrimental because the bond zone can be kept extremely thin.

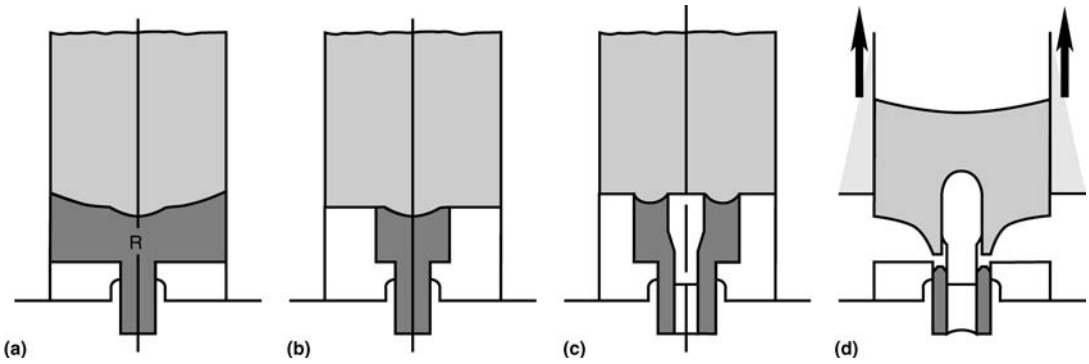

Fig. 4.56 Extrusion of aluminum "billet-on-billet" [Ake 92]. (a) Extrusion of a billet on the discard in the container. (b) With feeder die. (c) In the ports of a porthole die. (d) Pulling off the discard in a bridge die [Ake 92]

Table 4.1 Liquid phases between the cladding and the billet

Element	Melting point, °C	Transformation point, °C	Lowest temperature for the formation of liquid phases (°C) with		
			Copper	Nickel	Iron
Beryllium	1280	. . .	850	1157	1165
Titanium	1720	882	885	942	1085
Zirconium	1860	862	885	961	934
Vanadium	1900	. . .	. . .	1203	1468
Niobium	2410	. . .	1080	1175	1360
Tantalum	3000	. . .	1080	1360	1410

Source: [Ric 69]

It is not only the intermetallic phases that form during extrusion that can damage the surface zone of the extruded base material to such an extent that different properties exist relative to the core after removal of the cladding, e.g., corrosion susceptibility. The formation of a solid solution between the cladding material and the base metal can also result in the same problems. The selection of the cladding material and the extrusion parameters must, therefore, be carefully considered.

Other types of composite materials are produced so that a second or third material in the form of bar is added to the billet. Super conductors or contact wires can be produced by placing suitable bars or wires into holes in a copper billet. This is then extruded.

In certain cases extrusion is carried out with the knowledge that intermetallic phases will form between two adjacent materials, e.g., to achieve a high wear resistance or super conducting properties [Web 82].

There is also composite extrusion between two metals that exhibit extremely different properties and that apparently do not react with each other at the extrusion temperature. One example is the production of a composite of an aluminum section and a steel strip in which the wear resistance of the steel and its high hardness are utilized where the section is subjected to high stresses [Mie 87].

In fiber composite materials, metallic or nonmetallic fibers are embedded in a metallic matrix to improve the mechanical properties. The adhesive bonding between the fibers and the base material is usually low because the lattices are so different and, in the case of nonmetallic fibers, a metallic bond cannot be produced. Stiff fibers are broken into small pieces during extrusion by the elongation of the parent metal—the higher the extrusion ratio, the smaller the pieces. These pieces are mechanically held so tightly in the base material without adhesion that they can withstand tensile forces even during elongation of the extruded section and thus increase the strength. The softer metallic matrix transfers the forces under load into the fibers, which determine the strength [Kel 73].

The behavior of the fiber-reinforced metallic materials at different temperatures can only be explained to a limited extent by the behavior of the base material. At low temperatures, the fibers increase the strength. At high temperatures, in contrast, the base material can shear at the interface with the fibers. This can damage the material in such a way that it fails before a material without fibers [Scu 92].

4.12.4 Powder Extrusion

The process and the application of powder extrusion is described in detail in the section "Extrusion of Powder Metals" in Chapter 5 (see also [Sch 86]). This section covers the metallurgy of this process.

The particles of loose or cold compacted powder have a fill density of 50 to 80%; i.e., depending on the production process the round or angular particles contact each other, at best, incompletely. After cold compaction the particles have to some degree linked together and in some places even adhesively bonded so that the stabilized billet (green compact) can withstand the handling before extrusion without breaking. In the press the particles are initially to some extent plastically deformed so that they contact virtually over the entire surface. A certain amount of relative movement between the particles in this accommodation process results in the particles also rubbing together. This is believed to produce partial friction welding [She 72]. This process is either stopped in front of or at the start of the deformation zone by the plastic elongation corresponding to the extrusion ratio. The approximately round powder particles become elongated fibers. The surface area of the particles

is increased to such an extent that brittle surface coatings, usually oxides, break up to free the pure metal. A good lattice match, combined with transposition processes across the boundaries between the individual grains, develops a good adhesive bond by pressure welding [Rob 91].

The extruded section has a fine structure corresponding to the powder grain size that can scarcely be distinguished under the microscope from that of an extruded cast billet. However, the structure of a cast (or preforged) billet is usually coarse grained and exhibits in corresponding materials coarse primary precipitates that have a negative influence on the quality of the extruded section. The fine-grain structure of powder of the same composition is, in contrast, far more homogeneous (e.g., [Asl 81]).

With perfect bonding, the mechanical properties of a material produced from either a cast billet or a powder metallurgical material of the same composition are largely identical.

For dispersion hardening, hard particles of an intermetallic phase or a nonmetal (usually oxides, nitrides, or carbides) are embedded in the base material by powder extrusion. The effect of these particles corresponds exactly to that of precipitates described in section 4.7. They act as barriers to dislocation movement, which increases the yield strength and the work hardening. The number and distribution of the particles and not the size are important: the finer the distribution, the greater the effect.

The particles added by powder metallurgy are resistant to very high temperatures in contrast to precipitates in cast alloys. Coagulation and dissolution are impossible. Therefore, the application of dispersion-hardened materials is mainly attributable to the high-temperature properties. They are still effective at very high temperatures where other strength-increasing methods fail (work hardening, dissolved foreign atoms, precipitated particles), e.g., [Mat 90] (Fig. 4.57).

Very finely distributed dispersoids also hinder grain-boundary migration, which leads to recrystallization. Finely distributed aluminum oxide particles in a copper matrix can, for example, completely suppress recrystallization at 1000 °C, which is just below the melting point. This means that cold work-hardened materials also have a higher strength at high temperatures than the original soft material because of the retention of grain boundaries that hinder dislocation movement [Zwi 57].

The boundary surfaces matrix-hard particles do not usually have good adhesion, similar to fiber materials, because the adhesive effect is weak with different metallic lattices and completely absent with metallic inclusions. With their small size, however, they are embedded so securely in the base material that this is not important. If the hard particles or their material fraction are too large, tearing at the boundary surfaces can result in a decrease in strength. Volume fraction, size, and distribution of the hard particles have to be carefully balanced.

4.12.5 Friction between the Extruded Material and the Tooling

The friction conditions between the billet and the container as well as at the end faces and on the die working faces play a very important role in extrusion. This section discusses only the physical and metallurgical aspects of these processes. The basics of lubrication are also touched on (more information on adhesion is given in [Tyl 68]).

In the absence of lubrication, there is direct contact between the tooling and the extruded material. The roughness of the tool surface is determined by the machining. The high pressure in extrusion smears the plastically deformed material into the depressions and as it glides over the tool, it has to travel over the peaks and into the valleys. This process results in friction.

The adhesion between the tool and the material is more important. It occurs where there is metal-to-metal contact. The partial adhesion and breaking away of the material at the tool increases the friction between both. The adhesion can, however, be larger than the cohesion within the material. Particles of the material torn from its surface adhere to the tool. It is also possible for the pieces of the tool surface to be torn away and to pass out with the extruded section. This increases the roughness of the tool. High pressure and temperature increase the adhesive tendency.

This tendency to adhesion varies with the material/tool combination. It can be assumed that a slight adhesion tendency and thus a low friction force occurs where both partners only slightly dissolve in each other. Aluminum and titanium adhere very strongly with steel tooling. This, naturally, also applies to steel because the adhesion tendency between partners of the same material is particularly marked. On the other hand with copper the adhesion tendency to steel tooling is only half as high as that of aluminum [Czi 72].

The tooling surface is oxidized at the extrusion temperature. The adhesion tendency will be

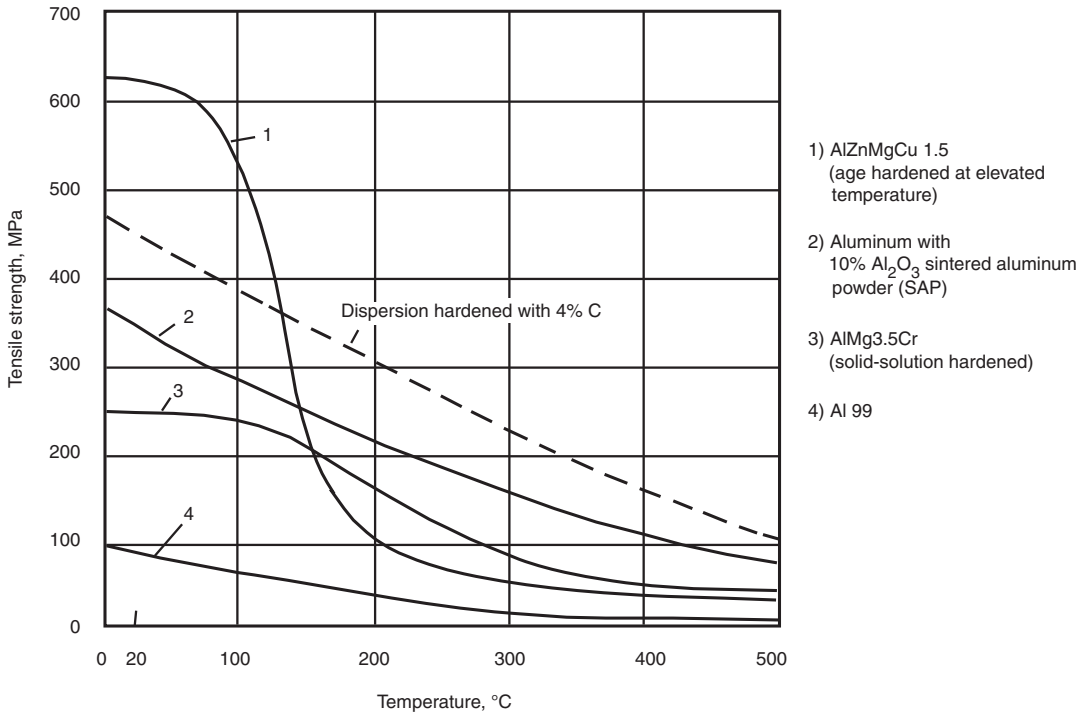

Fig. 4.57 Hot strength of normal and dispersion-hardened aluminum alloys [Jan 75]

reduced by this oxide coating on the hot tool. Its effect has still not been extensively studied. Probably, poorly bonding oxides are partly torn away and carried out with the extruded section so that the clean tool surface comes into contact with the material.

Even without taking into account the adhesion from the relative movement material/tooling, the plastic deformation needed for smearing at the surface structure of the hard tool produces heat. The catching on and releasing of the material caused by the adhesion can also produce local temperature peaks that can approach the melting point of the material. They are, however, immediately reduced by the good conductivity of the metal. Both processes are the cause for the temperature increase due to friction at the material surface.

The thin but firmly bonded oxide layer on aluminum is broken up by a large deformation even at high temperatures. The clean metal comes into contact with the tooling during extrusion. A thin layer of aluminum quickly forms on the bearing surface of the die, and this bonds so solidly because of the adhesion that the profile formed in the bearings largely slides along aluminum and not steel [Ake 83]. A smooth bearing surface thus behaves hardly differently from a slightly rougher one. The roughness measured perpendicular to the section corresponds to the roughness of the aluminum coating on the die bearing surface [The 93] (see also Chapter 6, the section on extrusion of aluminum alloys).

"Crow's feet" or "pickup" are particles that have been torn out within the die opening and have bonded to the tool. They produce grooves in the surface. They continue to grow until the shear force exerted by the extrusion is sufficient to tear them away and to carry them out with the extruded section [Mer 77].

Nitriding, which is usually used to harden the surface of extrusion dies for aluminum alloys, has only a slight effect on the adhesion behavior but does prevent premature wear of the tool surface. Grooves in the tool thus occur later, if at all. The aluminum coating does form later on nitrided tooling during extrusion than on unnitrided tooling. Once it has formed then, as far as the section surface is concerned, there is no longer any difference [The 93].

The container liner surface is coated with solidly bonded aluminum, even after the first extrusion, because of the strong adhesion tendency between steel and aluminum already mentioned.

After this, the billet no longer slides or, more correctly, shears, over steel during extrusion but over aluminum [Ake 83].

Only extrusion without lubrication has been considered so far, which is usual for aluminum. Lubricants—including certain oxides—should separate the material and the tooling and hinder any friction reaction between them (see [Sce 83] for a more detailed discussion).

The lubricant film has to bond both to the tooling and the material. The slip takes place within the lubricant film itself. The selected lubricant film has to be thick enough not to break down and must have the correct viscosity (toughness) at the extrusion temperature. The lubricant on one hand has to be able to follow the severe increase in the surface area in extrusion and, on the other hand, must not be squeezed out under the high extrusion pressure.

Only a few metal oxides act as lubricants and only copper oxide is so ductile at the extrusion temperature and bonds to the tooling and billet solidly enough while retaining the sliding effect that the container does not have to be lubricated at all and the die only slightly. However, an incomplete coating of the billet surface with oxide results in irregularities in the slip of the billet along the container liner wall and to defects in the extruded section (see the section on copper alloys in Chapter 5 for more information).

If nonlubricating oxides in copper alloys dominate, e.g., zinc oxide in CuZn alloys (brass), the lubricating effect of the copper oxide is lost.

The usual lubricants with copper alloys and other materials with moderate extrusion temperatures are graphite containing lubricating oils, which can be classified under the heading "solid lubrication." The hexagonal structure of graphite, the base surfaces of which exert only a weak attraction force between each other, is the reason that graphite plates easily slide over one another. The oil in which the graphite plates are embedded acts as a carrier and ensures that the lubricant bonds to the tooling with a suitable thickness.

If the extrusion temperature is higher than approximately 1000 °C, graphite is unsuitable as a lubricant because it is destroyed by oxidation, as is the carrier oil. Molybdenum disulfide, which exhibits at room temperature and slightly elevated temperatures outstanding lubrication properties—attributable like graphite to its crystal structure—loses its effect by oxidation above 300 °C. It is therefore not suitable for extrusion at higher temperatures.

Glass lubrication in the Séjournet process is the current practice for high-temperature extrusion (stainless steels, nickel alloys, etc.). This is described in detail in the section "Extrusion of Iron-Alloy Semifinished Products" in Chapter 5. It should also be mentioned that the thermal insulation between the material and the tooling plays an important role in addition to the good lubrication properties.

The billet and tooling have to be completely wetted by the glass lubricant. Good adhesion is also a requirement and it should also not attack the metal. The glass film on the extruded section should be approximately 10 to 30 μm thick.

The relative movement between the material and the tooling occurs entirely within the glass film, the viscosity of which corresponds to a first approximation to a Newtonian liquid:

$$\text{Viscosity } \eta = A \cdot \exp(E/RT)$$

The glass film becomes more fluid as the temperature increases. Pressure dependence of the glass viscosity has not been found.

Different glass compositions are recommended to give the correct viscosity, which should be between 10 and 100 Pa · s, at the different extrusion temperatures and extrusion ratios. The table in Fig 4.58 gives the composition of different glasses and shows some viscosity curves.

4.13 Extrudability of Metallic Materials

Good extrudability is a collective term for a low-extrusion load, high extrusion speed, good surface finish, freedom from defects, tight dimensional tolerances, and high tooling throughput. The breadth of the term makes definitions and deductions difficult. In general, a material is described as having a better extrudability than another if it has better hot-working characteristics in extrusion when specific extrusion parameters are held constant. Extrusion materials are classified by this term into high, moderate, and low extrudability.

One material from an alloy family can then have a higher extrudability than another if:

- The maximum extrusion speed before the occurrence of surface defects (roughness, grooves) under otherwise equal conditions (initial billet temperature, container temperature, extrusion ratio, die) is faster.

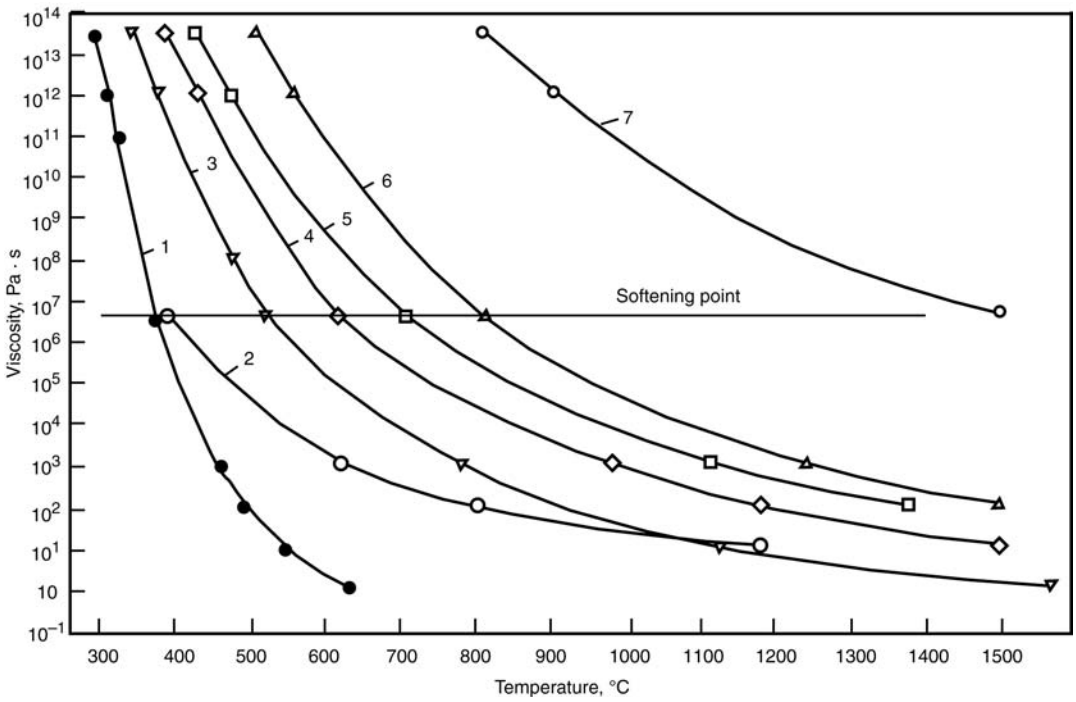

No.	Type of glass	Approximate composition	Recommended temperature range, °C
1	Lead-borate	10 B_2O_3, 82 PbO, 5 SiO_2 3 Al_2O_3	530
2	Borate	. . .	870
3	Potassium-lead-silicate	35 SiO_2, 7 K_2O, 58 PbO	870–1090
4	Potassium-sodium-lead-silicate	63 SiO_2, 8 Na_2O, 6 K_2O, 4 MgO, 21 PbO	1090–1430
5	Boron-silicate	70 SiO_2, 1 PbO, 28 B_2O_3, 1 Al_2O_3	1260–1730
6	Boron-silicate	81 SiO_2, 4 Na_2O, 13 B_2O, 2 Al_2O_3	1540–2100
7	Silicate (quartz)	96 + SiO_2	2210

Fig. 4.58 Dependence of the viscosity of glass lubricants on the temperature [Sce 83]

- The extrusion load under otherwise equal conditions (initial billet temperature, container temperature, extrusion ratio, die, extrusion speed) is lower.
- The initial billet temperature and the container temperature under otherwise equal conditions (extrusion ratio, die, and extrusion speed) are lower.

The material and its properties influence the extrudability in many ways:

- *The melting point* is a controlling factor for the deformation temperature and thus for the tooling life and for the subsequent processing of the extruded product by calibration or finish drawing.
- *Alloying additions* (type and content) determine the flow stress, extrusion speed, and the tendency to extrusion defects.
- *Large precipitates and inclusions* can result in the formation of surface defects (furrows, flaking, and cracks) and increase the tool wear.

From the practical point of view it is important to be able to use simple criteria before accepting an order and before using an unknown material to estimate whether and at what cost an order can be realized. The size and the type of press available, the tooling, and the dimensions of the extruded product play a role in addition to the material.

The theory of the extrusion load is given in Chapter 3. Reference should be made to section 3.1.1.4 and the calculation example in Fig. 3.18.

The values of k_f or k_w and η_u cannot be obtained from the data obtained from normal tensile tests since the strain that can be attained is too low because of the necking and because the rate of deformation in extrusion is several orders of magnitude higher than the experimental conditions on a tensile testing machine.

The logarithmic principle strain rate $\dot{\varphi}_g$ of 1 to 10 s^{-1} reached in torsion tests falls in the range of the average logarithmic principle strain rate in extrusion. In compression testing on fast presses, φ_g up to approximately 2 and $\dot{\varphi}_g$ up to 1000 s^{-1} are achieved.

The *Atlas of Hot-Working Properties of Non-Ferrous Metals* (Vol 1, *Aluminum Alloys*) [DGM 78] gathers the known data from the literature in a standard format (ordinate: flow stress k_f, abscissa: logarithmic principle strain φ_g with the parameters temperature and principle strain rate). For the extrusion press specialist it is difficult to find the necessary data for the extrusion ratios of $V = 10$ to 300, corresponding to principle strains φ_g between 2 and 6 and the logarithmic strain rates $\dot{\varphi}_g$ between 0.5 and 10 s^{-1} normally used in extrusion.

What helps in practice?

One suggestion made after trials with aluminum alloys was to define the extrusion behavior by using a standard two-hole die [Mon 75] (Fig. 4.59) as follows: The farther the thicker section travels during extrusion, the higher is the extrudability of the material. Tests with this process found it to be too insensitive. Seven-hole dies of a specific design have also been used for experiments [Mis 91].

Scharf estimated the extrudability of aluminum alloys in experimental extrusions from the extrusion time at a constant extrusion load. He therefore used indirectly the extrusion speed as the limiting parameter and could thus differentiate between alloys and their heat treatment [Sca 64].

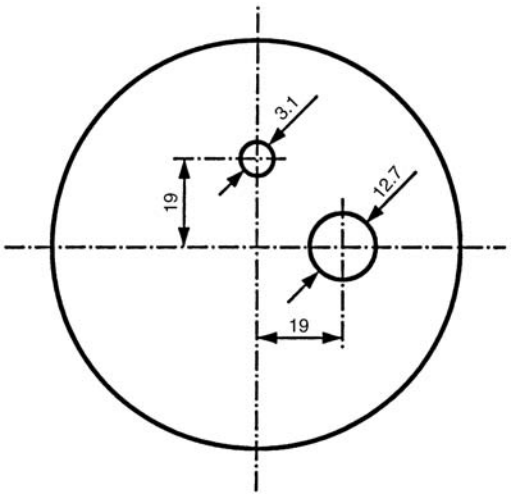

Fig. 4.59 Experimental die to determine extrudability

Castle and Lang [Cas 78] developed a test die and test section with which it was possible to make a meaningful assessment of the material properties of continuously cast material with and without heat treatment (Fig. 4.60). The limiting speed for poor shape or tearing away of the ribs was determined. The necessary extrusion load can also be used as a measure of the extrudability of a material.

Many extrusion plants use similar test dies—even dies for hollow sections with corresponding ribs.

Figure 4.61 shows the various limiting speeds for a range of alloys.

The extrusion speed does not play such a large role with materials that are extruded at moderate and high temperatures (e.g., copper alloys, steels); it is usually very high. In this case the

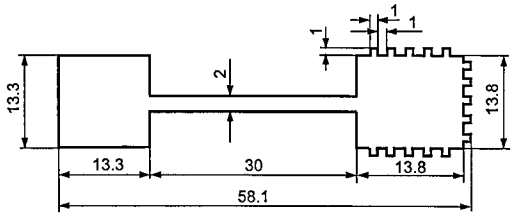

Fig. 4.60 Test section to estimate the extrudability of aluminum alloys using the extrusion speed as the limiting factor [Cas 78]

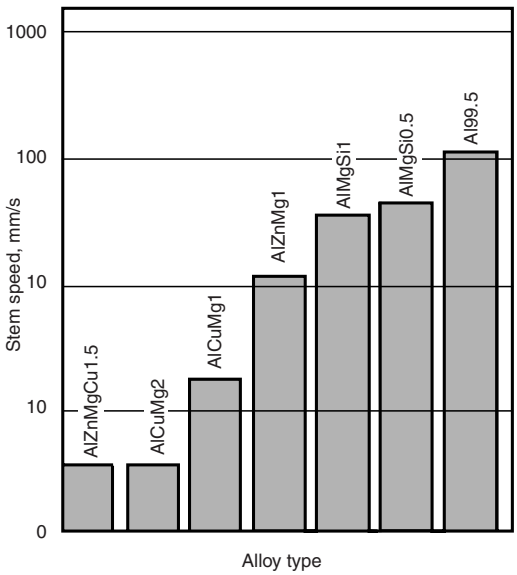

Fig. 4.61 Limiting extrusion speed measured on different aluminum alloys using the test section in Fig. 4.60 [Cas 78]

flow resistance and thus the limiting extrusion load have to be taken into account.

Hot-tearing tests can give a rough comparison between the different materials. The dependence of the strength of different materials on the temperature is in principle correctly reproduced. The k_f values obtained, however, cannot be used to calculate the extrusion load.

The following method is known from the copper alloy processing industry: Equations 3.4, 3.5, and 3.49 given in Chapter 3 in for the variation of the extrusion load during extrusion with and without lubrication are used.

For simplicity, the relevant formulae for the maximum extrusion load F_0 are:

Unlubricated container $F_{St\ max}$

$$= A_0 \cdot k_w \cdot \varphi_g + D_0 \cdot \pi \cdot (l_0 - l_R)\tau \quad \text{(Eq 4.1)}$$

and

Lubricated container $F_{St\ max}$

$$= A_0\{k_w \cdot \varphi_g \cdot e^{4(\mu_0/D_0)\cdot l_c} + k_{f_0}(1 - e^{4(\mu_0/D_0)\cdot l_c})\} \quad \text{(Eq 4.2)}$$

With glass lubrication the friction factor μ_0 is approximately zero. Then:

$$F_{St\ max} = A_0 \cdot k_w \cdot \varphi_g$$

where

$$k_w = \bar{k}_f/\eta$$

and

$$\varphi_g = \ln A_0/A_1$$

where A_0 is the container cross-sectional area; A_s is the section cross-sectional area; D_0 is the container bore; l_0 is the upset billet length in the container; k_f is the mean flow stress of the material being deformed in the deformation zone; η_u is deformation efficiency; k_{f_0} is flow stress in the billet outside the deformation zone; and, μ_0 is the coefficient of friction for the friction between the billet and the container.

Successive trials are carried out on the extrusion press in question with a standardized billet size (diameter, length) at the assumed temperature. Using initially large and then increasingly smaller extruded bar diameters, extrusions are carried out up to the maximum press capacity.

A value of k_w can then be calculated from Eq 4.1 (unlubricated container) or Eq 4.2 (lubricated container) using the coefficients η and μ_0 obtained from the practical measurements. It is then possible using Eq 4.1 or 4.2 to deduce possible billet or section dimensions for the material studied on this press [Ret 99].

The very specific test process described to estimate the extrudability reflects the extent of the problem and the complexity of this term. At the same time such tests have become useful aids to determine optimal deformation conditions. Many extrusion plants also use their own test methods.

Other criteria for the extrudability, including freedom from defects, dimensional tolerances, and tooling life do not lend themselves to model investigations and practical experience has to be used.

Appendix: Additional Information for Chapter 4 Metallurgical Principles

Additional Information 1: Miller's Indices to Describe a Space Lattice

Various planes can be drawn through the atomic points of a crystallite, referred to as *crystallographic planes*. Because there are numerous parallel crystallograhic planes, these are referred to as a family of crystallographic planes. The orientation of the crystallographic planes is described by a coordinate system, the axes *x*, *y*, and *z* coincide with the edges of the unit cell (edge length *a*, *b*, *c*) (Fig. 4.62).

The lengths *ma*, *nb*, and *pc* from the origin to the intersection points of the crystallographic planes define their location. The reciprocal values of m, n, p, are taken to give the Miller indices as follows:

$$h{:}k{:}l = 1/m{:}1/n{:}1/p$$

The Miller indices of closely packed planes consist of small whole numbers (in the diagram: m = 2, n = 4, p = 1 gives h:k:l = 2:1:4).

The indices are given in ( ): (*hkl*) = (214). Negative indices are described with ¯ (overbar)

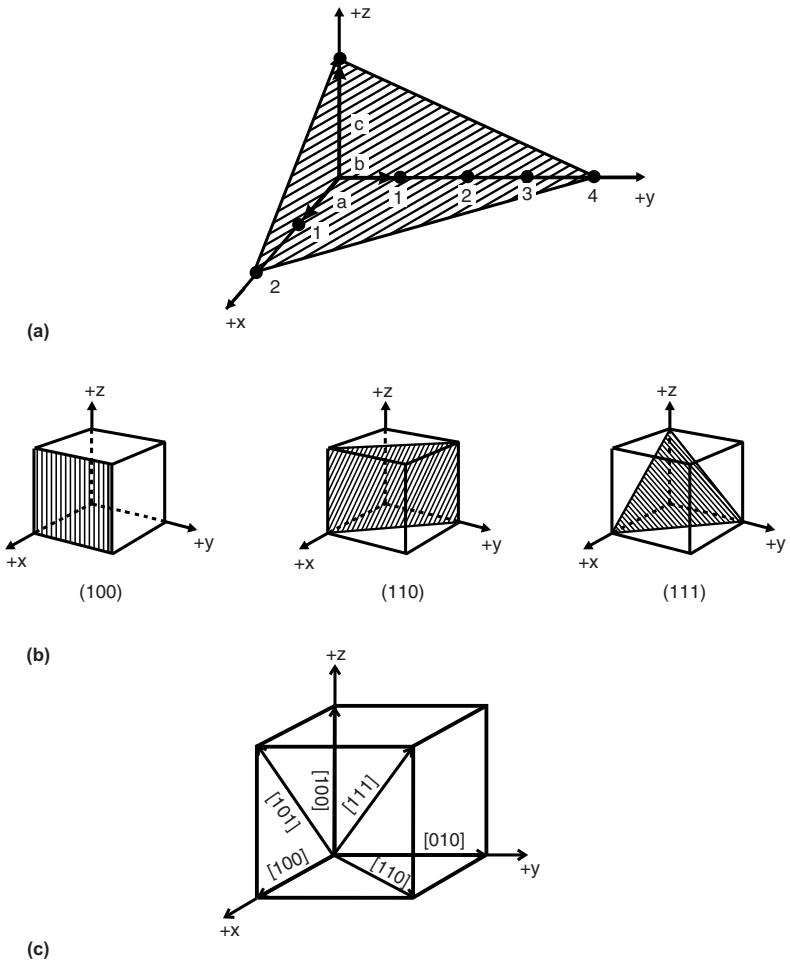

Fig. 4.62 Miller's indices for space lattices. (a) Designation of lattice planes. (b) Examples of planes in the cubic lattice. (c) Examples of directions in the cubic lattice

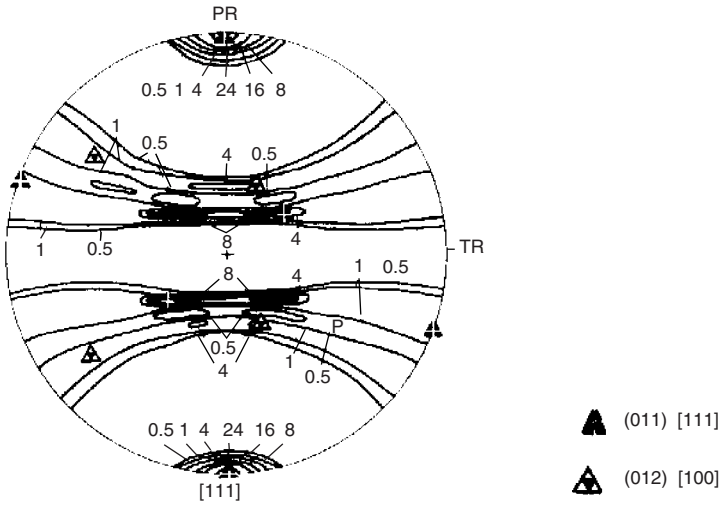

Fig. 4.63 Representation of textures in pole figures. [111] pole figure from the section core of an extruded AlCuMg bar [Moe 75]

over the number: e.g., $-1 = \bar{1}$. Figure 4.62(b) shows some examples of crystallographic planes in a cubic lattice.

Directions in the unit cell are described with the location coordinates of a point on a line going through the origin—also whole numbers but this time within angular brackets. A surface diagonal in the cubic lattice is designated with [011], and a spatial diagonal with [111] (Fig. 4.62c).

Additional Information 2: Representation of Textures in Pole Figures

In general, the orientation distribution in a textured structure is shown on a stereographic projection in which a spherical surface is represented on a plane (known as the projection plane).

The specimen is located in the center of the sphere, and the normals of the crystallographic planes penetrate the surface of the sphere. A texture is described by showing in the pole figure the frequency of the orientations of individual crystallographic planes (e.g., (111) or (100)). The pole plane coincides with a specific projection plane (e.g., the rolling plane in rolled sheets). In extruded or drawn bar the north-south direction of the pole figure is usually orientated along the bar axis (Fig. 4.63).

Additional Information 3: Temperature and Speed Dependence of the Flow Stress in Hot Working [Sel 79, Ake 70, McQ 90]

In the stationary region of the work-hardening curve where work hardening and recovery are in equilibrium, the flow stress is dependent on an exponential function of the temperature as deduced from diffusion. The activation energy is that for self diffusion:

$$k_f \approx f(Q/RT)$$

At the same flow stress there is a simple relationship between the strain rate and the absolute temperature T:

$$\dot{\varphi} = A \cdot \exp(-Q/RT)$$

If deformation is carried out at a higher temperature and higher speed then, according to this relationship, the flow stress is the same as that at a lower temperature and corresponding low speed:

$$k_f = f(\dot{\varphi}\exp(Q/RT))$$

Or, using the Zener-Hollomon parameter Z:

$$k_f = f(Z)$$
$$Z = \dot{\varphi}\exp(Q/RT)$$

There are various expressions for the relationship between the flow stress k_f and the Zener-Hollomon parameter Z that apply depending on the material and temperature-speed situation:

$$Z = a \cdot k_f^a \qquad Z = a \cdot \exp(b \cdot k_f)$$

REFERENCES

Books and Overviews

[Alt 94]: D. Altenpohl, *Aluminium von innen* (*Aluminum from the Inside*), Aluminium-Verlag, Düsseldorf, 1994

[Ber 83]: W. Bergmann, *Werkstofftechnik, Teil 1: Grundlagen, Teil 2: Anwendung* (*Material Technology, Part 1: Fundamentals, Part 2: Application*), Carl Hanser Verlag, Munich, Vienna, 1983

[Blu 93]: W. Blum, H. Mughrabi, and B. Reppich, *Grundlagen der Werkstoffkunde—Nichteisenmetalle* in *Umformtechnik* (*Fundamentals of Material Science*), Verlag Stahleisen, Düsseldorf, 1993

[Dah 93]: W. Dahl, R. Kopp, and O. Pawelski, *Umformtechnik—Plastomechanik und Werkstoffkunde* (*Non-Ferrous Metals in Deformation Technology*), Verlag Stahleisen, Düsseldorf, 1993

[Guz 70]: A.G. Guz and G. Petzow, *Metallkunde für Ingenieure* (*Metallurgy for Engineers*), Akad. Verlagsges, Frankfurt, 1970

[Hor 67]: E. Hornbogen and H. Warlimont, *Metallkunde* (*Metallurgy*), Springer-Verlag, 1967

[Hou 93]: H.P. Hougardy, *Grundlagen der Werkstoffkunde* (*Fundamentals of Metallurgy*), Stahl in *Umformtechnik,* Verlag Stahleisen, Düsseldorf, 1993

[Sce 83]: J.A. Schey, *Tribology in Metalworking,* ASM International, 1983

[Sch 81]: W. Schatt, *Einführung in die Werkstoffwissenschaft* (*Introduction to Material*

Science), VEB Deutscher Verlag für die Grundindustrie, Leipzig, 4, Auflage, 1981

[Tyl 68]: R.F. Tylecote, *The Solid Phase Welding of Metals,* Edward Arnold Ltd., London, U.K., 1968

[Wie 86]: A.G. Wielandwerke, *Ulm: Wieland-Buch Kupferwerkstoffe* (*Wieland-Book Copper Alloys*), Wieland-Werke AG, Ulm, 5, Auflage, 1986

Special Literature

[Ake 66]: R. Akeret and A. Künzli, Ermittlung der Formänderungsfestigkeitkf von Aluminiumlegierungen mit Hilfe von Torsionsversuchen und Vergleich der Er-gebnisse mit denjenigen von Strangpreßversuchen (Determination of the Flow Stress of Aluminum Alloys Using Torsion Tests and Comparison of the Results with Those from Conclusion Trials), *Z. Metallkde*., Vol 57, 1966, p 7789–7792

[Ake 70]: R. Akeret, "Fließspannung und Struktur bei der Warmumformung (von Aluminium)" ("Flow Stress and Structure in Hot Working **[of** Aluminum**]**"), Alusuisse report 220/70

[Ake 83]: R. Akeret, Einfluß der Querschnittform und der Werkzeuggestaltung beim Strangpressen von Aluminium, Teil II: Die Reibung im Preßkanal (Influence of the Cross-Section and Tool Design on the Extrusion of Aluminum, Part II: Friction in the Die Bearing), *Aluminium,* Vol 59, 1983, p 745–750

[Ake 88]: R. Akeret, A. Ried, and J. Theler, *J. Metall,* Vol 42, 1988, p 760–769

[Ake 90]: R. Akeret and M. Textor, *Strangpressen* (*Extrusion*), DGM-Informationsgesellschaft, Oberursel, Germany, 1990

[Ake 92]: R. Akeret, Strangpreßnähte in Aluminiumprofilen (Extrusion Welds in Aluminum Sections), Parts 1 and 2, *Aluminium,* Vol 68, 1992, p 877–886 and 965–973

[Ake 92a]: R. Akeret, "Extrusion Welds—Quality Aspects Are Now Center Stage," presented at International Aluminum Technology Seminar (Chicago, IL), May 20–22, 1992

[Alt 65]: D. Altenpohl, *Aluminium und Aluminiumlegierungen* (*Aluminum and Aluminum Alloys*), Springer-Verlag, 1965

[And 48]: W.A. Anderson and R.F. Mehl, *Trans. AIME,* Vol 161, 1948, p 140

[Ash 79]: M.F. Ashby, C. Gandhi, and D.M.R. Taplin, *Acta Metall.,* Vol 27, 1979, p 699–729

[Asl 81]: C. Aslund, G. Gemmel, and T. Andersson, Stranggepreßte Rohre auf pulvermetallurgischer Basis (Extruded Tubes with a Powder Metallurgy Base), *Bänder Bleche Rohre,* Vol 9, 1981, p 223–226

[Bag 81]: J. Baumgarten, W. Bunk, and K. Lücke, Strangpreßtexturen bei AlMgSi-Legierungen, Teil 1: Rundstangen (Extruded Texture in AlMgSi Alloys, Part 1: Round Poles), *Z. Metallkde.,* Vol 72, 1981, p 75–81

[Bau 59]: M. Bauser, "Einführung in die Physik der plastischen Verformung der Metalle" ("Introduction to the Physics of the Plastic Deformation of Metals"), unpublished manuscript

[Bau 61]: M. Bauser, *Verhalten von Nichteisen-Metallen bei der Warmumformung* (*Behavior of Nonferrous Metals in Hot-Working*), Vortrag Metallfachabend, Düsseldorf, 1961

[Bau 63]: M. Bauser, Verformbarkeit und Bruchverhalten bei der Warmformgebung (Workability and Fracture Behavior in Hot-Working), *Metall.,* Vol 17, 1963, p 420–429

[Bau 64]: M. Bauser, Zeit-temperatur-Auschärtungsschaubilder und die Festigkeit stranggepreßter aushärtbarer Aluminiumlegierungen (Time Temperature Age-Hardening Diagrams and the Mechanical Properties of Extruded Age-Hardening Aluminum Alloys), *Z. Metallkde,*Vol 55, 1964, p 816–821

[Bux 77]: K. Buxmann, *Metall.,* Vol 31, 1977, p 163–170

[Bux 77a]: K. Buxmann, Fachbericht (technical reports) FB 41/777/100 der Deutschen Gesellschaft für Materialkunde, Oberursel, Germany

[Cas 78]: A.F. Castle and G. Lang, *Proceedings Aluminium Konferencia 78,* Székesfehérvar, Vol 1, 1978

[Czi 72]: H. Czichos, *J. Appl. Phys.,* Vol 5, 1972, p 1980

[DGM 78]: Deutsche Gesellschaft für Metallkunde: *Atlas der Warmformgebungseigenschaften von Nichteisenmetallen, Aluminiumwerkstoffe* (*Atlas of Hot-Working Properties of Non-Ferrous Metals*), Vol 1, *Aluminum Alloys,* DGM, 1978

[DGM 78a]: Deutsche Gesellschaft für Metallkunde: *Atlas der Warmformgebungseigenschaften von Nichteisenmetallen,* Band 2, *Kupferwerkstoffe* (*Atlas of Hot-Working Properties of Non-Ferrous Metals*), Vol 2, *Copper Alloys*, DGM, 1978

[Die 77]: O. Diegritz, "Preßfehlerkatalog; Fehlererscheinungen bein direkten Strangpressen

von Kupferwerkstoffen" ("Defects in the Direct Extrusion of Copper Alloys"), manuscript, AK Schwermetall im Strangpreßausschuß, DGM

[Fie 57]: D.S. Fields and W.A. Backofen, Determination of Strain Hardening Characteristics by Torsion Testing, *Proc. Amer. Soc. Test. Mat.*, Vol 57, 1957, p 1259–1272

[Fle 74]: M.C. Flemings, *Solidification Processing,* McGraw-Hill Inc., 1974

[Fra 50]: F.C. Frank and W.T. Read, *Phys. Rev.,* Vol 79, 1950, p 722–723

[Got 84]: G. Gottstein, Rekrlstallisation metallischer Werkstoffe (Recrystallization of Metallic Materials), Deutsche Ges., *F. Metallkunde,* e.V., 1984

[Grz 93]: B. Grzemba and J. Hasenclever, *Non-Ferrous Metals Volume Using Aluminum and Copper as Examples,* Umformtechnik, Kopp und Pawelski, Ed., Verlag Stahleisen, Düsseldorf, 1993

[Haa 84]: P. Haasen, *Physikalische Metallkunde* (*Physical Metallurgy*), Springer-Verlag, Berlin, 1984

[Hof 62]: W. Hofmann, *Lead and Lead Alloys, Metallurgy and Technology,* Springer-Verlag, 2, Auflage, 1962

[Jan 75]: G. Jangg, F. Kutner, and G. Korb, Herstellung und Eigenschaften von dispersionsgehärtetem Aluminium (Production and Properties of Dispersion Hardened Aluminum), *Aluminium,* Vol 51, 1975, p 641–645

[Kat 67]: T.Z. Kattamis, J.C. Coughlin, and M.C. Flemings, *Trans. AIME,* Vol 239, 1967, p 1504–1511

[Kel 73]: A. Kell, *Werksstoffe hoher Festigkeit* (*High Strength Material*), Vol 4, Verlag Vieweg, Wiesbaden, Germany, 1973

[Lan 89]: G. Lang, Warmformverhalten von Aluminiumlegierungen beim direkten Strangpressen (Hot-Working Characteristics of Aluminum Alloys in Direct Extrusion), *Aluminium,* Vol 65, 1989, p 291–294

[Los 77]: E. Lossack, *Erzmetall,* Vol 30, 1977, p 243

[Los 83]: E. Lossack and W. Schneider, *Galvanotechnik,* Jahrg, Vol 74, 1983, p 787–794

[Mat 90]: K.H. Matucha, K. Drefahl, G. Korb, and M. Rühle, Neue oxiddispersionsge-härtete Legierungen für Hochtemperatur-Anwendungen (New Oxide Dispersion Hardened Alloy for High Temperature Application), *VDI-Berichte* (*VDI-Reported*), 1990, Vol 797, p 125–152

[McQ 75]: H.J. McQueen and J.J. Jonas, *Plastic Deformation of Materials. Treatise on Material Science and Technology,* Vol 6, Akad. Press, New York, 1975, p 393–493

[McQ 90]: H.J. McQueen, Micromechanisms of Dynamic Softening in Aluminum Alloys during Hot Working, *Hot Deformation of Aluminum Alloys Proc.* (Detroit, MI), 1990

[McQ 90a]: H.J. McQueen, Effect of Solutes and Precipitates on Hot Working Behavior of Al Alloys, *Hot Deformation of Aluminum Alloys Proc.* (Detroit, MI), 1990, p 105–120

[Mer 77]: G. Merk and S.E. Naess, Pick-Up Formation on Aluminium Extrusion, *Z. Metallkd.,* Vol 68, 1977, p 683–687

[Mie 87]: G. Mier, Verbundstromschienen Aluminium-Stahl für S-und U-Bahnen (Composite Bus-Bars in Aluminum Steel for S and U Trains), *Schweizerische Aluminium Rundschau* (*Swiss Aluminum Review*), 1987, p 12–17

[Mis 91]: W. Misiolek and J. Zasadzinski, Test-Die for Estimation of the Extrudability of Metals, *Aluminium,* Vol 67, 1991, p 85–89

[Möl 75]: M. Möller, "Werkstoffluß, Grobkornbildung und Preßeffekt bei stranggepreßtem Aluminium (AlCuMg)" ("Course Grain Formation and Extrusion Effect in Extruded Aluminum"), dissertation, Technical University of Clausthal, Germany, 1975

[Mon 75]: L.F. Mondolfo, A.R. Peel, and J.A. Marcantonio, *Met. Technol.,* Sept 1975, p 433

[Mor 69]: G. Moritz, *Z. Metallkde.,* Vol 60, 1969, p 742–749

[Mug 84]: H. Mughrabi, Mechanisms and Mechanics of Plasticity, *Rev. Phys. Appl.,* Vol 23, 1984, p 367–379

[Ohm 88]: L. Ohm and S. Engler, *Aluminium,* Vol 64, 1988, p 513–520

[Ohm 89]: L. Ohm and S. Engler, *Metall.,* Vol 43, 1989, p 539–543

[Ray 49]: G.V. Raynor, *Ann. Equilibr. Diagrams*, No. 2, 1949

[Rei 80]: W. Reif and W. Schneider, *Gießereiforschung,* Vol 32, 1980, p 53–60

[Res 92]: O. Reiso, Ph.D. thesis, Norwegian Institute of Technology, Trondheim, Norway, 1992

[Ret 99]: W. Rethmann, Pers Mitteilung KM-Kabelmetall AG (communication from KM-Kabelmetall AG), Osnabrück, Germany, 1999

[Ric 69]: H. Richter, Die Herstellung von Stangen, Rohren und Profilen durch Verbundstrangpressen (The Production of Bars, Tubes and Sections by Composite Extrusion), *Z. Metallkde.,* Vol 60, 1969, p 619–622

[Rie 87]: H. Riedel, *Fracture at High Temperatures,* Springer-Verlag, Berlin, 1987

[Rob 91]: Roberts and Ferguson, Strangpressen von Pulvermetallen (Extrusion of Powder Metals), *Int. Mater. Rev.,* Vol 36, 1991, p 62–79

[San 75]: R. Sandström and R. Lagneborg, *Acta Metall.,* Vol 23, 1975, p 387

[Sca 64]: G. Scharf, Einfluß der chemischen Zusammensetzung auf Preßbarkeit und Festigkeit von AlMgSi0.5 (Influence of the Chemical Composition on the Extrudability and Strength of AlMgSi0.5), *Z. Metallkde.,* Vol 55, 1964, p 740–744

[Sch 86]: W. Schatt, *Pulvermetallurgie* (*Powder Metallurgy*), Hüthig-erlag, Heidelberg, Germany, 1986

[Scn 85]: W. Schneider, *Aluminium,* Vol 61, 1985, p 338–345

[Scu 92]: K. Schulte, *Metal-Matrix Composites with Aluminium Matrix: Advanced Aerospace Materials,* Springer-Verlag, 1992, p 108–118

[See 85]: A. Seeger, *Kristallplastizität. Handbuch der Physik* (*Handbook of Physics*), Springer-Verlag, Berlin, VII/2, p 1–210

[Sel 79]: C.M. Sellars, The Physical Metallurgy of Hot Working, *Proc. Int. Conf. Hot Working and Forming Processes* (Sheffield, U.K.), 1979, p 3–15

[She 72]: T. Sheppard and P.J.M. Chare, *Powder Metall.,* Vol 15, 1972, p 17–41

[Stü 69]: H.-P. Stüwe, Einfluß einer plastischen Verformung auf Phasenumwandlungen in Metallen (Influence of a Plastic Deformation on the Phase Transformations in Metals), *Härt.-Tech. Mitt.,* Vol 24, 1969, p 1–5

[The 93]: W.W. Thedja, K. Müller, and D. Ruppin, Die Vorgänge im Preßkanal beim Warmstrangpressen von Aluminium: Reibung im Preßkanal und Matrizenverschleiß (The Processes in the Die Aperture in the Hot-Extrusion of Aluminum: Friction in the Die Aperture and Die Wear), *Aluminium,* Vol 69, 1993, p 524–528 and 649–653

[Web 82]: H.R. Weber, Extrusion of Technical Superconductors, *Extrusion* symposium, DGM, 1982, p 277–296

[Wei 94]: H. Weiland, T.N. Rouns, and J. Liu, The Role of Particle Stimulated Nucleation during Recrystallization of an Aluminum-Manganese Alloy, *Z. Metallkde.,* Vol 85, 1994, p 592–597

[Wev 54]: F. Wever and A. Rose, *Atlas zur Wärmebehandlung der Stähle* (*Atlas on the Heat Treatment of Steels*), Verlag Stahleisen, Düsseldorf, 1954

[Wie 86]: A.G. Wieland werke, *Wieland-Book Copper Alloys,* Ulm, 5, Auflage, 1986.

[Zwi 57]: K.M. Zwilsky and N.J. Grant, *J. Met.,* Vol 9, 1957, p 1197–1201